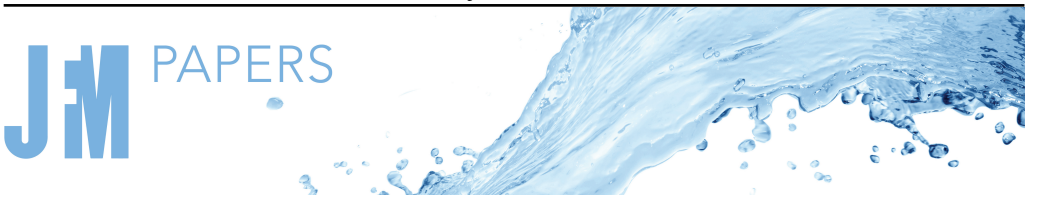
J. Fluid Mech. (2026), *vol.* 1034, A32, doi:10.1017/jfm.2026.11537



Beltrami fields in time-dependent spatially homogeneous velocity gradient background flows

Álvaro Viúdez

Department of Physical Oceanography and Technology, CSIC, Institute of Marine Sciences, Passeig Martim de la Barceloneta 37–49, Barcelona 08003, Spain

Corresponding author: Álvaro Viúdez, aviudez@cmima.csic.es

(Received 18 December 2025; revised 26 February 2026; accepted 9 April 2026)

The time evolution of Beltrami fields in the presence of a time-dependent background flow with spatially homogeneous velocity gradient is analysed using the barotropic vorticity equation. For backgrounds comprising a time-dependent isotropic expansion/contraction and a time-dependent solid-body rotation, we show that every scalar Laplacian eigenfunction generates an unsteady solution of the nonlinear vorticity equation in which the non-background component remains a time-dependent Beltrami field. We derive the evolution law for the background angular velocity in the presence of time-dependent deviatoric strain and velocity divergence, and we generalise the Chandrasekhar–Kendall construction to obtain unsteady Beltrami velocity fields. When the background deformation is a similarity (vanishing deviatoric strain), the Beltrami field is frozen into an advecting flow that differs from the background only by a spatially homogeneous, time-dependent drift. In general, deviatoric strain breaks the Beltrami property, but in regimes where departures are small, we introduce a 'Beltrami field approximation'. Because the background velocity gradient has nine time-dependent degrees of freedom, three of which are constrained by the vorticity equation, six remaining functions may be prescribed to drive the Beltrami field. We illustrate the approach by describing elastic scattering of Beltrami fields by a background-flow pulse.

Key words: compressible flows, general fluid mechanics, nonlinear dynamical systems

© The Author(s), 2026. Published by Cambridge University Press. This is an Open Access article, distributed under the terms of the Creative Commons Attribution licence (https://creativecommons.org/licenses/by/4.0/), which permits unrestricted re-use, distribution and reproduction, provided the original article is properly cited.

https://doi.org/10.1017/jfm.2026.11537 Published online by Cambridge University Press

1. Introduction

The dynamical behaviour of vortices and waves in background flows is central to classical fluid mechanics, including geophysical fluid dynamics. A particularly relevant example is in the ocean, where small-scale vortices and waves coexist with large-scale currents. Mesoscale eddies, with typical radii of 50–150 km and lifetimes of weeks to months, are ubiquitous; submesoscale fronts and vortices, with horizontal scales of 0.1–10 km, Rossby number $Ro = \mathcal{O}(1)$, and lifetimes of hours to days, are also common in the upper ocean (Klein & Lapeyre 2009; McWilliams 2016). At even smaller scales, 1–100 m, turbulence cascades energy forward to dissipation and the motions possess a strongly three-dimensional, ageostrophic character (Vallis 2017). However, the large-scale circulation comprises basin gyres that span 10^3–10^4 km horizontally and includes intense western boundary currents such as the Gulf Stream and the Kuroshio, narrow (∼50–200 km), deep jets that extend hundreds to a thousand km along the boundary, with typical depths of 500–1500 m (Stommel 1948; Munk 1950; Vallis 2017). The Antarctic Circumpolar Current forms a circumpolar band roughly 1000–2000 km wide that encircles the Southern Ocean along a path of order 2×10^4 km, with strong regional variability (Rintoul *et al.* 2001). Small-scale vortices and waves embedded within these background flows are advected, rotated, stretched and strained by the mean currents; many preserve a coherent identity while undergoing filamentation and vortex stretching, before their energy is ultimately dissipated by eddy or molecular viscosity (Chelton, Schlax & Samelson 2011; McWilliams 2016; Vallis 2017).

The main purpose of this paper is to show that, in the presence of a background current $\boldsymbol{u}_b(\boldsymbol{x}, t)$, a particular class of vortices and waves, namely Beltrami fields, which otherwise would be steady solutions, become unsteady and evolve, in a manner fully consistent with the governing dynamical equations, in the presence of a linear background current. The background current, having a time-dependent yet spatially uniform velocity gradient, defines a linear flow. Consequently, the background motion may include a time-dependent translation, isotropic expansion/contraction, pure strain and solid-body rotation. This formulation makes the resulting solutions applicable well beyond geophysical scales. Beltrami velocity fields, or force-free flows, $\boldsymbol{\mathcal{U}}(\boldsymbol{x}, t)$ that satisfy $\nabla \times \boldsymbol{\mathcal{U}} = -k_0 \boldsymbol{\mathcal{U}}$ are eigenfunctions of the curl operator (Woltjer 1958*b*; Dombre *et al.* 1986; Arnold & Khesin 1998; Enciso & Peralta-Salas 2012). In this setting, the Beltrami field is materially 'frozen in' to the background velocity. Its structure is advected, rotated and strained by the imposed linear flow. At laboratory scales, background strain and rotation reshape vortex kinematics and stability, as described by Kida's exact solution (Kida 1981; Robinson & Saffman 1984; Dritschel & Legras 1991; Legras & Dritschel 1991) that shows how an initially elliptic, uniform-vorticity patch embedded in steady planar strain preserves its ellipticity while its aspect ratio and orientation evolve, exhibiting regimes of rotation, nutation and extreme elongation. Subsequent work generalised this framework to rotating strain and analysed stability (Dritschel 1990).

The divergent component of the background flow is a time-dependent, spatially uniform isotropic expansion, mathematically identical to the 'Hubble flow' used to model cosmic expansion, so the time-dependent Beltrami solutions $\boldsymbol{\mathcal{U}}(\boldsymbol{x}, t)$ are compatible (Viúdez 2025*b*) with an arbitrary scale-factor history (Peacock 1999; Ryden 2017). The rotational component of the background motion is a time-dependent solid-body rotation. This component causes the Beltrami wavevector $\boldsymbol{k}_0$ to precess about the axis set by the background vorticity (Viúdez 2025*c*), in direct analogy with Larmor precession of a magnetic moment in a uniform external magnetic field (Jackson 1999). Finally, a time-dependent but spatially uniform strain tensor stretches and tilts the Beltrami field.

https://doi.org/10.1017/jfm.2026.11537 Published online by Cambridge University Press

This stretching usually breaks the Beltrami property, except in some particular stretch orientations in the case of Beltrami plane waves, and the advected Beltrami fields become solutions only in the particular approximation of linear dynamics, referred here to as the Beltrami field approximation, in which it is assumed that the nonlinear term in the vorticity equation, $(\boldsymbol{\nabla}(\boldsymbol{\nabla}\times\boldsymbol{\mathcal{U}}))\boldsymbol{\mathcal{U}}-(\boldsymbol{\nabla}\boldsymbol{\mathcal{U}})\boldsymbol{\nabla}\times\boldsymbol{\mathcal{U}}$, which represents the nonlinear departure from a Beltrami field in the vorticity equation, can be neglected in relation to the Beltrami advection terms due to the background velocity.

The formulation of the problem and the general solution are presented first in § 2. Given an initial steady Beltrami field $\boldsymbol{\mathcal{U}}_0(\boldsymbol{x}_0)$ and a background flow $\boldsymbol{u}_b(\boldsymbol{x},t)$, the vorticity equation reduces to the freezing condition of $\boldsymbol{\mathcal{U}}_0(\boldsymbol{x}_0)$ in the flow $\boldsymbol{v}_b(\boldsymbol{x},t)$, which differs from the background flow $\boldsymbol{u}_b(\boldsymbol{x},t)$ only by a time-dependent drift velocity $\boldsymbol{c}(t)$. The freezing condition of the Beltrami field is preserved at all times if the background flow has a homogeneous but time-dependent velocity gradient that induces a similarity map, which includes time-dependent rotations and expansion/contraction. The background flow must satisfy the vorticity equation, which leads to a compatibility condition (§ 3) expressing how the rate of change of the background angular velocity $\boldsymbol{v}(t)$, or vorticity $\boldsymbol{\omega}_b(t)=2\boldsymbol{v}(t)$, depends on the background deviatoric rate-of-deformation (strain) tensor $\mathsf{D}_0(t)$ and the background divergence $\delta(t)\equiv\boldsymbol{\nabla}\cdot\boldsymbol{u}_b$. Once this equation is solved, we obtain the flow map $\boldsymbol{r}_v(\boldsymbol{x}_0,t)$ of the advecting velocity $\boldsymbol{v}_b(\boldsymbol{x},t)$ and then the inverse map $\boldsymbol{R}_v(\boldsymbol{x},t)$, which is required to express explicitly the time-dependent Beltrami field $\boldsymbol{\mathcal{U}}(\boldsymbol{x},t)$. The Beltrami flows are analysed next (§ 4). The solutions $\boldsymbol{\mathcal{U}}(\boldsymbol{x},t)$ encompass a wide variety of Beltrami fields since, using the Chandrasekhar–Kendall procedure, they can be put into correspondence with any scalar Laplacian eigenfunction $\eta_0(\boldsymbol{x}_0)$ and a steady Beltrami flow $\boldsymbol{\mathcal{U}}_0(\boldsymbol{x}_0)$. This procedure is time-independent and, in § 4, it is explained how it may be applied to time-dependent fields frozen in the background flow $\boldsymbol{v}_b(\boldsymbol{x},t)$. Thus, Beltrami fields may be specified in many different geometries: Cartesian plane waves (leading to the Arnold–Beltrami–Childress, ABC flows), cylindrical vortices (yielding cylindrical Kelvin solutions), spherical geometry (leading to spherical vortices and, in particular, to the Hicks–Moffatt spherical vortex), ellipsoidal geometry and so on – corresponding to any coordinate system in which the scalar Helmholtz equation $\nabla^2\eta_0(\boldsymbol{x})=-k_0^2\eta_0(\boldsymbol{x})$ is separable. The time evolution of the Beltrami field $\boldsymbol{\mathcal{U}}(\boldsymbol{x},t)$ is prescribed by the background flow $\boldsymbol{u}_b(\boldsymbol{x},t)$, whose deviatoric strain tensor $\mathsf{D}_0(t)$ and divergence $\delta(t)$ are arbitrary time-dependent functions. The prescription of the time evolution of $\mathsf{D}_0(t)$ and $\delta(t)$, together with the initial Beltrami field $\boldsymbol{\mathcal{U}}_0(\boldsymbol{x}_0)$, fully determines the solution for the total flow $\boldsymbol{u}(\boldsymbol{x},t)\equiv\boldsymbol{\mathcal{U}}(\boldsymbol{x},t)+\boldsymbol{u}_b(\boldsymbol{x},t)$. These solutions are described (§ 5) in the case of plane Beltrami fields. In § 6, two examples are analysed. The first considers background rotation and expansion, with $\mathsf{D}_0(t)=\mathsf{0}$. In this case, only the magnitude $\|\boldsymbol{v}(t)\|$ of the background angular velocity may change; the direction $\hat{\boldsymbol{v}}\equiv\boldsymbol{v}(t)/\|\boldsymbol{v}(t)\|$ remains constant. The second example considers an isochoric background flow, $\delta(t)=0$, in which both the magnitude and the direction of the background angular velocity $\boldsymbol{v}(t)$ vary. As a third application example, § 7 addresses, using the Beltrami field approximation, the scattering of a Beltrami field by a time-dependent pulse of background flow. Finally, concluding remarks are given in § 8.

2. Formulation of the problem and general solution

We seek exact time-dependent velocity field solutions $\boldsymbol{u}(\boldsymbol{x},t)$ to the nonlinear barotropic vorticity equation for a perfect fluid,

https://doi.org/10.1017/jfm.2026.11537 Published online by Cambridge University Press

$$\frac{\partial \boldsymbol{\omega}}{\partial t} + \nabla\boldsymbol{\omega}\,\boldsymbol{u} - \nabla\boldsymbol{u}\,\boldsymbol{\omega} + \boldsymbol{\omega}\nabla\cdot\boldsymbol{u} = \boldsymbol{0}, \tag{2.1}$$

where $\boldsymbol{\omega}(\boldsymbol{x}, t) \equiv \nabla \times \boldsymbol{u}$ is the total vorticity field. We use $\nabla\boldsymbol{a}$ to denote the (covariant) gradient of vector $\boldsymbol{a}(\boldsymbol{x})$, i.e. the (1, 1) tensor defined by its action on any vector $\boldsymbol{b}$ as $\nabla\boldsymbol{a}\boldsymbol{b} = (\nabla\boldsymbol{a})\cdot\boldsymbol{b} = \nabla_{\boldsymbol{b}}\boldsymbol{a} = (\boldsymbol{b}\cdot\nabla)\boldsymbol{a}$. In Cartesian coordinates, $\nabla\boldsymbol{a} = (\partial a_i/\partial x_j)\hat{\boldsymbol{e}}_i \otimes \hat{\boldsymbol{e}}_j$. It is convenient to express (2.1) using the Cauchy vorticity formula in the spatial description as

$$\boldsymbol{\omega}(\boldsymbol{x}, t) = \frac{1}{J_T(\boldsymbol{x}, t)}\mathsf{F}_T(\boldsymbol{x}, t)\boldsymbol{\omega}_0(\boldsymbol{R}(\boldsymbol{x}, t)), \quad \boldsymbol{\omega}_0(\boldsymbol{x}) = \boldsymbol{\omega}(\boldsymbol{x}, 0). \tag{2.2}$$

In (2.2), $\mathsf{F}_T(\boldsymbol{x}, t) \equiv \partial(\boldsymbol{r}/\partial\boldsymbol{x}_0)(\boldsymbol{R}(\boldsymbol{x}, t))$ is the deformation gradient of the total flow in the spatial description, $\boldsymbol{r}(\boldsymbol{x}_0, t)$ is the flow map of the total flow, $\boldsymbol{R}(\boldsymbol{x}, t)$ is the inverse flow map and $J_T \equiv \det(\mathsf{F}_T)$.

The total velocity field $\boldsymbol{u}(\boldsymbol{x}, t)$ is decomposed into the sum of a time-dependent Beltrami flow $\boldsymbol{\mathcal{U}}(\boldsymbol{x}, t)$ and a time-dependent, non-Beltrami background velocity $\boldsymbol{u}_b(\boldsymbol{x}, t)$, that is,

$$\boldsymbol{u}(\boldsymbol{x}, t) \equiv \boldsymbol{\mathcal{U}}(\boldsymbol{x}, t) + \boldsymbol{u}_b(\boldsymbol{x}, t). \tag{2.3}$$

The time-dependent oscillating flow $\boldsymbol{\mathcal{U}}(\boldsymbol{x}, t)$, which is derived from steady Beltrami solutions $\boldsymbol{\mathcal{U}}_0(\boldsymbol{x})$ in the reference initial configuration in § 4, must remain a Beltrami flow at all times, that is,

$$\nabla \times \boldsymbol{\mathcal{U}}(\boldsymbol{x}, t) = -k(t)\boldsymbol{\mathcal{U}}(\boldsymbol{x}, t), \quad \forall t, \tag{2.4}$$

with a time-dependent eigenvalue $-k(t)$, where $k(t)$ is a time-dependent wavenumber. In the absence of background flow, $\boldsymbol{u}_b = \boldsymbol{0}$, the vorticity equation requires $\partial_t\boldsymbol{\mathcal{U}} = \boldsymbol{0}$ and, therefore, the time-dependence of the Beltrami flow $\boldsymbol{\mathcal{U}}(\boldsymbol{x}, t)$ is completely prescribed from the background velocity $\boldsymbol{u}_b(\boldsymbol{x}, t)$.

The background velocity $\boldsymbol{u}_b(\boldsymbol{x}, t)$ must satisfy the vorticity equation, that is, the vorticity equation for the total flow (2.1) in the case $\boldsymbol{\mathcal{U}} = \boldsymbol{0}$, which, assuming $k(t) \neq 0$, reduces to

$$\frac{\partial}{\partial t}(k\boldsymbol{\mathcal{U}}) + k\nabla\boldsymbol{\mathcal{U}}\,\boldsymbol{v}_b - k\nabla\boldsymbol{v}_b\,\boldsymbol{\mathcal{U}} + k\boldsymbol{\mathcal{U}}\,\nabla\cdot\boldsymbol{v}_b = \boldsymbol{0}, \tag{2.5}$$

where the advecting velocity $\boldsymbol{v}_b(\boldsymbol{x}, t)$ is defined from the background velocity $\boldsymbol{u}_b(\boldsymbol{x}, t)$ and the Beltrami wavenumber $k(t)$ as

$$\boldsymbol{v}_b \equiv \boldsymbol{u}_b + \frac{\nabla \times \boldsymbol{u}_b}{k(t)}. \tag{2.6}$$

Equation (2.5) follows by substituting $\boldsymbol{u} = \boldsymbol{u}_b + \boldsymbol{\mathcal{U}}$ (2.3) into the vorticity equation and subtracting the (generally nonlinear) vorticity equation satisfied by the background flow $\boldsymbol{u}_b$ (see § 3), so that no background self-advection term is neglected, while the spatial homogeneity $\nabla\boldsymbol{u}_b = \mathsf{L}(t)$ is used only to simplify the remaining coupling terms and yield a closed transport law for $k\boldsymbol{\mathcal{U}}$.

Since the Beltrami fields are isochoric $\nabla\cdot\boldsymbol{\mathcal{U}} = 0$, the divergence of the total flow $\boldsymbol{u}$ in (2.3) is due to the divergence of the background flow $\boldsymbol{u}_b$, which equals the divergence of the advecting flow $\boldsymbol{v}_b$,

$$\nabla\cdot\boldsymbol{u} = \nabla\cdot\boldsymbol{u}_b = \nabla\cdot\boldsymbol{v}_b. \tag{2.7}$$

Equation (2.5) means that the vorticity $-k(t)\boldsymbol{\mathcal{U}}(\boldsymbol{x}, t)$ of the Beltrami flow $\boldsymbol{\mathcal{U}}(\boldsymbol{x}, t)$ is frozen in the advecting flow $\boldsymbol{v}_b(\boldsymbol{x}, t)$. Assuming that $\boldsymbol{u}_b(\boldsymbol{x}, t)$ is a flow solution, the motion problem reduces therefore to find the fields $\{\boldsymbol{\mathcal{U}}, \boldsymbol{v}_b\}$ that satisfy the frozen condition (2.5), while $\boldsymbol{\mathcal{U}}$ remains a Beltrami flow (2.4) at all times.

https://doi.org/10.1017/jfm.2026.11537 Published online by Cambridge University Press

We obtain the time-dependent Beltrami flow $\boldsymbol{\mathcal{U}}(\boldsymbol{x}, t)$ from a Beltrami flow in the initial reference configuration $\boldsymbol{\mathcal{U}}_0(\boldsymbol{x})$ that is frozen in $\boldsymbol{v}_b(\boldsymbol{x}, t)$ in the following way. Let the flow map of the advecting velocity $\boldsymbol{v}_b(\boldsymbol{x}, t)$ be $\boldsymbol{r}_v(\boldsymbol{x}_0, t)$ and its inverse be $\boldsymbol{R}_v(\boldsymbol{x}, t)$. Then, the velocity in the material and spatial descriptions are respectively

$$\tilde{\boldsymbol{v}}_b(\boldsymbol{x}_0, t) \equiv \frac{\partial \boldsymbol{r}_v}{\partial t}(\boldsymbol{x}_0, t) \quad \text{and} \quad \boldsymbol{v}_b(\boldsymbol{x}, t) = \tilde{\boldsymbol{v}}_b(\boldsymbol{R}_v(\boldsymbol{x}, t), t). \tag{2.8a,b}$$

Introducing the deformation gradient of the advecting flow in the material and spatial descriptions as

$$\tilde{\mathsf{F}}_v(\boldsymbol{x}_0, t) \equiv \frac{\partial \boldsymbol{r}_v}{\partial \boldsymbol{x}_0}(\boldsymbol{x}_0, t) \quad \text{and} \quad \mathsf{F}_v(\boldsymbol{x}, t) = \tilde{\mathsf{F}}_v(\boldsymbol{R}_v(\boldsymbol{x}, t), t), \tag{2.9a,b}$$

the solution to (2.5) is the Cauchy formula

$$k(t)\boldsymbol{\mathcal{U}}_v(\boldsymbol{x}, t) = \frac{1}{J_v(\boldsymbol{x}, t)}\mathsf{F}_v(\boldsymbol{x}, t)\,(k_0\boldsymbol{\mathcal{U}}_0(\boldsymbol{R}_v(\boldsymbol{x}, t)))\,, \tag{2.10}$$

where the subscript v in $\boldsymbol{\mathcal{U}}_v$ is introduced to remind of its dependence with the advecting velocity $\boldsymbol{v}_b(\boldsymbol{x}, t)$. The vector $\boldsymbol{\mathcal{U}}_0(\boldsymbol{R}_v(\boldsymbol{x}, t))$ in (2.10) is the value of $\boldsymbol{\mathcal{U}}_0$ of the material particle, or spatial point in the reference configuration, which has been (parallel) advected to the point $(\boldsymbol{x}, t)$ by the advecting velocity $\boldsymbol{v}_b(\boldsymbol{x}, t)$. The term F_v/J_v rotates, stretches and compresses the vector $k_0\boldsymbol{\mathcal{U}}_0(\boldsymbol{R}_v(\boldsymbol{x}, t))$ in such a way that the final result $k(t)\boldsymbol{\mathcal{U}}_v(\boldsymbol{x}, t)$ in (2.10) represents the (frozen) advection of $k_0\boldsymbol{\mathcal{U}}_0$ by the advecting flow $\boldsymbol{v}_b(\boldsymbol{x}, t)$.

Since $\boldsymbol{\mathcal{U}}_v(\boldsymbol{x}, t)$ in (2.10) must remain a Beltrami flow at all times while it is (frozen) advected by $\boldsymbol{v}_b(\boldsymbol{x}, t)$, the motion problem is to find the properties of the advecting velocity $\boldsymbol{v}_b(\boldsymbol{x}, t)$ which transform a Beltrami flow into a Beltrami flow, that is, that leaves the Beltrami condition invariant.

To find these conditions, let $\boldsymbol{\mathcal{U}}_0(\boldsymbol{x}_0)$ be a Beltrami flow and consider the kinematic identity applied to (2.10) for the transformation of the curl,

$$\nabla_{\boldsymbol{x}} \times (\mathsf{F}_v(t)\boldsymbol{\mathcal{U}}_0(\boldsymbol{R}_v(\boldsymbol{x}, t))) = \frac{1}{J_v(t)}\mathsf{F}_v(t)\,\left(\nabla_{\boldsymbol{x}_0} \times \boldsymbol{\mathcal{U}}_0(\boldsymbol{x}_0))(\boldsymbol{R}_v(\boldsymbol{x}, t)\right). \tag{2.11}$$

If the homogeneous time-dependent deformation gradient is an isotropic stretch plus a rotation $\mathsf{F}_v = \lambda(t)\mathsf{Q}(t)$, $\mathsf{Q}(t) \in SO(3)$, thus $J(t) = \lambda(t)^3$, and the requirement that $\nabla \times \boldsymbol{\mathcal{U}} = -k(t)\boldsymbol{\mathcal{U}}$ forces $k(t) = k_0/\lambda(t)$, and therefore,

$$J_v(t) = \left(\frac{k_0}{k(t)}\right)^3, \quad \text{with} \quad J_v(0) = 1, \tag{2.12}$$

and the curl of (2.10), divided by $k(t)$, becomes

$$\nabla \times \boldsymbol{\mathcal{U}}_v(\boldsymbol{x}, t) = -k(t)\mathsf{F}_v(t)\boldsymbol{\mathcal{U}}_0(\boldsymbol{R}_v(\boldsymbol{x}, t)) = -k(t)\boldsymbol{\mathcal{U}}_v(\boldsymbol{x}, t). \tag{2.13}$$

In other words, since under a Piola transformation the velocity $\boldsymbol{\mathcal{U}}$ transforms as $\boldsymbol{\mathcal{U}} = \mathsf{F}^{-\top}\boldsymbol{\mathcal{U}}_0$ and the vorticity $\boldsymbol{\mathcal{W}}$ as $\boldsymbol{\mathcal{W}} = J^{-1}\mathsf{F}\boldsymbol{\mathcal{W}}_0$, the Beltrami condition $\boldsymbol{\mathcal{W}} = -k(t)\boldsymbol{\mathcal{U}}$ is preserved if $\mathsf{F}(t)^\top\mathsf{F}(t) = J(t)(k(t)/k_0)\mathsf{I}$. Using the polar decomposition $\mathsf{F}(t) = \mathsf{R}(t)\mathsf{U}(t)$ of the deformation gradient $\mathsf{F}(t)$ into a rotation $\mathsf{R}(t)$ and a positive-definite symmetric right stretch tensor $\mathsf{U}(t)$, the right Cauchy–Green deformation tensor is $\mathsf{C}(t) \equiv \mathsf{F}^\top(t)\mathsf{F}(t) = \mathsf{U}(t)^2$. Therefore, the right stretch tensor

$$\mathsf{U}^2(t) = J(t)\frac{k(t)}{k_0}\mathsf{I}, \tag{2.14}$$

https://doi.org/10.1017/jfm.2026.11537 Published online by Cambridge University Press

and since U is symmetric positive-definite, we have $\mathsf{U}(t)=\lambda(t)\mathsf{I}$ for some scalar function $\lambda(t)>0$. Since $J=\det\mathsf{F}=\det\mathsf{U}=\lambda^3$, the deformation gradient must be $\mathsf{F}(t)=(k_0/k(t))\mathsf{R}(t)$, that is, the deformation gradient is an isotropic stretch and a rotation.

Therefore, $\boldsymbol{\mathcal{U}}(\boldsymbol{x},t)$ remains a Beltrami flow if is initially a Beltrami flow $\boldsymbol{\mathcal{U}}(\boldsymbol{x},0)=\boldsymbol{\mathcal{U}}_0(\boldsymbol{x})$, with initial wavenumber $k_0\equiv k(0)$, and the deformation gradient of the background flow is an isotropic stretch and a rotation. This result is independent of the particular geometry of the Beltrami flow $\boldsymbol{\mathcal{U}}_0(\boldsymbol{x})$. In the more general case in which the deformation gradient F_v is required only to be only time-dependent $\mathsf{F}_v=\mathsf{F}_v(t)$, so it may include a time-dependent deviatoric strain $\mathsf{D}_0(t)$, the Beltrami property (2.13) does not follow from (2.10) for every steady Beltrami flow $\boldsymbol{\mathcal{U}}_0(\boldsymbol{x})$. Plane Beltrami flows, however, may satisfy (2.13), as is explained in more detail in § 5. We henceforth assume the more general condition for $\mathsf{F}_v(t)$ and consider an advecting velocity field $\boldsymbol{v}_b(\boldsymbol{x},t)$ having a linear dependence on $\boldsymbol{x}$ such that its deformation gradient is only time-dependent $\mathsf{F}_v=\mathsf{F}_v(t)$.

To obtain the permissible initial Beltrami flows in many different geometries, say Cartesian plane waves, spherical, cylindrical, ellipsoidal, etc., we follow the steady Chandrasekhar–Kendall approach (Morse & Feshbach 1953; Chandrasekhar & Kendall 1957; Chandrasekhar & Woltjer 1958; Woltjer 1958*a*,*b*) which, from a scalar Laplacian eigenfunction $\eta_0(\boldsymbol{x})$,

$$\nabla^2\eta_0=-k_0^2\eta_0, \tag{2.15}$$

and a constant unit vector $\hat{\boldsymbol{n}}_0$, obtains a Beltrami flow, say $\boldsymbol{\mathcal{U}}_\eta(\boldsymbol{x})$, as

$$\boldsymbol{\mathcal{U}}_\eta(\boldsymbol{x})\equiv\boldsymbol{\nabla}\times\left(\eta_0\hat{\boldsymbol{n}}_0-k_0^{-1}\boldsymbol{\nabla}\times(\eta_0\hat{\boldsymbol{n}}_0)\right),\quad\text{such that}\quad\boldsymbol{\nabla}\times\boldsymbol{\mathcal{U}}_\eta=-k_0\boldsymbol{\mathcal{U}}_\eta. \tag{2.16a,b}$$

Using this Beltrami flow $\boldsymbol{\mathcal{U}}_\eta(\boldsymbol{x})$, associated with the scalar Laplacian eigenfunction $\eta_0(\boldsymbol{x})$ we may write, in the case of background isotropic stretch and rotation, as it is shown in § 4, the Beltrami solution as

$$\boldsymbol{\mathcal{U}}(\boldsymbol{x},t)=\boldsymbol{\mathcal{U}}_{\eta v}(\boldsymbol{x},t)=\mathsf{F}_v(t)\boldsymbol{\mathcal{U}}_\eta(\boldsymbol{R}_v(\boldsymbol{x},t)), \tag{2.17}$$

where the notation $\boldsymbol{\mathcal{U}}_{\eta v}(\boldsymbol{x},t)$ makes explicit that the particular Beltrami solution $\boldsymbol{\mathcal{U}}(\boldsymbol{x},t)$ depends on the Laplacian eigenfunction $\eta_0(\boldsymbol{x})$ and on the advecting flow $\boldsymbol{v}_b(\boldsymbol{x},t)$ or, alternatively, on the background flow $\boldsymbol{u}_b(\boldsymbol{x},t)$). Equation (2.17) states that the Beltrami field is advected isochorically by the non-isochoric flow $\boldsymbol{v}_b(\boldsymbol{x},t)$.

In addition to the Beltrami condition for $\boldsymbol{\mathcal{U}}(\boldsymbol{x},t)$, the background flow $\boldsymbol{u}_b(\boldsymbol{x},t)$ must satisfy the vorticity equation and this requirement imposes a constraint to the time-dependent background velocity gradient tensor $\mathsf{L}(t)\equiv\boldsymbol{\nabla}\boldsymbol{u}_b(t)$, which is considered in the next section. Independently of this constraint, the background flow has uniform vorticity $\boldsymbol{\omega}_b(t)=(\boldsymbol{\nabla}\times\boldsymbol{u}_b)(t)$ and, therefore, we may introduce a vector drift velocity $\boldsymbol{c}(t)$ given by

$$\boldsymbol{c}(t)\equiv\frac{\boldsymbol{\nabla}\times\boldsymbol{u}_b(\boldsymbol{x},t)}{k(t)}=\frac{\boldsymbol{\omega}_b(t)}{k(t)}=\frac{2\boldsymbol{v}(t)}{k(t)}, \tag{2.18}$$

where $\boldsymbol{v}(t)\equiv\boldsymbol{\omega}_b(t)/2$ is the angular velocity of the background flow $\boldsymbol{u}_b$. Thus, the advecting velocity

$$\boldsymbol{v}_b(\boldsymbol{x},t)=\boldsymbol{u}_b(\boldsymbol{x},t)+\boldsymbol{c}(t) \tag{2.19}$$

differs from the background velocity $\boldsymbol{u}_b(\boldsymbol{x},t)$ by the time-dependent drift $\boldsymbol{c}(t)$.

The subtle difference between the background velocity $\boldsymbol{u}_b$ and the advecting velocity $\boldsymbol{v}_b$ has far-reaching physical consequences. For example, if the background flow $\boldsymbol{u}_b$ is reduced to a steady solid body rotation with constant angular velocity $\boldsymbol{v}_0$, that is, $\boldsymbol{u}_b(\boldsymbol{x})=\boldsymbol{v}_0\times\boldsymbol{x}$, then the background deformation gradient $\mathsf{F}_v(t)=\mathsf{R}_{\hat{\boldsymbol{v}}_0}(v_0t)$ is a constant-rate rotation around the angle defined by the unit vector $\hat{\boldsymbol{v}}_0\equiv\boldsymbol{v}_0/\|\boldsymbol{v}_0\|$. If this external

https://doi.org/10.1017/jfm.2026.11537 Published online by Cambridge University Press

flow $\boldsymbol{u}_b$ is interpreted as generated by an external measuring device acting on a Beltrami field $\boldsymbol{\mathcal{U}}_0(\boldsymbol{x})$, the presence of this external flow $\boldsymbol{u}_b$ not only causes the Beltrami field $\boldsymbol{\mathcal{U}}(\boldsymbol{x}, t)$ to precess, due to the $\boldsymbol{u}_b$ component on the advecting velocity $\boldsymbol{v}_b$ in (2.19), but also to displace with the drift velocity $2\boldsymbol{v}_0/k_0$ present in $\boldsymbol{R}_v(\boldsymbol{x}, t)$ in (2.17). This displacement velocity $\boldsymbol{c}_0 = 2\boldsymbol{v}_0/k_0$, which depends on the amplitude and direction of the background field $\boldsymbol{v}_0$ and on the Beltrami wavenumber k_0, is an interaction term between the Beltrami field and the measuring field, and therefore, can be used as a measure of the Beltrami field wavenumber k_0. In this case, correlations between measures i in an ensemble ($i = 1, \cdots, N$) using different apparatus configurations $\boldsymbol{v}[i]$, of two Beltrami fields, say $\boldsymbol{\mathcal{U}}_a(\boldsymbol{x}, t; k_a)$ and $\boldsymbol{\mathcal{U}}_b(\boldsymbol{x}, t; k_b)$, must depend on the correlation between $\boldsymbol{c}_a[i] \equiv 2\boldsymbol{v}_a[i]/k_a[i]$ and $\boldsymbol{c}_b[i] \equiv 2\boldsymbol{v}_b[i]/k_b[i]$. This property, which is independent of the particular geometry of the Beltrami field, has been used, with spherical Beltrami fields (Viúdez 2025), to suggest a classical fluid mechanics explanation of the correlation experimentally found in quantum particle entanglement experiments. We see here that this drift velocity is a general property of Beltrami fields independent of their particular geometry.

Once a permissible time-dependent, with homogeneous velocity gradient $\mathsf{L}(t)$, background flow $\boldsymbol{u}_b(\boldsymbol{x}, t)$, or equivalently $\boldsymbol{v}_b(\boldsymbol{x}, t)$, and a particular Laplacian eigenfunction $\eta_0(\boldsymbol{x})$ which specifies the Beltrami flow, are chosen, the resulting oscillatory motion is given by (2.17). An economical way of visualising the time evolution of the Beltrami motion is from the time-dependent scalar density function $\eta(\boldsymbol{x}, t)$,

$$\eta(\boldsymbol{x}, t) \equiv \left(\frac{k(t)}{k_0}\right)^3 \eta_0(\boldsymbol{R}_v(\boldsymbol{x}, t) - \boldsymbol{o}(0)), \tag{2.20}$$

where $\boldsymbol{o}(0)$ is the value at the initial time $t = 0$ of an arbitrary time-dependent vector $\boldsymbol{o}(t)$. The scalar function $\eta(\boldsymbol{x}, t)$ (2.20) is, by construction, frozen in the advecting flow $\boldsymbol{v}_b(\boldsymbol{x}, t)$,

$$\frac{\partial \eta}{\partial t} + \boldsymbol{v}_b \cdot \boldsymbol{\nabla}\eta + \eta \boldsymbol{\nabla} \cdot \boldsymbol{v}_b = 0. \tag{2.21}$$

The Beltrami field $\boldsymbol{\mathcal{U}}(\boldsymbol{x}, t)$ can be obtained at any time t from $\eta(\boldsymbol{x}, t)$ given by (2.20).

3. Time-dependent background velocity field $\boldsymbol{u}_b(\boldsymbol{x}, t)$

The purpose of this section is to obtain the conditions that must satisfy the background flow $\boldsymbol{u}_b(\boldsymbol{x}, t)$ to be a solution to the vorticity equation, as well as to obtain the inverse map $\boldsymbol{R}_v(\boldsymbol{x}, t)$. The inverse map $\boldsymbol{R}_v(\boldsymbol{x}, t)$ is required to prescribe the time evolution of the Beltrami field $\boldsymbol{\mathcal{U}}(\boldsymbol{x}, t)$ described in the previous section.

The background velocity field $\boldsymbol{u}_b(\boldsymbol{x}, t)$, with vorticity $\boldsymbol{\omega}_b \equiv \boldsymbol{\nabla} \times \boldsymbol{u}_b$, must satisfy the vorticity equation, that is,

$$\frac{\partial \boldsymbol{\omega}_b}{\partial t} + \boldsymbol{\nabla}\boldsymbol{\omega}_b\, \boldsymbol{u}_b - \boldsymbol{\nabla}\boldsymbol{u}_b\, \boldsymbol{\omega}_b + \boldsymbol{\nabla} \cdot \boldsymbol{u}_b\, \boldsymbol{\omega}_b = \boldsymbol{0}. \tag{3.1}$$

As explained in § 2, the background flow $\boldsymbol{u}_b(\boldsymbol{x}, t)$ must have a homogeneous velocity gradient $\mathsf{L}(t)$ and, consequently, we set

$$\boldsymbol{u}_b(\boldsymbol{x}, t) = \dot{\boldsymbol{o}}(t) + \mathsf{L}(t)(\boldsymbol{x} - \boldsymbol{o}(t)), \tag{3.2}$$

where $\boldsymbol{o}(t)$ is an arbitrary time-dependent vector, interpreted as the origin of the spatial frame, and is included in the term $\mathsf{L}(t)(\boldsymbol{x} - \boldsymbol{o}(t))$ to simplify the mathematical expressions. The origin of the spatial frame $\boldsymbol{o}(t)$ as a free parameter allows us to assign the drift velocity $\boldsymbol{c}(t)$ entirely to the advecting flow $\boldsymbol{v}_b(\boldsymbol{x}, t)$ setting $\dot{\boldsymbol{o}}(t) \mapsto \boldsymbol{0}$, or entirely to the background

https://doi.org/10.1017/jfm.2026.11537 Published online by Cambridge University Press

flow $\boldsymbol{u}_b(\boldsymbol{x}, t)$ setting $\dot{\boldsymbol{o}}(t) \mapsto -\boldsymbol{c}(t)$. In the advecting flow, the origin $\boldsymbol{o}_v(t)$ of the frame respect to which fluid particle positions are referenced is given by

$$\boldsymbol{o}_v(t) \equiv \boldsymbol{o}(t) + \mathsf{F}(t) \int_0^t \mathsf{F}^{-1}(\tau)\, \boldsymbol{c}(\tau)\, \mathrm{d}\tau, \quad \boldsymbol{o}_v(0) = \boldsymbol{o}(0). \tag{3.3}$$

Thus, we may write

$$\boldsymbol{R}_v(\boldsymbol{x}, t) - \boldsymbol{o}(0) = \mathsf{F}^{-1}(t)\, (\boldsymbol{x} - \boldsymbol{o}_v(t)) \equiv \boldsymbol{z}_v(\boldsymbol{x}, t), \tag{3.4}$$

which serves as a definition of the material variable $\boldsymbol{z}_v(\boldsymbol{x}, t)$. Thus, the time-dependence of the Beltrami field $\boldsymbol{\mathcal{U}}_\eta(\boldsymbol{x}, t)$ is fully described by the scalar field

$$\eta(\boldsymbol{x}, t) \equiv \frac{1}{J(t)} \eta_0(\boldsymbol{R}_v(\boldsymbol{x}, t) - \boldsymbol{o}(0)) = \frac{1}{J(t)} \eta_0(\boldsymbol{z}_v(\boldsymbol{x}, t)), \tag{3.5}$$

through the advection as a density of the Laplacian eigenfunction $\eta_0(\boldsymbol{x}_0)$ by the advecting velocity $\boldsymbol{v}_b(\boldsymbol{x}, t)$.

Since the drift velocity $\boldsymbol{c}(t)$ only depends on time, the background velocity gradient $\mathsf{L}(t)$ is the same for both background $\boldsymbol{u}_b$ and advecting $\boldsymbol{v}_b$ velocity fields,

$$\mathsf{L}(t) = \mathsf{L}_u(t) \equiv \boldsymbol{\nabla} \boldsymbol{u}_b = \mathsf{L}_v(t) \equiv \boldsymbol{\nabla} \boldsymbol{v}_b. \tag{3.6}$$

To facilitate the analysis, it is useful to separate the background velocity gradient $\mathsf{L}(t)$ into its symmetric strain tensor $\mathsf{D}(t)$ and skew-symmetric spin tensor $\mathsf{W}(t)$ components, and then express the strain $\mathsf{D}(t)$ as the sum of the deviatoric traceless strain tensor $\mathsf{D}_0(t)$ and the volumetric strain $(1/3)\mathrm{tr}(\mathsf{D}(t))\mathsf{I}$. That is, when acting on an arbitrary vector $\boldsymbol{e}$,

$$\mathsf{L}(t)\boldsymbol{e} = (\mathsf{D}(t) + \mathsf{W}(t))\, \boldsymbol{e} = \left(\mathsf{D}_0(t) + \frac{1}{3}\delta(t)\mathsf{I}\right) \boldsymbol{e} + \boldsymbol{v}(t) \times \boldsymbol{e}, \tag{3.7}$$

where the divergence $\delta(t)$, deviatoric strain $\mathsf{D}_0(t)$ and angular velocity $\boldsymbol{v}(t)$ are

$$\delta(t) \equiv \boldsymbol{\nabla} \cdot \boldsymbol{u}_b = \mathrm{tr}(\mathsf{D}(t)), \quad \mathsf{D}_0(t) \equiv \mathsf{D}(t) - \frac{1}{3}\mathrm{tr}(\mathsf{D}(t))\mathsf{I}, \quad \boldsymbol{v}(t) \equiv \frac{1}{2}\boldsymbol{\omega}_b(t), \tag{3.8a,b,c}$$

where the angular velocity $\boldsymbol{v}(t)$ is the axial vector of the spin tensor $\mathsf{W}(t)$,

$$\mathsf{W}(t)\boldsymbol{e} = [\boldsymbol{v}(t)\times]\boldsymbol{e} = \boldsymbol{v}(t) \times \boldsymbol{e}. \tag{3.9}$$

Since the relation between the background velocity $\boldsymbol{u}_b(\boldsymbol{x}, t)$ and the advecting velocity $\boldsymbol{v}_b(\boldsymbol{x}, t)$ is a time-dependent drift,

$$\boldsymbol{v}_b(\boldsymbol{x}, t) \equiv \boldsymbol{u}_b + \frac{\boldsymbol{\nabla} \times \boldsymbol{u}_b}{k(t)} = \boldsymbol{u}_b(\boldsymbol{x}, t) + \frac{2\boldsymbol{v}(t)}{k(t)} \tag{3.10}$$

if $\boldsymbol{u}_b(\boldsymbol{x}, t)$ is a flow solution to the vorticity equation, then $\boldsymbol{v}_b(\boldsymbol{x}, t)$ is also a flow solution.

From the vorticity equation for the background flow (3.1), the background velocity (3.2) and the background velocity gradient (3.7), we obtain the compatibility condition for the background flow,

$$\dot{\boldsymbol{v}}(t) = \left(\mathsf{D}_0(t) - \frac{2}{3}\delta(t)\mathsf{I}\right) \boldsymbol{v}(t), \tag{3.11}$$

which prescribes a constraint between the time rate of change of the angular velocity $\dot{\boldsymbol{v}}(t)$ and the actual values of deviatoric and volumetric strains acting on the angular velocity $\boldsymbol{v}(t)$. Clearly, fluid expansion/contraction described by the background divergence $\delta(t)$ is associated with changes in the magnitude $v(t)$ of the angular velocity $\boldsymbol{v}(t) = v(t)\hat{\boldsymbol{v}}(t)$, and not with changes in its direction $\hat{\boldsymbol{v}}(t)$.

https://doi.org/10.1017/jfm.2026.11537 Published online by Cambridge University Press

It is necessary to time-integrate (3.11) to find $\boldsymbol{v}(t)$ and hence obtain the permissible advecting velocity $\boldsymbol{v}_b(\boldsymbol{x}, t)$ from which to derive the inverse map $\boldsymbol{R}_v(\boldsymbol{x}, t)$. With this objective, it is useful to factorise the right-hand side of the compatibility condition (3.11) introducing the time integral $\Delta(t)$ of the divergence,

$$\Delta(t) \equiv \int_0^t \delta(\tau)\, \mathrm{d}\tau, \tag{3.12}$$

in such a way that the compressibility effects on the time-rate of change of $\boldsymbol{v}(t)$ are solved explicitly,

$$\boldsymbol{v}(t) = \mathrm{e}^{-\frac{2}{3}\Delta(t)} \boldsymbol{v}_D(t), \tag{3.13}$$

where

$$\dot{\boldsymbol{v}}_D(t) = \mathsf{D}_0(t)\boldsymbol{v}_D(t), \quad \text{with} \quad \boldsymbol{v}_D(0) = \boldsymbol{v}(0). \tag{3.14a,b}$$

The vector $\boldsymbol{v}_D(t)$ is the background angular velocity that is related to the background deviatoric strain tensor and is not affected by the fluid expansion/compression. It remains to solve the more complicated (3.14), which explains how time changes on both amplitude and direction of the angular velocity $\boldsymbol{v}_D(t)$ are related to the actual values of the deviatoric strain tensor $\mathsf{D}_0(t)$. The general solution to (3.14) is

$$\boldsymbol{v}_D(t) = \mathrm{OE}[\mathsf{D}_0](t)\boldsymbol{v}_0 = \mathcal{T}\exp\left(\int_0^t \mathsf{D}_0(\tau)\, \mathrm{d}\tau\right)\boldsymbol{v}_0, \tag{3.15}$$

where $\mathcal{T}$ is the time-ordered exponential $\mathrm{OE}[a](t)$, which is the unique solution of the differential equation of initial value

$$\frac{d}{\mathrm{d}t}\mathrm{OE}[a](t) = a(t)\mathrm{OE}[a](t), \quad \text{with} \quad \mathrm{OE}[a](0) = 1. \tag{3.16a,b}$$

For non-commuting $\mathsf{D}_0(t)$, the fundamental matrix $\mathsf{U}_0(t, t_0)$ in $\boldsymbol{v}_D(t) = \mathsf{U}_0(t, t_0)\boldsymbol{v}_0$ is given by the time-ordered exponential (equivalently its Dyson-series expansion) in (3.15). The close analogy with the quantum evolution operator in time-dependent Schrödinger/quantum field theory dynamics is described in Appendix B.

The factorisation (3.13) suggests that it is convenient to factorise the background deformation gradient $\mathsf{F}(t)$ as

$$\mathsf{F}(t) = \mathrm{e}^{\Delta(t)/3}\boldsymbol{\mathcal{F}}(t), \tag{3.17}$$

where the gradient deformation tensor $\boldsymbol{\mathcal{F}}(t)$ carries the isochoric deformation and rotation. Defining the isochoric velocity gradient $\boldsymbol{\mathcal{L}}(t)$ as

$$\boldsymbol{\mathcal{L}}(t) \equiv \mathsf{D}_0(t) + \mathsf{W}(t) = \mathsf{L}(t) - \frac{1}{3}\delta(t)\mathsf{I}, \tag{3.18}$$

we see that $\boldsymbol{\mathcal{F}}(t)$ satisfies an equation analogous to the kinematic identity, $\dot{\mathsf{F}} = \mathsf{LF}$, that is,

$$\dot{\boldsymbol{\mathcal{F}}}(t) = \boldsymbol{\mathcal{L}}(t)\boldsymbol{\mathcal{F}}(t). \tag{3.19}$$

The solution to (3.19) is again the time-ordered exponential

$$\boldsymbol{\mathcal{F}}(t) = \mathrm{OE}[\boldsymbol{\mathcal{L}}](t) = \mathcal{T}\exp\left(\int_0^t \boldsymbol{\mathcal{L}}(\tau)\, \mathrm{d}\tau\right), \quad \text{with} \quad \boldsymbol{\mathcal{F}}(0) = \mathsf{I}, \tag{3.20a,b}$$

which provides the flow map $\boldsymbol{r}_v(\boldsymbol{x}_0, t)$ of the advecting flow, $\boldsymbol{v}_b(\boldsymbol{x}, t)$,

$$\boldsymbol{r}_v(\boldsymbol{x}_0, t) = \boldsymbol{o}_v(t) + \mathrm{e}^{\Delta(t)/3}\boldsymbol{\mathcal{F}}(t)(\boldsymbol{x}_0 - \boldsymbol{o}(0)), \tag{3.21}$$

https://doi.org/10.1017/jfm.2026.11537 Published online by Cambridge University Press

and hence, the inverse map

$$\boldsymbol{R}_v(\boldsymbol{x}, t) = \boldsymbol{o}(0) + \mathrm{e}^{-\Delta(t)/3}\boldsymbol{\mathcal{F}}^{-1}(t)(\boldsymbol{x} - \boldsymbol{o}_v(t)). \tag{3.22}$$

The Jacobian $J(t)$ of the advecting flow map $\boldsymbol{r}_v(\boldsymbol{x}, t)$, which is equal to the Jacobian of the background flow map $\boldsymbol{r}_u(\boldsymbol{x}, t)$, is

$$J(t) = J_v(t) = J_u(t) = \det(\mathsf{F}(t)) = \mathrm{e}^{\Delta(t)}, \tag{3.23}$$

and its rate of change,

$$\frac{\dot{J}(t)}{J(t)} = \dot{\Delta}(t) = \delta(t) = \boldsymbol{\nabla} \cdot \boldsymbol{u}, \tag{3.24}$$

expresses the rate of change of volume in the background flow. The advecting velocity $\boldsymbol{v}_b$ in the material description is

$$\begin{aligned}
&\tilde{\boldsymbol{v}}_b(\boldsymbol{x}_0, t) \equiv \frac{\partial \boldsymbol{r}_v}{\partial t}(\boldsymbol{x}_0, t) = \boldsymbol{v}_b(\boldsymbol{r}_v(\boldsymbol{x}_0, t), t) \\
&= \dot{\boldsymbol{o}}_v(t) + \mathsf{L}(t)\mathsf{F}(t)(\boldsymbol{x}_0 - \boldsymbol{o}(0)) = \dot{\boldsymbol{o}}_v(t) + \mathsf{L}(t)(\boldsymbol{r}_v(\boldsymbol{x}_0, t) - \boldsymbol{o}_v(t)) \\
&= \dot{\boldsymbol{o}}_v(t) + \frac{1}{3}\delta(t)(\boldsymbol{r}_v(\boldsymbol{x}_0, t) - \boldsymbol{o}_v(t)) \\
&\quad + \mathsf{D}_0(t)(\boldsymbol{r}_v(\boldsymbol{x}_0, t) - \boldsymbol{o}_v(t)) + \boldsymbol{v}(t) \times (\boldsymbol{r}_v(\boldsymbol{x}_0, t) - \boldsymbol{o}_v(t)) \,,
\end{aligned} \tag{3.25}$$

which shows in the material description four contributing terms: homogeneous displacement, isotropic expansion/contraction, isochoric stretching and rotation. The background velocity $\boldsymbol{u}_b$ in the material description becomes identical to $\boldsymbol{v}_b$ once the origin $\boldsymbol{o}_v(t)$ is replaced with $\boldsymbol{o}(t)$,

$$\begin{aligned}
&\tilde{\boldsymbol{u}}_b(\boldsymbol{x}_0, t) \equiv \frac{\partial \boldsymbol{r}_u}{\partial t}(\boldsymbol{x}_0, t) = \boldsymbol{u}_b(\boldsymbol{r}_u(\boldsymbol{x}_0, t), t) \\
&= \boldsymbol{v}_b(\boldsymbol{r}_v(\boldsymbol{x}_0, t), t) - \frac{2\boldsymbol{v}(t)}{k_0} \\
&= \dot{\boldsymbol{o}}(t) + \frac{1}{3}\delta(t)(\boldsymbol{r}_u(\boldsymbol{x}_0, t) - \boldsymbol{o}(t)) \\
&\quad + \mathsf{D}_0(t)(\boldsymbol{r}_u(\boldsymbol{x}_0, t) - \boldsymbol{o}(t)) + \boldsymbol{v}(t) \times (\boldsymbol{r}_u(\boldsymbol{x}_0, t) - \boldsymbol{o}(t)) \,.
\end{aligned} \tag{3.26}$$

Since the background vorticity is spatially uniform, the background vorticity in the spatial and material descriptions coincide $\tilde{\boldsymbol{\omega}}_b(\boldsymbol{x}_0, t) = \boldsymbol{\omega}_b(t) = 2\boldsymbol{v}(t)$, and the Cauchy vorticity formula for the background flow $\boldsymbol{u}_b$ is

$$\boldsymbol{v}(t) = \frac{1}{J(t)}\mathsf{F}(t)\boldsymbol{v}_0, \tag{3.27}$$

whose time derivative leads, using $\dot{\mathsf{F}} = \mathsf{L}\mathsf{F}$, to the compatibility condition for the background flow (3.11).

In summary, since there are six time-dependent degrees of freedom in the way the velocity field, the velocity gradient of the background flow $\mathsf{L}(t)$ is defined, one needs to specify six time-dependent functions to obtain a compatible velocity gradient $\mathsf{L}(t)$. For example, one may specify five components of $\mathsf{D}_0(t)$ and $\delta(t)$, and then solving for $\boldsymbol{v}_D(t)$ using (3.15). With $\mathsf{D}_0(t)$, $\delta(t)$ and $\boldsymbol{v}_D(t)$ available, one may obtain $\boldsymbol{\mathcal{L}}(t)$ using (3.18) and then solve (3.20*a*) to obtain $\boldsymbol{\mathcal{F}}(t)$, and finally the inverse map $\boldsymbol{R}_v(\boldsymbol{x}, t)$ using (3.22).

https://doi.org/10.1017/jfm.2026.11537 Published online by Cambridge University Press

4. Beltrami field $\mathcal{U}(\boldsymbol{x}, t)$

So far, we have been concerned with the background flow $\boldsymbol{u}_b(\boldsymbol{x}, t)$ with a homogeneous velocity gradient $\mathsf{L}(t)$. In laboratory and field practice, flow diagnostics such as particle image velocimetry (PVI)/laser light sheets, dye or seeded Lagrangian tracers are typically designed to be weakly intrusive, so that at continuum scales the measured velocity may be regarded as unaffected to leading order; nevertheless, any observation ultimately relies on a physical coupling (illumination/scattering, tracer inertia and diffusion, finite-size effects) and it is useful in some contexts to represent such a coupling explicitly as an 'environment' acting on a coherent structure. This viewpoint is particularly natural in a broader programme of modelling spin-like degrees of freedom with coherent spherical vortical excitations, where the 'state' is defined relative to a chosen axis/observer and external couplings can induce precession or drift, as explored, for example, in the precession of spherical spin-1 vortices (Viúdez 2025*c*), in the fluid-mechanical spin-up/spin-down construction associated with Clauser–Horne–Shimony–Holt inequality tests (Viúdez 2025), and in Euler solutions reproducing Dirac-type dynamics using multipolar oscillations in spherical geometry (Viúdez 2025*a*). Accordingly, we use the background-flow superposition framework here as a controlled model of environmental coupling that yields observable drift/deflection of coherent modes, without implying that practical macroscopic measurements generally require, or are well approximated by, a dynamically significant interaction flow.

Thus, some practical applications, in particular, those at quantum scales, require including a second flow entity in such a way that the interaction between both flows becomes relevant. For example, at these very small spatial scales, a steady Beltrami flow $\mathcal{U}_0(\boldsymbol{x})$ in a three-dimensional space cannot be observed in isolation; it becomes measurable only through interaction with another flow. Conversely, a large-scale background flow can be detected through the advection of an extensive structure, such as a Beltrami field. In any case, whether the background flow is used to measure the properties of the vortex, or the vortex is used to measure the properties of the background flow, two flow entities are required and what is measured is the interaction between them.

In the set-up explained in the previous sections, the time evolution of the Beltrami flow $\mathcal{U}(\boldsymbol{x}, t)$ is completely described by (2.17) once an initial Beltrami flow $\mathcal{U}_0(\boldsymbol{x})$ is given. This initial Beltrami flow can be prescribed by a Chandrasekhar–Kendall (CK) procedure, which provides a Beltrami vector field from a scalar Laplacian eigenfunction $\eta_0(\boldsymbol{x})$. The Laplacian eigenvalue of $\eta_0(\boldsymbol{x})$ is $-k_0^2$. Such a procedure is independent of time, but it can be used to provide a time-dependent Beltrami field $\mathcal{U}(\boldsymbol{x}, t)$ from a time-dependent function $\eta_0(\boldsymbol{x}, t)$ as long as the procedure is generalised to time-dependent flows. The purpose of this section is to explain that generalisation.

Let us assume that $\eta_0(\boldsymbol{x}_0)$ is a Laplacian eigenfunction with eigenvalue $-k_0^2$. The frozen-in condition of the density $\eta_0(\boldsymbol{x})$ in the advecting flow $\boldsymbol{v}_b(\boldsymbol{x}, t)$ is

$$\eta(\boldsymbol{x}, t) = \frac{1}{J(t)}\eta_0(\boldsymbol{z}_v(\boldsymbol{x}, t)), \quad \text{where} \quad \boldsymbol{z}_v(\boldsymbol{x}, t) \equiv \boldsymbol{R}_v(\boldsymbol{x}, t) - \boldsymbol{o}(0). \tag{4.1a,b}$$

These relations immediately imply, in the spatial description, that

$$\frac{\partial \eta}{\partial t} + \boldsymbol{v}_b \cdot \nabla \eta + \eta \nabla \cdot \boldsymbol{v}_b = 0. \tag{4.2}$$

The transformation (4.1*a*) does not preserve the Laplacian eigenfunction property, unless $\boldsymbol{z}_v(\boldsymbol{x}, t)$ (4.1*b*) is a similarity, that is, a rigid body rotation and an isotropic expansion (case $\mathsf{D}_0(t) = 0$). A direct application of the CK procedure to time-dependent flows requires $\eta(\boldsymbol{x}, t)$ be a Laplacian eigenfunction at every time t and that $\mathsf{D}_0(t) = 0$ for

https://doi.org/10.1017/jfm.2026.11537 Published online by Cambridge University Press

general Beltrami flows. We assume therefore implicitly that the deviatoric stretch tensor $\mathsf{D}_0(t) = \mathsf{0}$. In this case, we have

$$\frac{1}{J(t)} = \frac{k(t)^3}{k_0^3}, \tag{4.3}$$

and $k(t)$ decays or grows as the inverse cubic root of the volume change induced by the background flow, as expected for a wavenumber carried by an isotropically expanding/compressing medium. The time-independent CK procedure can be recovered by setting $\mathsf{F}(t) = \mathsf{I}$, so that $J(t) = 1$ and $z_v(\boldsymbol{x}, t) = \boldsymbol{x}$. In any case, this time-dependent procedure can be omitted since $\boldsymbol{\mathcal{U}}(\boldsymbol{x}, t)$ can be always obtained more directly from $\eta_0(\boldsymbol{x})$, in a first step computing $\boldsymbol{\mathcal{U}}_\eta(\boldsymbol{x})$ using the standard CK procedure (2.16*a*) and in a second step using (2.17) to obtain $\boldsymbol{\mathcal{U}}(\boldsymbol{x}, t)$.

There are several, but equivalent, ways to define the time-dependent fields, analogous to those in the CK procedure, $\boldsymbol{\chi}(\boldsymbol{x}, t)$, $\boldsymbol{t}(\boldsymbol{x}, t)$, $\boldsymbol{p}(\boldsymbol{x}, t)$, streamfunction $\boldsymbol{\psi}(\boldsymbol{x}, t)$ and $\boldsymbol{\mathcal{U}}(\boldsymbol{x}, t)$. In the following procedure, we define them from their reference initial counterparts $\boldsymbol{\chi}_0(\boldsymbol{x})$, $\boldsymbol{t}_0(\boldsymbol{x})$, $\boldsymbol{p}_0(\boldsymbol{x})$, $\boldsymbol{\psi}_0(\boldsymbol{x})$ and $\boldsymbol{\mathcal{U}}_0(\boldsymbol{x})$, and hence show their relations. The starting point in the CK procedure is to assume that $\eta_0(\boldsymbol{x})$ is a scalar Laplacian eigenfunction,

$$\nabla^2 \eta_0(\boldsymbol{x}) = -k_0^2 \eta_0(\boldsymbol{x}). \tag{4.4}$$

The steady vector function $\boldsymbol{\chi}_0(\boldsymbol{x})$ is defined from the scalar Laplacian eigenfunction $\eta_0(\boldsymbol{x})$ as

$$\boldsymbol{\chi}_0(\boldsymbol{x}) \equiv \eta_0(\boldsymbol{x})\, \hat{\boldsymbol{n}}_0, \tag{4.5}$$

where $\hat{\boldsymbol{n}}_0$ is a constant unit vector that defines the direction of the Beltrami field, and from (4.5), or (4.1*a*), we define its generalisation by a Piola push-forward transformation

$$\frac{k(t)}{k_0}\boldsymbol{\chi}(\boldsymbol{x}, t) \equiv \frac{1}{J(t)}\mathsf{F}(t)\boldsymbol{\chi}_0(z_v(\boldsymbol{x}, t)) = \eta(\boldsymbol{x}, t)\mathsf{F}(t)\hat{\boldsymbol{n}}_0 = \eta(\boldsymbol{x}, t)\boldsymbol{n}(t), \tag{4.6}$$

where the time-dependent vector $\boldsymbol{n}(t)$ satisfies

$$\boldsymbol{n}(t) \equiv \mathsf{F}(t)\hat{\boldsymbol{n}}_0 \quad \text{and} \quad \dot{\boldsymbol{n}}(t) = \mathsf{L}(t)\boldsymbol{n}(t). \tag{4.7a,b}$$

The next step in the Chandrasekhar–Kendall procedure is to define from (4.5) the velocity potential $\boldsymbol{\psi}_0(\boldsymbol{x})$ as

$$\boldsymbol{\psi}_0(\boldsymbol{x}) \equiv \boldsymbol{\chi}_0(\boldsymbol{x}) - \frac{\nabla \times \boldsymbol{\chi}_0(\boldsymbol{x})}{k_0}, \tag{4.8}$$

or, alternatively, the divergence-free functions $\boldsymbol{t}_0(\boldsymbol{x})$ and $\boldsymbol{p}_0(\boldsymbol{x})$ as

$$\boldsymbol{t}_0(\boldsymbol{x}) \equiv \nabla \times \boldsymbol{\chi}_0(\boldsymbol{x}) \quad \text{and} \quad \boldsymbol{p}_0(\boldsymbol{x}) \equiv \frac{1}{k_0}\nabla \times \boldsymbol{t}_0(\boldsymbol{x}), \tag{4.9a,b}$$

which are commonly referred to as the toroidal ($\boldsymbol{t}_0$) and poloidal ($\boldsymbol{p}_0$) components. The relation between the poloidal component and the Gauss potential is described in Appendix C. By construction, the fields $\boldsymbol{t}_0$ and $\boldsymbol{p}_0$ are vector Laplacian eigenfunctions,

$$\nabla^2 \boldsymbol{t}_0 = -k_0^2 \boldsymbol{t}_0 \quad \text{and} \quad \nabla^2 \boldsymbol{p}_0 = -k_0^2 \boldsymbol{p}_0, \tag{4.10a,b}$$

and satisfy

$$\nabla \times \boldsymbol{t}_0 = k_0 \boldsymbol{p}_0 \quad \text{and} \quad \nabla \times \boldsymbol{p}_0 = k_0 \boldsymbol{t}_0. \tag{4.11a,b}$$

Thus, $\boldsymbol{t}_0(\boldsymbol{x})$ and $\boldsymbol{p}_0(\boldsymbol{x})$ are not Beltrami functions, but their helical combinations $\boldsymbol{\mathcal{U}}_\pm(\boldsymbol{x}) \equiv \boldsymbol{t}_0(\boldsymbol{x}) \pm \boldsymbol{p}_0(\boldsymbol{x})$ are the positive-helicity and negative-helicity Beltrami modes.

https://doi.org/10.1017/jfm.2026.11537 Published online by Cambridge University Press

We therefore define the Beltrami velocity $\boldsymbol{\mathcal{U}}_0$ as

$$\boldsymbol{\mathcal{U}}_0(\boldsymbol{x}) \equiv \boldsymbol{\mathcal{U}}_-(\boldsymbol{x}) \equiv \boldsymbol{\nabla} \times \boldsymbol{\psi}_0(\boldsymbol{x}) = \boldsymbol{t}_0(\boldsymbol{x}) - \boldsymbol{p}_0(\boldsymbol{x}), \tag{4.12}$$

where the minus sign option is used to be consistent with the minus sign in the definition of $\boldsymbol{\psi}_0(\boldsymbol{x})$ (4.8). We therefore consider k_0 as a signed wavenumber, the Beltrami eigenvalue being $-k_0$, and the wavenumber magnitude $|k_0|$. The positive sign solution may be recovered from the negative sign solution through the transformation $k_0 \to -k_0$. Otherwise, one may define $k_0 \equiv |k_0| > 0$ and work with both polarised solutions explicitly $\boldsymbol{\mathcal{U}}_\pm(\boldsymbol{x})$ which satisfy $\boldsymbol{\nabla} \times \boldsymbol{\mathcal{U}}_\pm = \pm k_0 \boldsymbol{\mathcal{U}}_\pm$. The velocity $\boldsymbol{\mathcal{U}}_0$ is therefore a Beltrami flow satisfying

$$\boldsymbol{\nabla} \times \boldsymbol{\mathcal{U}}_0 = -k_0 \boldsymbol{\mathcal{U}}_0. \tag{4.13}$$

We recall the curl identity applied to a vector function $\boldsymbol{w}(\boldsymbol{z})$ and a vector mapping $\boldsymbol{z}(\boldsymbol{x}, t)$,

$$\boldsymbol{\nabla}_{\boldsymbol{x}} \times \left(\mathsf{F}^{-\top}(t) \boldsymbol{w}(\boldsymbol{z}(\boldsymbol{x}, t)) \right) = \frac{1}{J(t)} \mathsf{F}(t) \left(\boldsymbol{\nabla}_{\boldsymbol{z}} \times \boldsymbol{w} \right) (\boldsymbol{z}(\boldsymbol{x}, t)). \tag{4.14}$$

In the time-dependent procedure, we define the vector potential $\boldsymbol{\psi}(\boldsymbol{x}, t)$ from $\boldsymbol{\psi}_0$ as a pseudovector

$$\frac{k(t)}{k_0} \boldsymbol{\psi}(\boldsymbol{x}, t) \equiv \frac{1}{J(t)} \mathsf{F}(t) \boldsymbol{\psi}_0(\boldsymbol{z}_v(\boldsymbol{x}, t)), \tag{4.15}$$

and the time-dependent $\boldsymbol{t}(\boldsymbol{x}, t)$ and $\boldsymbol{p}(\boldsymbol{x}, t)$ counterparts to $\boldsymbol{t}_0(t)$ and $\boldsymbol{p}_0(t)$ as

$$\frac{k(t)}{k_0} \boldsymbol{t}(\boldsymbol{x}, t) \equiv \frac{\mathsf{F}(t)}{J(t)} \boldsymbol{t}_0(\boldsymbol{z}_v(\boldsymbol{x}, t)), \quad \frac{k(t)}{k_0} \boldsymbol{p}(\boldsymbol{x}, t) \equiv \frac{\mathsf{F}(t)}{J(t)} \boldsymbol{p}_0(\boldsymbol{z}_v(\boldsymbol{x}, t)), \tag{4.16a,b}$$

which satisfy similar relations to (4.9),

$$\boldsymbol{t}(\boldsymbol{x}, t) = \frac{1}{k(t)} \boldsymbol{\nabla} \times \boldsymbol{\chi}(\boldsymbol{x}, t) \quad \text{and} \quad \boldsymbol{p}(\boldsymbol{x}, t) = \frac{1}{k(t)} \boldsymbol{\nabla} \times \boldsymbol{t}(\boldsymbol{x}, t). \tag{4.17a,b}$$

Therefore, $\boldsymbol{t}(\boldsymbol{x}, t)$ and $\boldsymbol{p}(\boldsymbol{x}, t)$ are time-dependent Laplacian eigenfunctions,

$$\nabla^2 \boldsymbol{t} = -k(t)^2 \boldsymbol{t} \quad \text{and} \quad \nabla^2 \boldsymbol{p} = -k(t)^2 \boldsymbol{p}. \tag{4.18a,b}$$

Finally, the time-dependent Beltrami field $\boldsymbol{\mathcal{U}}(\boldsymbol{x}, t)$ is defined from $\boldsymbol{\mathcal{U}}_0(\boldsymbol{x})$ as

$$\begin{aligned} \boldsymbol{\mathcal{U}}(\boldsymbol{x}, t) &\equiv \frac{k_0}{k(t)} \frac{\mathsf{F}(t)}{J(t)} \boldsymbol{\mathcal{U}}_0(\boldsymbol{z}_v(\boldsymbol{x}, t)) = \frac{k_0}{k(t)} \frac{\mathsf{F}(t)}{J(t)} \left(\boldsymbol{\nabla}_{\boldsymbol{z}} \times \boldsymbol{\psi}_0 \right) (\boldsymbol{z}_v(\boldsymbol{x}, t)) \\ &= \boldsymbol{\nabla} \times \boldsymbol{\psi}(\boldsymbol{x}, t) = \boldsymbol{t}(\boldsymbol{x}, t) - \boldsymbol{p}(\boldsymbol{x}, t), \end{aligned} \tag{4.19}$$

from which the Beltrami property follows,

$$\boldsymbol{\nabla} \times \boldsymbol{\mathcal{U}} = -k(t) \boldsymbol{\mathcal{U}}, \tag{4.20}$$

and therefore,

$$k(t) \boldsymbol{\mathcal{U}}(\boldsymbol{x}, t) = \frac{\mathsf{F}(t)}{J(t)} \left(k_0 \boldsymbol{\mathcal{U}}_0(\boldsymbol{z}_v(\boldsymbol{x}, t)) \right). \tag{4.21}$$

Similarly, the vorticity of the Beltrami field,

$$\boldsymbol{\mathcal{W}}(\boldsymbol{x}, t) \equiv \boldsymbol{\nabla} \times \boldsymbol{\mathcal{U}}(\boldsymbol{x}, t) = -k(t) \boldsymbol{\mathcal{U}}(\boldsymbol{x}, t) = \frac{\mathsf{F}(t)}{J(t)} \boldsymbol{\mathcal{W}}_0(\boldsymbol{z}(\boldsymbol{x}, t)), \tag{4.22}$$

https://doi.org/10.1017/jfm.2026.11537 Published online by Cambridge University Press

is just the Piola pushforward operation on the material vorticity $\boldsymbol{\mathcal{W}}_0 = -k_0\boldsymbol{\mathcal{U}}_0$. Therefore, the total velocity

$$\boldsymbol{u}(\boldsymbol{x}, t) \equiv \boldsymbol{\mathcal{U}}(\boldsymbol{x}, t) + \boldsymbol{u}_b(\boldsymbol{x}, t), \tag{4.23}$$

with vorticity

$$\boldsymbol{\omega}(\boldsymbol{x}, t) \equiv \nabla \times \boldsymbol{u}(\boldsymbol{x}, t) = \boldsymbol{\mathcal{W}}(\boldsymbol{x}, t) + 2\boldsymbol{v}(t) = -k(t)\boldsymbol{\mathcal{U}}(\boldsymbol{x}, t) + 2\boldsymbol{v}(t), \tag{4.24}$$

satisfies the time-dependent vorticity (2.1).

The key result of this section is that from a scalar Laplacian eigenfunction $\eta_0(\boldsymbol{x})$ and a background flow $\boldsymbol{u}_b(\boldsymbol{x}, t)$ with time-dependent homogeneous velocity gradient $\mathsf{L}(t)$, with vanishing deviatoric strain tensor $\mathsf{D}_0(t) = \mathsf{0}$, it is possible to obtain a time-dependent Beltrami flow $\boldsymbol{\mathcal{U}}(\boldsymbol{x}, t)$ that is materially advected by the background flow $\boldsymbol{v}_b(\boldsymbol{x}, t)$ and, therefore, becomes a solution to the time-dependent vorticity equation. Since there are 11 coordinate systems in which the Helmholtz equation is separable, we have $\boldsymbol{\mathcal{U}}_0(\boldsymbol{x})$ modes in 11 different geometries. For example, in Cartesian geometry, with coordinates $\{x, y, z\}$, the plane wave seed function

$$\eta_0(\boldsymbol{x}) \equiv \hat{\eta}_0 \mathrm{e}^{i(k_x x + k_y y + k_z z)}, \quad \text{with} \quad k_0^2 = k_x^2 + k_y^2 + k_z^2, \tag{4.25a,b}$$

leads to the family of Arnold–Beltrami–Childress (ABC) flows (Arnold 1965; Childress 1970; Dombre *et al.* 1986; Galloway & Frisch 1986; Soward 1987). In cylindrical coordinates $\{\rho, \varphi, z\}$, the seed function

$$\eta_0(\boldsymbol{x}) \equiv \hat{\eta}_0 R_m(\kappa\rho)\mathrm{e}^{im\varphi}\mathrm{e}^{ik_z z}, \quad R_m(\cdot) \in \left\{J_m(\cdot), Y_m(\cdot), H_m^{(1,2)}(\cdot)\right\}, \quad k_0^2 = \kappa^2 + k_z^2, \tag{4.26}$$

where $\{J_m, Y_m, H_m^{(1,2)}\}$ are the cylindrical Bessel and Hankel functions, leads to the cylindrical Kelvin modes (Kelvin 1880; Dritschel 1991). In spherical geometry, with coordinates $\{r, \theta, \varphi\}$, the function

$$\eta_0(\boldsymbol{x}) \equiv \hat{\eta}_0 \Psi_\ell(k_0 r) Y_\ell^m(\theta, \varphi), \quad \text{where} \quad \Psi(\cdot) \in \{j_\ell(\cdot), y_\ell(\cdot), h_\ell(\cdot)\}, \tag{4.27}$$

where $\{j_\ell, y_\ell, h_\ell\}$ are the spherical Bessel and Hankel functions, leads to the spherical vortices, including the Hicks–Moffatt vortex (Hicks 1899; Moffatt 1969, 2017; Viúdez 2022). An application of these spherical modes to physical oceanography is described in Appendix A. In parabolic cylindrical geometry, with coordinates $\{u, v, z\}$, the seed function is

$$\eta_0(\boldsymbol{x}) = \hat{\eta}_0 D_\nu(\sqrt{\kappa}u) D_\nu(\sqrt{\kappa}v)\mathrm{e}^{ik_z z}, \quad k_0^2 = \kappa^2 + k_z^2, \tag{4.28}$$

where D_ν are parabolic-cylinder functions. In confocal ellipsoidal geometry, with coordinates $\{\lambda, \mu, \nu\}$, the seed function

$$\eta_0(\boldsymbol{x}) \equiv L(\lambda)M(\mu)N(\nu) \tag{4.29}$$

is defined as the product of Lamé wave functions in ellipsoidal coordinates. And so on, in parabolic three-dimensional geometry, elliptic cylindrical geometry, prolate and oblate spheroidal geometries, and conical geometry. Using a different procedure, namely the Bragg–Hawthorne equation, steady-state solutions in the case of axisymmetric flows were given by Bělík *et al.* (2020) in cylindrical, spherical, paraboloidal, and prolate and oblate spheroidal geometries. The generalised CK procedure described in this section helps to classify all time-dependent Beltrami flows in different geometries within the same family of flow solutions.

https://doi.org/10.1017/jfm.2026.11537 Published online by Cambridge University Press

5. Plane Beltrami fields

In this section, we consider the particular case in which the Beltrami fields have a plane wave geometry. In the general case considered in the previous section, the background deviatoric tensor $\mathsf{D}_0(t)$ must vanish to allow the advected Beltrami field to preserve its Beltrami property. In the particular case of a plane Beltrami field, it is shown in the following that it is possible to have $\mathsf{D}_0(t) \neq \mathsf{0}$ as long as $\mathsf{D}_0(t)$ is in the direction of the plane wavevector $\boldsymbol{k}(t)$.

5.1. *Plane Beltrami flows*

The Laplacian eigenfunction for a plane wave is

$$\eta_0(\boldsymbol{x}_0) = \mathrm{e}^{i\boldsymbol{k}_0\cdot\boldsymbol{x}_0}, \quad \text{with} \quad \nabla^2\eta_0 = -|\boldsymbol{k}_0|^2\eta_0. \tag{5.1a,b}$$

For a linear invertible transformation $\mathsf{A}(t)$, it follows that

$$\eta(\boldsymbol{x},t) \equiv \eta_0(\mathsf{A}(t)\boldsymbol{x}) = \mathrm{e}^{i(\mathsf{A}(t)^\top\boldsymbol{k}_0)\cdot\boldsymbol{x}}, \quad \nabla^2\eta(\boldsymbol{x},t) = -|\mathsf{A}(t)^\top\boldsymbol{k}_0|^2\eta(\boldsymbol{x},t), \tag{5.2}$$

that is, $\eta(\boldsymbol{x},t)$ is a Laplacian eigenfunction with eigenvalue $-|\mathsf{A}(t)^\top\boldsymbol{k}_0|^2$. This property allows us to use the CK procedure at all times. In the CK procedure, the steady material vector plane waves are

$$\{\boldsymbol{\chi}_0(\boldsymbol{x}_0),\, \boldsymbol{t}_0(\boldsymbol{x}_0),\, \boldsymbol{p}_0(\boldsymbol{x}_0)\} = \left\{\hat{\boldsymbol{n}}_0,\, \boldsymbol{k}_0\times\hat{\boldsymbol{n}}_0,\, -\frac{1}{k_0}\boldsymbol{k}_0\times(\boldsymbol{k}_0\times\hat{\boldsymbol{n}}_0)\right\}\mathrm{e}^{i\boldsymbol{k}_0\cdot\boldsymbol{x}_0}. \tag{5.3}$$

The case $\boldsymbol{k}_0\|\hat{\boldsymbol{n}}_0$ produces a zero Beltrami field. In the equivalent time-dependent vector plane waves procedure, the initial seed function is a plane wave

$$\eta_0(\boldsymbol{x}_0) = \mathrm{e}^{i\boldsymbol{k}_0\cdot(\boldsymbol{x}_0-\boldsymbol{o}(0))}, \quad \nabla^2\eta_0 = -|\boldsymbol{k}_0|^2\eta_0, \tag{5.4a,b}$$

whose phase evolves, under the transformation (3.4), as

$$\boldsymbol{k}_0\cdot\left(\mathsf{F}^{-1}(t)(\boldsymbol{x}-\boldsymbol{o}_v(t))\right) = \boldsymbol{k}(t)\cdot(\boldsymbol{x}-\boldsymbol{o}_v(t)), \quad \text{where } \boldsymbol{k}(t) \equiv \mathsf{F}^{-\top}(t)\boldsymbol{k}_0. \tag{5.5a,b}$$

The corresponding scalar density function evolves as

$$\eta(\boldsymbol{x},t) = \frac{1}{J(t)}\mathrm{e}^{i\boldsymbol{k}(t)\cdot(\boldsymbol{x}-\boldsymbol{o}_v(t))} = A(t)\mathrm{e}^{i\boldsymbol{k}(t)\cdot\boldsymbol{x}}, \quad A(t) \equiv \frac{1}{J(t)}\mathrm{e}^{-i\boldsymbol{k}(t)\cdot\boldsymbol{o}_v(t)}, \tag{5.6a,b}$$

where $A(t)$ is a time-dependent complex-valued amplitude. The rate of change of the time-dependent wavevector is

$$\dot{\boldsymbol{k}}(t) = -\mathsf{L}^\top(t)\boldsymbol{k}(t), \tag{5.7}$$

and we may check that the rate of change of the phase in the material space is

$$\frac{\partial}{\partial t}\left(\boldsymbol{r}_v(\boldsymbol{x}_0,t)-\boldsymbol{o}_v(t)\right)\cdot\boldsymbol{k}(t)\right) = \mathsf{L}(t)\left[\mathsf{F}(t)(\boldsymbol{x}_0-\boldsymbol{o}(0)-(\boldsymbol{r}_v(\boldsymbol{x}_0,t)-\boldsymbol{o}_v(t)))\right]\boldsymbol{k}(t) = 0, \tag{5.8}$$

so that the phase in the material space,

$$\boldsymbol{r}_v(\boldsymbol{x}_0,t)-\boldsymbol{o}_v(t))\cdot\boldsymbol{k}(t) = (\boldsymbol{x}_0-\boldsymbol{o}(0))\cdot\boldsymbol{k}_0, \tag{5.9}$$

is stationary. Since $\eta(\boldsymbol{x},t)$ is a Laplacian eigenfunction at all times t,

$$\nabla^2\eta(\boldsymbol{x},t) = -k(t)^2\eta(\boldsymbol{x},t), \tag{5.10}$$

https://doi.org/10.1017/jfm.2026.11537 Published online by Cambridge University Press

we carry on with the time-dependent CK procedure and define the corresponding fields

$$\boldsymbol{\chi}(\boldsymbol{x},t)\equiv\eta(\boldsymbol{x},t)\hat{\boldsymbol{n}}(t),\quad \boldsymbol{t}(\boldsymbol{x},t)\equiv\nabla\times\boldsymbol{\chi}(\boldsymbol{x},t),\quad \boldsymbol{p}(\boldsymbol{x},t)\equiv\frac{\nabla\times\boldsymbol{\chi}(\boldsymbol{x},t)}{k(t)},\tag{5.11a,b,c}$$

which become

$$\boldsymbol{t}=\mathrm{i}\eta\boldsymbol{k}\times\hat{\boldsymbol{n}},\quad \text{and}\quad \boldsymbol{p}=\eta\left(k\hat{\boldsymbol{n}}-\frac{\boldsymbol{k}\cdot\hat{\boldsymbol{n}}}{k}\boldsymbol{k}\right).\tag{5.12a,b}$$

Next, we obtain, from (5.12a,b), the Beltrami velocity field

$$\boldsymbol{\mathcal{U}}(\boldsymbol{x},t)\equiv\boldsymbol{t}(\boldsymbol{x},t)-\boldsymbol{p}(\boldsymbol{x},t),\tag{5.13}$$

and hence, the Beltrami vorticity field $\boldsymbol{\mathcal{W}}(\boldsymbol{x},t)$ as

$$\boldsymbol{\mathcal{W}}(\boldsymbol{x},t)=\boldsymbol{W}(t)\mathrm{e}^{i\boldsymbol{k}(t)\cdot\boldsymbol{x}},\tag{5.14}$$

where the polarisation vector $\boldsymbol{W}(t)$ of the Beltrami vorticity field is a function of $\{\boldsymbol{k}(t),\hat{\boldsymbol{n}}(t),A(t)\}$,

$$\boldsymbol{W}(t)=\boldsymbol{W}(\boldsymbol{k}(t),\hat{\boldsymbol{n}}(t),A(t)),\tag{5.15}$$

and is given by

$$\boldsymbol{W}(t)=A(t)\big(k(t)^2\hat{\boldsymbol{n}}(t)-(\boldsymbol{k}(t)\cdot\hat{\boldsymbol{n}}(t))\boldsymbol{k}(t)-\mathrm{i}k(t)\boldsymbol{k}(t)\times\hat{\boldsymbol{n}}(t)\big).\tag{5.16}$$

Clearly,

$$\boldsymbol{W}(t)\cdot\boldsymbol{k}(t)=0,\tag{5.17}$$

so that the polarisation vector $\boldsymbol{W}(t)$ is tangent to the wavefronts and there is no vorticity component along the propagation direction $\boldsymbol{k}(t)$. This is equivalent to the property $\nabla\cdot\boldsymbol{\mathcal{W}}(\boldsymbol{x},t)=0$ in terms of the polarisation vector $\boldsymbol{W}(t)$. The vorticity mode $\boldsymbol{\mathcal{W}}(\boldsymbol{x},t)$, as well as the velocity mode $\boldsymbol{\mathcal{U}}(\boldsymbol{x},t)$, are transverse waves. This is analogous to the electromagnetic monochromatic plane waves with wavevector $\boldsymbol{k}$, where the electric $\boldsymbol{E}(\boldsymbol{x},t)$ and magnetic $\boldsymbol{B}(\boldsymbol{x},t)$ fields,

$$\boldsymbol{E}(\boldsymbol{x},t)\equiv\Re\big\{\boldsymbol{E}_0\mathrm{e}^{i(\boldsymbol{k}\cdot\boldsymbol{x}-\omega t)}\big\},\quad \boldsymbol{B}(\boldsymbol{x},t)\equiv\Re\big\{\boldsymbol{B}_0\mathrm{e}^{i(\boldsymbol{k}\cdot\boldsymbol{x}-\omega t)}\big\},\tag{5.18a,b}$$

satisfy the Maxwell equations for the propagation of electromagnetic waves in vacuum, which imply

$$\boldsymbol{k}\cdot\boldsymbol{E}_0=0,\quad \boldsymbol{k}\cdot\boldsymbol{B}_0=0,\quad \mathrm{i}\boldsymbol{k}\times\boldsymbol{E}_0=\omega\boldsymbol{B}_0,\quad \mathrm{i}\boldsymbol{k}\times\boldsymbol{B}_0=-\frac{\omega}{c_0^2}\boldsymbol{E}_0.\tag{5.19a,b,c,d}$$

So, in vacuum, the time dependence of the electromagnetic plane waves is purely oscillatory via the phase $\exp(-\mathrm{i}\omega t)$, and the polarisations $\boldsymbol{E}_0$ and $\boldsymbol{B}_0$ are constant. This analogy is pursued in § 5.2. The fluid mechanics analogues to the electromagnetic relations (5.19) are

$$\begin{gathered}\boldsymbol{k}(t)\cdot\boldsymbol{U}(t)=0,\quad \boldsymbol{k}(t)\cdot\frac{\boldsymbol{W}(t)}{k(t)}=0,\quad \mathrm{i}\boldsymbol{k}(t)\times\boldsymbol{U}(t)=\boldsymbol{W}(t),\\ \mathrm{i}\boldsymbol{k}(t)\times\left(\frac{\boldsymbol{W}(t)}{k(t)}\right)=-k(t)\boldsymbol{U}(t).\end{gathered}\tag{5.20}$$

Given the relation between $\boldsymbol{k}(t)$ and $\mathsf{L}(t)$ (5.7), the problem is to find the relations between the parameters of the advecting flow and the parameters of the Beltrami flow such that the

https://doi.org/10.1017/jfm.2026.11537 Published online by Cambridge University Press

vorticity polarisation is frozen in the advecting flow, that is,

$$\dot{\boldsymbol{W}}(t) = \left(\mathsf{D}_0(t) - \frac{2}{3}\delta(t)\mathsf{I} + \mathsf{W}(t)\right)\boldsymbol{W}(t), \tag{5.21}$$

or, in an equivalent way using the Piola transformation, that

$$\boldsymbol{W}(t) = \frac{1}{J(t)}\mathsf{F}(t)\boldsymbol{W}(0). \tag{5.22}$$

Time differentiation of (5.22) leads to (5.21). Thus, the polarisation vector $\boldsymbol{W}(t)$ obeys the same time evolution equation as the background vorticity $2\boldsymbol{v}(t)$ and $\boldsymbol{W}(t)$ is frozen in the flow $\boldsymbol{v}_b(\boldsymbol{x}, t)$.

Using (5.16), we may express the rate of change of $\boldsymbol{W}(t)$ as

$$\dot{\boldsymbol{W}}(t) = \partial_{\boldsymbol{k}}\boldsymbol{W}\dot{\boldsymbol{k}} + \partial_{\hat{\boldsymbol{n}}}\boldsymbol{W}\dot{\hat{\boldsymbol{n}}} + \partial_A\boldsymbol{W}\dot{A}. \tag{5.23}$$

At every time t, relations (5.7) and (5.21) imply six real linear constraints on the nine real components of $\mathsf{L}(t)$, so that in the generic case, for non-degenerate $\{\boldsymbol{k}(t), \boldsymbol{W}(t)\}$, there is a three-parameter family of homogeneous flows with velocity gradient $\mathsf{L}(t)$ in which the vorticity $\boldsymbol{\mathcal{W}}(\boldsymbol{x}, t)$ is frozen for any given choice of $\boldsymbol{k}(t)$, $\hat{\boldsymbol{n}}(t)$ and $A(t)$. The deviatoric strain tensor $\mathsf{D}_0(t)$ causes the anisotropic stretching and tilting of the polarisation, the divergence $\delta(t)$ is responsible for the isotropic amplification/decay of the magnitude of $\boldsymbol{W}(t)$, while the background spin causes a rigid body rotation, or precession, of $\boldsymbol{W}(t)$ via $\mathsf{W}(t)\boldsymbol{W}(t) = \boldsymbol{v}(t) \times \boldsymbol{W}(t)$. A Beltrami plane wave $\boldsymbol{\mathcal{W}}(\boldsymbol{x}, t)$ (5.14)

$$\nabla \times \boldsymbol{\mathcal{W}} = -k\boldsymbol{\mathcal{W}} \quad \Longleftrightarrow \mathcal{C}_{\boldsymbol{k}}\boldsymbol{W} = -k\boldsymbol{W}, \quad \text{where } \mathcal{C}_{\boldsymbol{k}} \equiv \mathrm{i}\boldsymbol{k}\times. \tag{5.24}$$

Thus, the Beltrami condition implies that the polarisation vector $\boldsymbol{W}(t)$ is an eigenvector of the operator $\mathcal{C}_{\boldsymbol{k}}$ with eigenvalue $-k(t)$. This means that in the complex representation

$$\boldsymbol{W}(t) = \Re\boldsymbol{W}(t) + \mathrm{i}\Im\boldsymbol{W}(t), \tag{5.25}$$

the real vectors $\Re\boldsymbol{W}(t)$ and $\Im\boldsymbol{W}(t)$ are orthogonal $\Re\boldsymbol{W}\cdot\Im\boldsymbol{W} = 0$, and have the same norm $||\Re\boldsymbol{W}|| = ||\Im\boldsymbol{W}||$, which means that $\boldsymbol{W}(t)$ must have circular polarisation in the plane perpendicular to $\boldsymbol{k}(t)$.

To find the background velocity gradient $\mathsf{L}(t)$ that preserves the Beltrami condition of the plane wave, we assume that the deviatoric tensor $\mathsf{D}_0(t)$ is axisymmetric about the direction of $\boldsymbol{k}(t)$ and that the spin tensor $\mathsf{W}(t)$ generates a rotation about the same axis. We define orthonormal basis vectors $\{\hat{\boldsymbol{e}}_1, \hat{\boldsymbol{e}}_2, \hat{\boldsymbol{e}}_3\}$ such that

$$\hat{\boldsymbol{e}}_3 \equiv \hat{\boldsymbol{k}}(t) = \frac{\boldsymbol{k}(t)}{k(t)}. \tag{5.26}$$

In that orthogonal basis, the deviatoric $\mathsf{D}_0(t)$ and spin $\mathsf{W}(t)$ tensors are

$$\mathsf{D}_0(t) = \begin{pmatrix} \sigma(t) & 0 & 0 \\ 0 & \sigma(t) & 0 \\ 0 & 0 & -2\sigma(t) \end{pmatrix}, \quad \mathsf{W}(t) = \begin{pmatrix} 0 & -\nu(t) & 0 \\ \nu(t) & 0 & 0 \\ 0 & 0 & 0 \end{pmatrix}, \tag{5.27}$$

and therefore, the velocity gradient is

$$\mathsf{L}(t) = \begin{pmatrix} \sigma(t) + \delta(t)/3 & -2\nu(t) & 0 \\ 2\nu(t) & \sigma(t) + \delta(t)/3 & 0 \\ 0 & 0 & -2\sigma(t) + \delta(t)/3 \end{pmatrix}. \tag{5.28}$$

https://doi.org/10.1017/jfm.2026.11537 Published online by Cambridge University Press

Since $\mathsf{L}(t)$ is block-diagonal with respect to the split $\mathbb{R}^3 = \text{span}\{\hat{\boldsymbol{e}}_1, \hat{\boldsymbol{e}}_2\} \oplus \text{span}\{\hat{\boldsymbol{e}}_3\}$, the solution $\mathsf{F}(t)$ to $\dot{\mathsf{F}} = \mathsf{L}\mathsf{F}$ has the same block-diagonal form

$$\mathsf{F}(t) = \begin{pmatrix} \mathsf{F}_\perp(t) & 0 \\ 0 & \mathsf{F}_\parallel(t) \end{pmatrix}, \tag{5.29}$$

where $\mathsf{F}_\perp(t)$ is a 2×2 matrix acting on the transverse plane and $\mathsf{F}_\parallel(t)$ is a scalar function acting on $\hat{\boldsymbol{e}}_3$.

We first solve the transverse block with evolution equation $\dot{\mathsf{F}}_\perp(t) = \mathsf{L}_\perp(t)\mathsf{F}_\perp(t)$, with $\mathsf{F}_\perp(0) = \mathsf{I}_2$, in which the transverse velocity gradient is

$$\mathsf{L}_\perp(t) = \begin{pmatrix} \sigma(t) + \delta(t)/3 & -2\nu(t) \\ 2\nu(t) & \sigma(t) + \delta(t)/3 \end{pmatrix}. \tag{5.30}$$

The transverse deformation gradient $\mathsf{F}_\perp(t)$ can be explicitly integrated and the solution is

$$\mathsf{F}_\perp(t) = \Lambda_\perp(t)\mathsf{R}(\theta(t)), \tag{5.31}$$

where

$$\Lambda_\perp(t) \equiv \exp\left(\int_0^t \left(\sigma(\tau) + \frac{1}{3}\delta(\tau)\right) \mathrm{d}\tau\right), \tag{5.32}$$

and the rotation matrix $\mathsf{R}(\theta)$ and rotation angle $\theta(t)$ are

$$\mathsf{R}(\theta) = \begin{pmatrix} \cos\theta & -\sin\theta \\ \sin\theta & \cos\theta \end{pmatrix}, \quad \theta(t) \equiv \int_0^t \nu(\tau)\,\mathrm{d}\tau. \tag{5.33a,b}$$

Thus, in the transverse plane, the deformation is a uniform stretch $\Lambda_\perp(t)$ plus a rotation by an angle $\theta(t)$.

The axial component of the deformation $\mathsf{F}_\parallel(t)$ satisfies $\dot{\mathsf{F}}_\parallel(t) = \mathsf{L}_\parallel(t)\mathsf{F}_\parallel(t)$, with $\mathsf{F}_\parallel(0) = 1$, and

$$\mathsf{L}_\parallel(t) \equiv -2\sigma(t) + \delta(t)/3. \tag{5.34}$$

Therefore, the axial component of the deformation gradient $\mathsf{F}_\parallel(t)$ is

$$\mathsf{F}_\parallel(t) = \Lambda_\parallel(t) = \exp\left(\int_0^t \left(-2\sigma(\tau) + \frac{1}{3}\delta(\tau)\right) \mathrm{d}\tau\right). \tag{5.35}$$

The determinant of the transformation is simply

$$J(t) \equiv \det\mathsf{F}(t) = \Lambda_\parallel^2(t)\Lambda_\perp(t) = \exp\left(\int_0^t \delta(\tau)\,\mathrm{d}\tau\right). \tag{5.36}$$

The time evolution of the wavenumber $k(t)$ is

$$k(t) = \frac{k_0}{\Lambda_\parallel(t)} = k_0 \exp\left(\int_0^t \left(2\sigma(\tau) - \frac{1}{3}\delta(\tau)\right) \mathrm{d}\tau\right), \tag{5.37}$$

unit vector $\hat{\boldsymbol{n}}(t)$,

$$\hat{\boldsymbol{n}}(t) = \mathsf{R}(\theta(t))\hat{\boldsymbol{n}}_0, \quad \hat{\boldsymbol{n}}_0 \perp \hat{\boldsymbol{e}}_3, \tag{5.38}$$

and the time evolution of the amplitude $A(t)$ is

$$A(t) = A_0 \frac{\Lambda_\parallel(t)}{\Lambda_\perp(t)} = A_0 \exp\left(\int_0^t -3\sigma(\tau)\,\mathrm{d}\tau\right). \tag{5.39}$$

https://doi.org/10.1017/jfm.2026.11537 Published online by Cambridge University Press

We may summarise the results as follows. An initial helical vector $\boldsymbol{W}(0)$ in $\boldsymbol{k}(0)_\perp$ must evolve as $\boldsymbol{W}(t) = (1/J(t))\mathsf{F}(t)\boldsymbol{W}(0)$ and must remain a helical eigenvector of $\mathrm{i}\boldsymbol{k}(t)\times$ at all times t, that is, it must conserve its circular polarisation. If the transverse part of $\mathsf{F}(t)$ is a similarity, consisting of a uniform stretch plus a rotation, the Piola evolution keeps $\boldsymbol{W}(t)$ inside the helical subspace in the plane perpendicular to $\boldsymbol{k}(t)$; therefore, the Beltrami property survives and the CK representation is possible at all times. In this particular solution, the free parameters of the background flow are the main parameter, namely, the principal deviatoric strain rate $\sigma(t)$ in the two transverse directions, the velocity divergence $\delta(t)$, and the angular velocity $\nu(t)$. The anisotropic strain rate $\sigma(t)$ stretches/compresses the wavelength along $\boldsymbol{k}(t)$ and exponentially amplifies or damps the plane-wave amplitude $A(t)$. The isotropic expansion/compression $\delta(t)$ modifies the growth/decay of the wavenumber $k(t)$ via volume change through $J(t)$, but cancels out $A(t)$ in this CK–frozen solution. The background rotation rate $\nu(t)$ rigidly rotates the polarisation direction $\hat{\boldsymbol{n}}(t)$ in the plane orthogonal to $\boldsymbol{k}(t)$ without changing $|k(t)|$ or $|A(t)|$.

From (5.36), (5.37) and (5.39), we obtain a time invariant

$$J(t)A(t)^2k(t)^3 = \text{const.} \tag{5.40}$$

For the CK Beltrami plane-wave, the vorticity amplitude, up to a fixed numerical factor coming from the precise CK normalisation that the vorticity amplitude $\|\boldsymbol{\mathcal{W}}\| \sim Ak^2$, the velocity $\|\boldsymbol{\mathcal{U}}\| \sim Ak$ implies that the helicity density $\mathcal{H} \equiv \boldsymbol{\mathcal{U}} \cdot \boldsymbol{\mathcal{W}} \sim A^2k^3$ and, therefore, $H_0 = J(t)A(t)^2k(t)^3$ represents the helicity content of the mode per material volume element.

5.2. *Electromagnetic wave analogy: Jones vector and matrix representation*

For a monochromatic plane wave propagating along the z-axis, we only need the transverse electric field components, say E_x and E_y. Their complex amplitudes are collected into a column vector called the Jones vector (Jones 1941; Collett 2005),

$$\boldsymbol{E} = \begin{pmatrix} E_x \\ E_y \end{pmatrix}. \tag{5.41}$$

For example,

$$\boldsymbol{E}_x = \begin{pmatrix} 1 \\ 0 \end{pmatrix}, \quad \boldsymbol{E}_y = \begin{pmatrix} 0 \\ 1 \end{pmatrix}, \quad \boldsymbol{E}_R = \frac{1}{\sqrt{2}}\begin{pmatrix} 1 \\ -\mathrm{i} \end{pmatrix}, \quad \boldsymbol{E}_L = \frac{1}{\sqrt{2}}\begin{pmatrix} 1 \\ \mathrm{i} \end{pmatrix}, \tag{5.42}$$

represent linear polarisation along x and along y, and right and left circular polarizations, respectively. The relative phase between E_x and E_y is encoded in the complex entries of the Jones vector. The polarisation changes caused by a linear optical element can be represented by a 2×2 complex matrix J, called the the Jones matrix, acting on the Jones vector,

$$\boldsymbol{E}_{out} = \mathsf{J}\,\boldsymbol{E}_{in}. \tag{5.43}$$

For example,

$$\mathsf{J} = \begin{pmatrix} 1 & 0 \\ 0 & 1 \end{pmatrix}, \quad \mathsf{J}_{pol,x} = \begin{pmatrix} 1 & 0 \\ 0 & 0 \end{pmatrix}, \quad \mathsf{J}_{ret}(\phi) = \begin{pmatrix} 1 & 0 \\ 0 & e^{i\phi} \end{pmatrix}, \tag{5.44}$$

represent free space (no change), ideal linear polariser transmitting only the x-component, phase retarder, waveplate that introduces a phase shift ϕ in the y-component. Thus, a Jones matrix is simply the linear operator in the two-dimensional polarisation space that maps an input Jones vector to an output Jones vector.

https://doi.org/10.1017/jfm.2026.11537 Published online by Cambridge University Press

In the fluid mechanics solution, the polarisation vector $\boldsymbol{W}(t)$, or the velocity polarisation $\boldsymbol{U}(t)$, in the plane orthogonal to $\boldsymbol{k}(t)$ plays the role of a Jones vector

$$\boldsymbol{W}(t) \in \boldsymbol{k}(t)^{\perp} \cong \mathbb{C}^2, \tag{5.45}$$

that is, the plane $\boldsymbol{k}(t)^{\perp}$ is isomorphic to $\mathbb{C}^2$. The restriction of the time-dependent deformation gradient $\mathsf{F}(t)$ of the background flow to the transverse plane,

$$\mathsf{F}_{\perp}(t) : \boldsymbol{k}(t)^{\perp} \to \boldsymbol{k}(t)^{\perp}, \tag{5.46}$$

acts on $\boldsymbol{W}(t)$ exactly like a Jones matrix J (5.43) acts on a Jones vector,

$$\boldsymbol{W}(t) \propto \mathsf{F}_{\perp}(t)\, \boldsymbol{W}_0. \tag{5.47}$$

If $\mathsf{F}_{\perp}(t)$ is of the form

$$\mathsf{F}_{\perp}(t) = \lambda(t)\mathsf{R}(\theta(t)), \tag{5.48}$$

that is, a scalar stretch $\lambda(t)$ times a rotation $\mathsf{R}(\theta(t))$ in the transverse plane, that is, transverse isotropy about $\boldsymbol{k}(t)$, then it preserves circular polarisation, and a Beltrami (helical) polarisation remains Beltrami, exactly as an isotropic optical medium preserves circular polarisation. If, instead, $\mathsf{F}_{\perp}(t)$ contains anisotropic shear (is not a pure stretch plus rotation), then it acts like a birefringent Jones matrix: a circular (Beltrami) polarisation is mapped into an elliptical polarisation in $\boldsymbol{k}(t)^{\perp}$, and the mode ceases to be Beltrami, even though the vorticity remains frozen-in. We notice that the Jones matrix transformation is an instantaneous transformation, while its fluid mechanics counterpart (5.47) is a continuous deformation. In practice, the scattering of Beltrami fields may be described, under the Beltrami field approximation, by finite-time, or pulses, of a background velocity gradient $\mathsf{L}(t)$, and consequently, pulses of the background deformation gradient $\mathsf{F}(t)$ acting on the Beltrami field. An example of a scattering process is given in § 7.

6. Two examples using particular forms of the velocity gradient $\mathsf{L}(t)$

The time-dependent Beltrami flow $\boldsymbol{\mathcal{U}}(\boldsymbol{x}, t)$ is completely determined by the initial Beltrami flow $\boldsymbol{\mathcal{U}}_0(\boldsymbol{x})$ and the background flow $\boldsymbol{u}_b(\boldsymbol{x}, t)$. The temporal changes in $\boldsymbol{\mathcal{U}}(\boldsymbol{x}, t)$, apart from those derived from the arbitrary rigid translation $\boldsymbol{o}(t)$, are due to the time evolution of the background flow $\boldsymbol{u}_b(\boldsymbol{x}, t)$, which are themselves prescribed by the time evolution of the background velocity gradient tensor $\mathsf{L}(t)$. The nine independent components of $\mathsf{L}(t)$ correspond to the expansion/contraction term $\delta(t)$ (one component), vorticity tensor $\mathsf{W}(t)$ (three components) and deviatoric tensor $\mathsf{D}_0(t)$ (five components, namely two normal/extensional components and three shear-rate components). However, the three components of the angular velocity $\boldsymbol{\nu}(t)$ must satisfy the vorticity equation, which implies that there are six degrees of freedom in the way the time evolution of $\mathsf{L}(t)$ can be arbitrarily prescribed. These degrees of freedom allow us to prescribe the time-evolution of the Beltrami field. This freedom can be viewed as the possibilities to prescribe external time-dependent potential, i.e. conservative, forces in the Euler momentum equation. The introduction of forces, however, is not required in this vorticity equation approach, which only assumes that the flow acceleration $\boldsymbol{a}(\boldsymbol{x}, t)$ is irrotational, $\boldsymbol{\nabla} \times \boldsymbol{a} = \boldsymbol{0}$. This section provides two examples of how particular solutions of $\mathsf{L}(t)$ prescribe the time evolution of a Beltrami field.

6.1. *Case* $\mathsf{D}_0(t) = \mathsf{0}$*: background rigid-body rotation with isotropic dilatation*

In the case where the deviatoric tensor of the background flow vanishes $\mathsf{D}_0(t) = \mathsf{0}$, the background flow $\boldsymbol{u}_b(\boldsymbol{x}, t)$ is a rigid-body rotation with isotropic expansion/contraction

https://doi.org/10.1017/jfm.2026.11537 Published online by Cambridge University Press

and there is only one degree of freedom available. In this case, the compatibility condition (4.2) reduces to

$$\dot{\boldsymbol{v}}(t) = -\frac{2}{3}\delta(t)\boldsymbol{v}(t) \tag{6.1}$$

and therefore, only changes in magnitude, and not in orientation, of the background angular velocity $\boldsymbol{v}(t)$ are possible, and hence, only changes in the speed of the displacement velocity $\boldsymbol{c}(t) = 2\boldsymbol{v}(t)/k(t)$ of the Beltrami field. These changes are related to the isotropic expansion/contraction caused by the divergence $\delta(t)$,

$$\dot{\nu}(t) = -\frac{2}{3}\delta(t)\nu(t). \tag{6.2}$$

In terms of the time-integrated divergence $\Delta(t)$, relation (6.2) is

$$\frac{\dot{\nu}(t)}{\nu(t)} = -\frac{2}{3}\dot{\Delta}(t), \quad \text{where } \dot{\Delta}(t) = \delta(t), \tag{6.3a,b}$$

whose time-integration leads to the solution

$$\boldsymbol{v}(t) = \boldsymbol{v}_0 \mathrm{e}^{-\frac{2}{3}\Delta(t)}, \quad \nu(t) = \nu_0 \mathrm{e}^{-\frac{2}{3}\Delta(t)}, \quad \boldsymbol{v}_0 \equiv \boldsymbol{v}(0), \tag{6.4a,b,c}$$

which provides the time-evolution of the background angular velocity $\boldsymbol{v}(t)$ as a function of the time-integral of the background divergence $\delta(t)$. Using Euler's identity

$$\dot{J}(t) = J(t)\delta(t), \quad \text{where} \quad J(t) \equiv \det(\mathsf{F}), \tag{6.5a,b}$$

the relation between $\dot{\nu}(t)$ and $\dot{J}(t)$ is

$$\frac{\dot{\nu}(t)}{\nu(t)} = -\frac{2}{3}\frac{\dot{J}(t)}{J(t)}, \tag{6.6}$$

whose time integration yields the relation between the time-dependent volume and angular velocity,

$$\frac{\nu(t)}{\nu(0)} = \left(\frac{J(t)}{J(0)}\right)^{-2/3}. \tag{6.7}$$

Relation (6.3a) implies that the background velocity $\boldsymbol{u}_b(\boldsymbol{x}, t)$ may be written in terms of the time-integrated divergence $\Delta(t)$, or in terms of the angular velocity $\nu(t)$, as

$$\boldsymbol{u}_b(\boldsymbol{x}, t) = \dot{\boldsymbol{o}}(t) + \frac{1}{3}\dot{\Delta}(t)(\boldsymbol{x} - \boldsymbol{o}(t)) + \mathrm{e}^{-\frac{2}{3}\Delta(t)}\nu_0\hat{\boldsymbol{v}}_0 \times (\boldsymbol{x} - \boldsymbol{o}(t)) \tag{6.8a}$$

$$= \dot{\boldsymbol{o}}(t) - \frac{1}{2}\frac{\dot{\nu}(t)}{\nu(t)}(\boldsymbol{x} - \boldsymbol{o}(t)) + \nu(t)\hat{\boldsymbol{v}}_0 \times (\boldsymbol{x} - \boldsymbol{o}(t)). \tag{6.8b}$$

In the case of vanishing background divergence, $\delta(t) = 0$, the background flow reduces to a constant rotation and arbitrary time-dependent translation given by $\boldsymbol{o}(t)$.

The advecting velocity $\boldsymbol{v}_b(\boldsymbol{x}, t)$ is

$$\boldsymbol{v}_b(\boldsymbol{x}, t) = \boldsymbol{u}_b(\boldsymbol{x}, t) + \frac{2\mathrm{e}^{-\frac{2}{3}\Delta(t)}\nu_0\hat{\boldsymbol{v}}_0}{k(t)} = \boldsymbol{u}_b(\boldsymbol{x}, t) + \frac{2\nu(t)}{k(t)}\hat{\boldsymbol{v}}_0. \tag{6.9}$$

In this case, the deformation gradient reduces to the isotropic expansion/contraction and rotation,

$$\mathsf{F}(t) = \mathrm{e}^{\Delta(t)/3}\mathsf{R}(t), \tag{6.10}$$

https://doi.org/10.1017/jfm.2026.11537 Published online by Cambridge University Press

where the rotation tensor

$$\mathsf{R}(t) \equiv \mathsf{R}_{\hat{\boldsymbol{v}}}(\vartheta(t)) = \mathrm{e}^{[\hat{\boldsymbol{v}}\times]\vartheta(t)}, \tag{6.11}$$

expresses the rotation around the constant axis defined by $\hat{\boldsymbol{v}}$ by an angle $\vartheta(t)$ given by

$$\vartheta(t) \equiv \int_0^t \nu(\tau)\,\mathrm{d}\tau, \quad \text{with} \quad \dot{\vartheta}(t) = \nu(t). \tag{6.12a,b}$$

These relations imply that any spatial dependence in the Beltrami field given by a dimensionless scalar term in the form $\boldsymbol{k}_0 \cdot \boldsymbol{z}_v(\boldsymbol{x}, t)$, where $\boldsymbol{k}_0$ is a constant wavevector, or co-vector, transform as

$$\begin{aligned}\boldsymbol{k}_0 \cdot \boldsymbol{z}_v(\boldsymbol{x}, t) &= \boldsymbol{k}_0 \cdot \left(\mathrm{e}^{-\Delta(t)/3}\mathsf{R}(t)^\top(\boldsymbol{x} - \boldsymbol{o}(0))\right) = \mathrm{e}^{-\Delta(t)/3}\,(\mathsf{R}(t)\boldsymbol{k}_0)\cdot(\boldsymbol{x} - \boldsymbol{o}(0)) \\ &= \boldsymbol{k}(t)\cdot(\boldsymbol{x} - \boldsymbol{o}(0)).\end{aligned} \tag{6.13}$$

That is, if $\boldsymbol{x} - \boldsymbol{o}(0)$ transforms contravariantly $\boldsymbol{z}_v(\boldsymbol{x}, t) = (\partial \boldsymbol{r}_v/\partial \boldsymbol{x}_0)(\boldsymbol{x} - \boldsymbol{o}(0)) = \mathsf{F}(t)(\boldsymbol{x} - \boldsymbol{o}(0))$, then the covector $\hat{\boldsymbol{k}}_0$ transforms covariantly into the time-dependent covector $\boldsymbol{k}(t)$ defined as

$$\boldsymbol{k}(t) \equiv \mathrm{e}^{-\Delta(t)/3}\mathsf{R}(t)\boldsymbol{k}_0, \quad \text{with} \quad \boldsymbol{k}_0 \equiv \boldsymbol{k}(0), \tag{6.14a,b}$$

which implies that the solid-body rotation plus isotropic expansion/contraction background flow causes a rotation and an expansion/contraction of the initial wavevector $\boldsymbol{k}_0$, that is, an expansion/contraction and precession of the Beltrami field with an angular frequency $\nu(t)$ modulated by the background expansion/contraction.

Since $\mathsf{R}(t)^\top = \mathsf{R}_{\hat{\boldsymbol{v}}}(-\vartheta(t))$ is a rotation, it preserves norms and, hence, the norm of $\boldsymbol{z}_v(\boldsymbol{x}, t)$ transforms as

$$\|\mathrm{e}^{-\Delta(t)/3}\mathsf{R}(t)^\top(\boldsymbol{x} - \boldsymbol{o}(t))\| = \mathrm{e}^{-\Delta(t)/3}\|(\boldsymbol{x} - \boldsymbol{o}(t))\|. \tag{6.15}$$

The flow map $\boldsymbol{R}_v(\boldsymbol{x}, t)$ of the advecting velocity $\boldsymbol{v}(\boldsymbol{x}, t)$ is a composition of a translation, a rotation and a uniform scaling by $\exp(-\Delta(t)/3)$. The Laplacian is invariant under rigid motions and under uniform scaling, it transforms by a constant factor, consequently,

$$\nabla^2\eta(\boldsymbol{x}, t) = -k_0^2\eta(\boldsymbol{x}, t). \tag{6.16}$$

We may define a time-dependent radial scalar wavenumber $k(t)$ as

$$k(t) \equiv k_0\mathrm{e}^{-\Delta(t)/3} \tag{6.17}$$

in such a way that the time evolution of $k_0\|\boldsymbol{x}\|$ is expressed as the transformation

$$k_0\|\boldsymbol{x}\| \mapsto k(t)\|(\boldsymbol{x} - \boldsymbol{o}(t))\|. \tag{6.18}$$

Relations (6.17) and (6.4*b*) imply that

$$-\frac{\dot{k}(t)}{k(t)} = \frac{\dot{\Delta}(t)}{3} = \frac{\delta(t)}{3} = -\frac{1}{2}\frac{\dot{\nu}(t)}{\nu(t)}, \tag{6.19}$$

and therefore, the relation between angular frequency $\nu(t)$ and wavenumber $k(t)$ is

$$\frac{\nu(t)}{\nu_0} = \frac{k^2(t)}{k_0^2}. \tag{6.20}$$

https://doi.org/10.1017/jfm.2026.11537 Published online by Cambridge University Press

As a consequence, the background velocity $\boldsymbol{u}_b(\boldsymbol{x}, t)$ (6.8a) can be written in terms of the radial wavenumber $k(t)$, or in terms of the angular velocity $\nu(t)$, as

$$\boldsymbol{u}_b(\boldsymbol{x}, t) = \dot{\boldsymbol{o}}(t) - \frac{\dot{k}(t)}{k(t)}(\boldsymbol{x} - \boldsymbol{o}(t)) + \frac{k^2(t)}{k_0^2}\nu_0\hat{\boldsymbol{v}}_0 \times (\boldsymbol{x} - \boldsymbol{o}(t)) \tag{6.21a}$$

$$= \dot{\boldsymbol{o}}(t) - \frac{1}{2}\frac{\dot{\nu}(t)}{\nu(t)}(\boldsymbol{x} - \boldsymbol{o}(t)) + \nu(t)\hat{\boldsymbol{v}}_0 \times (\boldsymbol{x} - \boldsymbol{o}(t)). \tag{6.21b}$$

The radial velocity $\dot{k}(t)/k(t)(\boldsymbol{x} - \boldsymbol{o}(t))$ in (6.21a, b) is a Hubble flow. This relation to the Hubble flow becomes explicit upon defining a dimensionless spatial scale factor $a(t)$ as

$$a(t) \equiv \frac{k_0}{k(t)}. \tag{6.22}$$

Using material coordinates (R, t), the flow map $\boldsymbol{r}_H(R, t)$ of this radial Hubble flow is

$$\boldsymbol{r}_H(R, t) = \frac{k_0}{k(t)}R\hat{\boldsymbol{r}} = Ra(t)\hat{\boldsymbol{r}}. \tag{6.23}$$

The velocity of the fluid particles is therefore

$$\tilde{\boldsymbol{u}}_H(R, t) = R\dot{a}(t)\hat{\boldsymbol{r}} = D(t)H(t)\hat{\boldsymbol{r}}, \quad D(t) \equiv Ra(t), \quad H(t) \equiv \frac{\dot{a}(t)}{a(t)}, \tag{6.24a,b,c}$$

which is the Hubble flow (Barnes *et al.* 2006) in a universe with dimensionless scale factor $a(t)$. Term $D(t)$ is called the proper distance between galaxies, and (6.24c) is the definition of the Hubble parameter $H(t)$. In this fluid mechanics description, the expansion of the space is interpreted as the expansion of the fluid by the background flow in which the Beltrami fields are frozen. The time dependence of the wavenumber $k(t)$ of the Beltrami field is used to describe this space expansion.

For example, we may consider Beltrami flows with spherical geometry in which the radial part is given by the spherical Bessel functions $j_\ell(k_0 r)$ and the angular part is given by the spherical harmonics $Y_\ell^m(\theta, \varphi)$. The corresponding function $\eta_0(\boldsymbol{x})$, simplifying $\boldsymbol{o}(t) = \boldsymbol{0}$, is

$$\eta_0(\boldsymbol{x}) = \sum_{\ell \geq 0} \sum_{|m| \leq \ell} \hat{\eta}_{\ell m} j_\ell\,(k_0 r)\, Y_\ell^m(\theta, \varphi), \tag{6.25}$$

where $\hat{\eta}_{\ell m}$ are constants. The simplest mode $\ell = 0$ is

$$\eta_0(\boldsymbol{x}) = \hat{\eta}_0 j_0(k_0 r), \tag{6.26}$$

which, using the CK procedure, leads to a Hicks–Moffatt spherical vortex spatially oriented along $\hat{\boldsymbol{n}}_0$. The next mode $\ell = 1$, in Cartesian coordinates, can be written as

$$\eta_0(\boldsymbol{x}) = j_1\,(k_0\|\boldsymbol{x}\|)\,\boldsymbol{k}_0 \cdot \frac{\boldsymbol{x}}{\|\boldsymbol{x}\|}. \tag{6.27}$$

Here, we have used the unnormalised real spherical harmonics of order $\ell = 1$ and degree $m = \{-1, 0, 1\}$, which are x/r, y/r and z/r, with $r \equiv \|\boldsymbol{x}\|$. The arbitrary constant $\hat{\eta}_1$ can be used to normalise the radial wavevector $|\hat{\boldsymbol{k}}_0| = 1$. In this case, the time-dependent seed function $\eta(\boldsymbol{x}, t)$ becomes

https://doi.org/10.1017/jfm.2026.11537 Published online by Cambridge University Press

$$\eta(\boldsymbol{x},t)=\left(\frac{k(t)}{k_0}\right)^3 j_1\left(k(t)\|\boldsymbol{x}-\boldsymbol{c}(t)\|\right)\frac{\boldsymbol{k}(t)\cdot(\boldsymbol{x}-\boldsymbol{c}(t))}{|k(t)|\|\boldsymbol{x}-\boldsymbol{c}(t)\|}$$
$$=\left(\frac{k(t)}{k_0}\right)^3 j_1\left(k(t)\|\boldsymbol{x}-\boldsymbol{c}(t)\|\right)\hat{\boldsymbol{k}}(t)\cdot\frac{\boldsymbol{x}-\boldsymbol{c}(t)}{\|\boldsymbol{x}-\boldsymbol{c}(t)\|}. \tag{6.28}$$

This represents a field $\eta_0(\boldsymbol{x})$ that is displacing with velocity $\boldsymbol{c}(t)$, whose radial part is expanding/contracting by the presence of the time-dependent wavenumber $k(t)$ in the spherical Bessel function $j_1(\cdot)$, and whose angular part is rotating by the time-dependent unit vector $\hat{\boldsymbol{k}}(t)$, which describes the precession of the Beltrami field.

The same interpretation may be applied to the Beltrami fields in different geometries, and therefore flow expansion/contraction and flow precession are general properties of the Beltrami fields in the presence of a background velocity field with homogeneous but time-dependent divergence $\delta(t)$ and vorticity $2\boldsymbol{v}(t)$. In this background flow, the angular velocity $\boldsymbol{v}(t)$ cannot change direction $\hat{\boldsymbol{v}}$ and, therefore, the displacement velocity of the Beltrami field $\boldsymbol{c}(t)=2\boldsymbol{v}(t)/k_0$ cannot change its direction either. Changes in the direction of the displacement velocity of the Beltrami field $\boldsymbol{c}(t)$ are related to the presence of a background deviatoric deformation gradient tensor $\mathsf{D}_0(t)\neq\mathsf{0}$. An example of this possibility is considered in the next subsection.

6.2. *Deviatoric deformation gradient* $\mathsf{D}_0(t)$ *is diagonalisable in the same basis*

We consider in this section a deviatoric tensor $\mathsf{D}_0(t)\neq\mathsf{0}$ and assume the Beltrami field approximation. In the case where the deviatoric deformation gradient tensor $\mathsf{D}_0(t)$ is diagonalisable in the same basis at all times,

$$\mathsf{D}_0(t)=\sum_{i=1}^{3}\lambda_i(t)\hat{\boldsymbol{e}}_i\otimes\hat{\boldsymbol{e}}_i,\quad\text{with}\quad\sum_{i=1}^{3}\lambda_i(t)=0, \tag{6.29a,b}$$

the deviatoric deformation gradient $\mathsf{D}_0(t)$ commutes with itself at all times,

$$[\mathsf{D}_0(t_1),\mathsf{D}_0(t_2)]\equiv\mathsf{D}_0(t_1)\mathsf{D}_0(t_2)-\mathsf{D}_0(t_2)\mathsf{D}_0(t_1)=\mathsf{0}\quad\text{for all } t_1,t_2. \tag{6.30}$$

This condition implies that we can avoid the time-ordered exponential integral in (3.15) and obtain that the isochoric dependence of the background angular velocity $\boldsymbol{v}_D(t)$ is given by

$$\boldsymbol{v}_D(t)=\mathrm{e}^{\boldsymbol{\Delta}_0(t)}\boldsymbol{v}(0),\quad\text{where}\quad\boldsymbol{\Delta}_0(t)\equiv\int_0^t\mathsf{D}_0(\tau)\,\mathrm{d}\tau. \tag{6.31a,b}$$

This relation provides the dynamical dependence that $\boldsymbol{v}_D(t)$ and $\mathsf{D}_0(t)$ must satisfy for the background flow to be a solution to the vorticity equation.

The next step is to obtain the relation between $\boldsymbol{v}_D(t)$ and the principal deviatoric stretches $\lambda_i(t)$. To do so, we define the tensor

$$\mathsf{A}(t)\equiv\mathsf{D}_0(t)-\frac{2}{3}\delta(t)\mathsf{I}, \tag{6.32}$$

in terms of which the vorticity equation for the background flow is expressed as

$$\dot{\boldsymbol{v}}(t)=\mathsf{A}(t)\boldsymbol{v}(t). \tag{6.33}$$

https://doi.org/10.1017/jfm.2026.11537 Published online by Cambridge University Press

Defining the angular velocity components along the direction of the principal stretches

$$\nu_i(t) \equiv \boldsymbol{\nu}(t) \cdot \hat{\boldsymbol{e}}_i, \quad \text{so that} \quad \boldsymbol{\nu}(t) = \sum_{i=1}^{3} \nu_i(t) \hat{\boldsymbol{e}}_i, \tag{6.34a,b}$$

we obtain the decoupled ordinary differential equations for the angular velocity components $\nu_i(t)$ along the deviatoric stretching directions,

$$\dot{\nu}_i(t) = \left(\lambda_i(t) - \frac{2}{3}\delta(t) \right) \nu_i(t) \quad \text{for } i = 1, 2, 3, \tag{6.35}$$

which have the solutions

$$\nu_i(t) = \mathrm{e}^{-\frac{2}{3}\Delta(t)} \mathrm{e}^{\Lambda_i(t)} \nu_i(0), \quad \text{where} \quad \Lambda_i(t) \equiv \int_0^t \lambda_i(\tau)\, \mathrm{d}\tau. \tag{6.36a,b}$$

Thus, the time evolution of the background angular velocity vector is given by

$$\boldsymbol{\nu}(t) = \mathrm{e}^{-\frac{2}{3}\Delta(t)} \sum_{i=1}^{3} \nu_i(0) \mathrm{e}^{\Lambda_i(t)} \hat{\boldsymbol{e}}_i, \tag{6.37}$$

which provides the background angular velocity in terms of the time-integrated principal deviatoric stretches $\Lambda_i(t)$ and time-integrated divergence $\Delta(t)$. The background expansion/contraction $\delta(t)$ affects the amplitude of the angular velocity, while the deviatoric stretches affect the components of $\boldsymbol{\nu}(t)$ along the principal deviatoric directions.

The changes of $\nu_i(t)$ related to the changes of $\lambda_i(t)$ are not independent since the deviatoric stretches must satisfy the condition $\lambda_1 + \lambda_2 + \lambda_3 = 0$. To avoid this lack of independence, we may include the isotropic expansion in the effective stretches

$$\bar{\lambda}_i(t) \equiv \lambda_i(t) - \frac{2}{3}\delta(t), \tag{6.38}$$

so that

$$\boldsymbol{\nu}(t) = \sum_{i=1}^{3} \nu_i(0) \mathrm{e}^{\bar{\Lambda}_i(t)} \hat{\boldsymbol{e}}_i, \quad \text{where} \quad \bar{\Lambda}_i(t) \equiv \int_0^t \bar{\lambda}_i(\tau)\, \mathrm{d}\tau, \tag{6.39a,b}$$

where now the three effective stretches $\bar{\lambda}_i(t)$ are free parameters. Thus, the components of $\boldsymbol{\nu}(t)$ along the principal deviatoric strain directions change exponentially according to $\exp(\bar{\Lambda}_i(t))$. The direction of $\boldsymbol{\nu}(t)$ changes, unless the growth rates $\bar{\lambda}_i(t)$ along each direction are all equal, which would imply an isotropic expansion, or $\boldsymbol{\nu}(t)$ is initially aligned with a single eigenvector $\hat{\boldsymbol{e}}_N$, so that $\nu_i(0) = 0$, for $i \neq N$. In any other cases, the background angular velocity vector $\boldsymbol{\nu}(t)$, and hence the background vorticity vector $\boldsymbol{\omega}_b(t) = 2\boldsymbol{\nu}(t)$, align over time with the fastest-growing eigen-direction $\hat{\boldsymbol{e}}_M$, that is, along the direction having the largest eigenvalue $\bar{\lambda}_M(t) \equiv \max\{\bar{\lambda}_1(t), \bar{\lambda}_2(t), \bar{\lambda}_3(t)\}$. When $\boldsymbol{\nu}(t)$ is initially aligned with a single eigenvector $\hat{\boldsymbol{e}}_N \in \{\hat{\boldsymbol{e}}_1, \hat{\boldsymbol{e}}_2, \hat{\boldsymbol{e}}_3\}$, the background angular velocity $\boldsymbol{\nu}(t) = \nu_N(t)\hat{\boldsymbol{e}}_N$ preserves its direction along $\hat{\boldsymbol{e}}_N$ and scales exponentially. If the initial orientation of the background angular velocity does not correspond to the direction of the largest effective stretching $\hat{\boldsymbol{e}}_N \neq \hat{\boldsymbol{e}}_M$, any small perturbation at a given time t_1 $\delta\nu_M(t_1) \neq 0$ involving a change in the background angular velocity $\boldsymbol{\nu}(t_1)$ in the direction of $\hat{\boldsymbol{e}}_M$ equal to $\delta\nu_M(t_1)\hat{\boldsymbol{e}}_M$, will produce an exponential change of $\delta\nu_M(t_1)$, and therefore the state $\boldsymbol{\nu}(t) = \boldsymbol{\nu}_N(t)\hat{\boldsymbol{e}}_N$ is unstable.

We consider now a unidirectional velocity of the Beltrami field. In the particular case of isochoric background motion $\delta(t) = 0$, a unidirectional velocity of a Beltrami field

https://doi.org/10.1017/jfm.2026.11537 Published online by Cambridge University Press

described by the drift $\boldsymbol{c}(t) = 2\boldsymbol{v}(t)/k_0$ would imply

$$\delta(t) = 0, \quad \lambda_z(t) = -\lambda_x(t) - \lambda_y(t). \tag{6.40}$$

Consequently, the time evolution of the components of the angular velocity $\boldsymbol{v}(t)$ are

$$v_x(t) = v_x(0)\mathrm{e}^{\Lambda_x(t)}, \quad v_x(t) = v_y(0)\mathrm{e}^{\Lambda_y(t)}, \quad v_z(t) = v_z(0)\mathrm{e}^{-\Lambda_x(t)-\Lambda_y(t)}. \tag{6.41}$$

In this case, unidirectional velocity is possible if the angular velocity vector $\boldsymbol{v}(0)$ at $t = 0$ is aligned with one of the strain directions $\hat{\boldsymbol{v}} = \hat{\boldsymbol{e}}_{\hat{\imath}}$ for some $\hat{\imath} = \{1, 2, 3\}$. To avoid the growth of the angular velocity components along the normal strain directions the stretches should be negative, say $\Lambda_x(t) < 0$ and say $\Lambda_y(t) < 0$, but this would imply $-\Lambda_x(t) - \Lambda_y(t) > 0$ and therefore the exponential growth of $v_z(t)$. However, for compressible background flows, $\delta(t) \neq 0$, we may set

$$\lambda_x(t) = \lambda_y(t) = \frac{2}{3}\delta(t), \quad \lambda_z(t) = -\frac{4}{3}\delta(t), \tag{6.42}$$

so that

$$\dot{v}_x(t) = \dot{v}_y(t) = 0, \quad \dot{v}_z(t) = -2\delta(t)v_z(t), \tag{6.43}$$

and therefore,

$$v_x(t) = v_x(0), \quad v_y(t) = v_y(0), \quad v_z(t) = v_z(0)\mathrm{e}^{-2\Delta(t)}. \tag{6.44}$$

In this case, the isotropic expansion/contraction cancels the normal stretches along the $\hat{\boldsymbol{x}}$ and $\hat{\boldsymbol{y}}$ directions, and increases/decreases the stretch along the $\hat{\boldsymbol{z}}$ direction, and only the $\hat{\boldsymbol{z}}$ component of the angular background velocity $v_z(t)$ is time-dependent.

7. Elastic scattering of Beltrami fields in the Beltrami field approximation

Scattering usually refers to the process by which particles or waves are deflected from their straight path due to interactions with other particles or non-uniformities in a medium, involving a change in the direction, and sometimes energy, of the incoming particle or wave. Usually, the medium is a steady inhomogeneous field. However, we may investigate scattering of a Beltrami field $\boldsymbol{\mathcal{U}}(\boldsymbol{x}, t)$ by an unsteady homogeneous velocity field $\boldsymbol{u}_b(\boldsymbol{x}, t)$, under the Beltrami field approximation, assuming that, if the amplitude of the Beltrami flow decays to zero at distances far from the Beltrami field centre, as it happens with spherical Beltrami flows, what the Beltrami vortex experiences along its path is a temporal change in the background homogeneous flow. The process of elastic scattering of a Lamb–Chaplygin dipole (Lamb 1895; Chaplygin 1903, 2007), a particular case of finite size Beltrami flow in two dimensions, by a background potential flow generated by a central vortex, has been numerically investigated in two-dimensional flows (Zoeller & Viúdez 2023). These results show that the Lamb–Chaplygin dipole experiences small deformations during the elastic scattering interaction.

As a particular example of scattering, we consider the case in which the background angular velocity $\boldsymbol{v}(t)$ evolves from an initial value, say $\boldsymbol{v}_1 = v_1\hat{\boldsymbol{e}}_1$ at $t = t_1$, to a final value $\boldsymbol{v}_2 = v_2\hat{\boldsymbol{e}}_2$ at $t = t_2$. Changes in the background angular velocity require, to be consistent with the vorticity equation, the presence of a deviatoric tensor $\mathsf{D}_0(t)$ and, hence, we take in this section the assumption of the Beltrami field approximation. The objective is to define the background velocity field $\boldsymbol{v}_b(\boldsymbol{x}, t)$ that, satisfying the vorticity equation, accelerates the Beltrami field. For simplicity, we assume isochoric background flow $\delta(t) = 0$. Next, we may define a scalar function $s(t)$ such that $s(t_1) = 0$ and $s(t_2) = 1$ to model a smooth

https://doi.org/10.1017/jfm.2026.11537 Published online by Cambridge University Press

transition between the scattering angular velocities. For example,

$$s_1(t) \equiv \frac{1}{2}\left(1 + \tanh(\mu_0 t)\right) \in (0,\, 1), \quad \mu_0 > 0, \tag{7.1}$$

so that $s(t) \to 0$ as $t \to -\infty$ and $s(t) \to 1$ as $t \to +\infty$. Using the functions $s_\nu(t)$ and $s_\theta(t)$, the angular velocity component $\nu(t)$ and phase $\theta_\nu(t)$ evolve as

$$\nu(t) = \nu_1 + (\nu_2 - \nu_1)s_\nu(t), \quad \theta_\nu(t) = \theta_2 + (\theta_2 - \theta_1)s_\theta(t). \tag{7.2}$$

Next, we define the time-dependent background angular velocity,

$$\boldsymbol{\nu}(t) \equiv \nu(t)\left(\sin\left(\theta_\nu(t)\right)\hat{\boldsymbol{x}}\right) + \left(\cos\left(\theta_\nu(t)\right)\hat{\boldsymbol{z}}\right). \tag{7.3}$$

The rates of change of the frequency and direction are defined as

$$\alpha_\nu(t) \equiv \frac{\dot{\nu}(t)}{\nu(t)} \quad \text{and} \quad \beta_\nu(t) \equiv \dot{\theta}_\nu(t). \tag{7.4a,b}$$

We seek solutions $\boldsymbol{\nu}(t)$ to the vorticity equation such that $\alpha_\nu(t) \to 0$ and $\beta_\nu(t) \to 0$ as $t \to \pm\infty$. Defining the orthonormal vectors $\{\hat{\boldsymbol{\nu}}(t),\, \hat{\boldsymbol{\nu}}_\perp(t)\}$ in the xz-plane as

$$\hat{\boldsymbol{\nu}}(t) \equiv \sin(\theta_\nu(t))\hat{\boldsymbol{x}} + \cos(\theta_\nu(t))\hat{\boldsymbol{z}}, \quad \hat{\boldsymbol{\nu}}_\perp(t) \equiv \cos(\theta_\nu(t))\hat{\boldsymbol{x}} - \sin(\theta_\nu(t))\hat{\boldsymbol{z}}, \tag{7.5a,b}$$

the rate of change of $\nu(t)$ and $\hat{\boldsymbol{\nu}}(t)$ are

$$\boldsymbol{\nu}(t) = \nu(t)\hat{\boldsymbol{\nu}}(t) \quad \text{and} \quad \dot{\hat{\boldsymbol{\nu}}}(t) = \dot{\theta}_\nu(t)\hat{\boldsymbol{\nu}}_\perp(t), \tag{7.6a,b}$$

so that the rate of change of $\boldsymbol{\nu}(t)$ is

$$\dot{\boldsymbol{\nu}}(t) = \dot{\nu}(t)\hat{\boldsymbol{\nu}}(t) + \nu(t)\dot{\theta}_\nu(t)\hat{\boldsymbol{\nu}}_\perp(t). \tag{7.7}$$

Then, a simple deviatoric strain tensor $\mathsf{D}_0(t)$ satisfying the compatibility condition,

$$\mathsf{D}_0\boldsymbol{\nu} = \dot{\boldsymbol{\nu}} = \dot{\nu}\hat{\boldsymbol{\nu}} + \nu\dot{\theta}_\nu\hat{\boldsymbol{\nu}}_\perp, \tag{7.8}$$

may be written, in tensor form, as

$$\mathsf{D}_0 = \alpha_\nu\left(\hat{\boldsymbol{\nu}} \otimes \hat{\boldsymbol{\nu}} - \hat{\boldsymbol{\nu}}_\perp \otimes \hat{\boldsymbol{\nu}}_\perp\right) + \beta_\nu\left(\hat{\boldsymbol{\nu}} \otimes \hat{\boldsymbol{\nu}}_\perp + \hat{\boldsymbol{\nu}}_\perp \otimes \hat{\boldsymbol{\nu}}\right). \tag{7.9}$$

It may be checked out that $\mathrm{tr}\mathsf{D}_0 = 0$, $\mathsf{D}_0^\top = \mathsf{D}_0$ and that $\mathsf{D}_0\boldsymbol{\nu} = \dot{\boldsymbol{\nu}}$. Since, for the example of smooth function $s_1(t)$ given by (7.1), its time derivative

$$\dot{s}_1(t) = \frac{\mu_0}{2}\mathrm{sech}^2(\mu_0 t) \tag{7.10}$$

decays at both ends $t \to \pm\infty$, we have $\alpha_\nu(t) \to 0$ and $\beta_\nu(t) \to 0$ as $t \to \pm\infty$, and therefore, $\mathsf{D}_0(t) \to \mathsf{0}$ as $t \to \pm\infty$. Thus, $\mathsf{D}_0(t)$ is a localised-in-time strain pulse that smoothly re-orients the angular velocity $\boldsymbol{\nu}(t)$. The velocity gradient L of the background flow is

$$\mathsf{L} = \alpha_\nu\left(\hat{\boldsymbol{\nu}} \otimes \hat{\boldsymbol{\nu}} - \hat{\boldsymbol{\nu}}_\perp \otimes \hat{\boldsymbol{\nu}}_\perp\right) + \beta_\nu\left(\hat{\boldsymbol{\nu}} \otimes \hat{\boldsymbol{\nu}}_\perp + \hat{\boldsymbol{\nu}}_\perp \otimes \hat{\boldsymbol{\nu}}\right) + \nu\left(\hat{\boldsymbol{y}} \otimes \hat{\boldsymbol{\nu}}_\perp - \hat{\boldsymbol{\nu}}_\perp \otimes \hat{\boldsymbol{y}}\right). \tag{7.11}$$

In the $\hat{\boldsymbol{\nu}}$–$\hat{\boldsymbol{\nu}}_\perp$ plane, the deviatoric strain tensor $\mathsf{D}_0(t)$ (7.9) is

$$\mathsf{D}_0|_{plane} = \begin{pmatrix} \alpha_\nu & \beta_\nu \\ \beta_\nu & -\alpha_\nu \end{pmatrix}, \tag{7.12}$$

whose eigenvalues $\lambda_\pm(t)$ are

$$\lambda_\pm(t) \equiv \pm\sigma_\nu(t), \quad \text{where} \quad \sigma_\nu(t) \equiv \sqrt{\alpha_\nu^2(t) + \beta_\nu^2(t)}. \tag{7.13a,b}$$

https://doi.org/10.1017/jfm.2026.11537 Published online by Cambridge University Press

The eigenvector $\hat{\boldsymbol{e}}_M$ for the largest eigenvalue $\lambda_+ = +\sigma_v$ is

$$\hat{\boldsymbol{e}}_{\mathrm{M}} \propto \beta_v \hat{\boldsymbol{v}} + (\sigma_v - \alpha_v)\hat{\boldsymbol{v}}_\perp. \tag{7.14}$$

The objective now is to find the inverse map $\boldsymbol{R}_v(\boldsymbol{x}, t)$ of the background advecting velocity

$$\boldsymbol{v}_b(\boldsymbol{x}, t) = \mathsf{D}_0(t)\boldsymbol{x} + \boldsymbol{v}(t) \times \boldsymbol{x} = \mathsf{A}(t)\boldsymbol{x}, \quad \text{where} \quad \mathsf{A}(t) \equiv \mathsf{D}_0(t) + [\boldsymbol{v}(t)\times], \tag{7.15a,b}$$

or in material variables,

$$\dot{\boldsymbol{r}} = \mathsf{A}(t)\boldsymbol{r}. \tag{7.16}$$

To find the deformation gradient $\mathsf{F}(t)$, we work in the time-dependent frame with unit vectors $\{\hat{\boldsymbol{v}}(t), \hat{\boldsymbol{y}}, \hat{\boldsymbol{v}}_\perp(t)\}$ that co-rotates around the $\boldsymbol{y}$-axis. To do this, we define the rotation tensor $\mathsf{Q}(t)$ about the $\boldsymbol{y}$-axis, normal to $\hat{\boldsymbol{v}}$ and $\hat{\boldsymbol{v}}_\perp$, by an angle $\theta_v(t)$,

$$\mathsf{Q}(t) \equiv \mathsf{R}_{\boldsymbol{y}}(\theta_v(t)) = \begin{pmatrix} \cos(\theta_v(t)) & 0 & \sin(\theta_v(t)) \\ 0 & 1 & 0 \\ -\sin(\theta_v(t)) & 0 & \cos(\theta_v(t)) \end{pmatrix}, \tag{7.17}$$

whose value at $t = t_1$ is $\mathsf{Q}(t_1) = \mathsf{R}_{\boldsymbol{y}}(\theta_1)$. We introduce the vector $\boldsymbol{\xi}$ in the rotated frame

$$\boldsymbol{\xi} \equiv \mathsf{Q}^\top \boldsymbol{r}, \quad \boldsymbol{r} = \mathsf{Q}\boldsymbol{\xi} \quad , \tag{7.18a,b}$$

and therefore,

$$\dot{\boldsymbol{\xi}} = \hat{\mathsf{A}}\boldsymbol{\xi}, \quad \hat{\mathsf{A}} \equiv \mathsf{Q}^\top \mathsf{A}\mathsf{Q} - \mathsf{Q}^\top \dot{\mathsf{Q}}, \tag{7.19a,b}$$

expresses the rate of change of $\boldsymbol{\xi}$ in terms of the tensor $\hat{\mathsf{A}}(t)$. In this tilted reference frame, we introduce an orthogonal basis vector $\{\hat{\boldsymbol{e}}_x, \hat{\boldsymbol{e}}_y, \hat{\boldsymbol{e}}_z\}$ such that the vectors $\hat{\boldsymbol{v}}(t) \mapsto \hat{\boldsymbol{e}}_z$ and $\hat{\boldsymbol{v}}_\perp(t) \mapsto \hat{\boldsymbol{e}}_x$, and the different terms in (7.19) are

$$\mathsf{Q}^\top \mathsf{D}_0 \mathsf{Q} = \alpha_v(t)\left(\hat{\boldsymbol{e}}_z \otimes \hat{\boldsymbol{e}}_z - \hat{\boldsymbol{e}}_x \otimes \hat{\boldsymbol{e}}_x\right) + \beta_v(t)\left(\hat{\boldsymbol{e}}_z \otimes \hat{\boldsymbol{e}}_x + \hat{\boldsymbol{e}}_x \otimes \hat{\boldsymbol{e}}_z\right), \tag{7.20a}$$

$$\mathsf{Q}^\top [\boldsymbol{v}\times] \mathsf{Q} = [v\hat{\boldsymbol{e}}_z\times] = v\left(\hat{\boldsymbol{e}}_y \otimes \hat{\boldsymbol{e}}_x - \hat{\boldsymbol{e}}_x \otimes \hat{\boldsymbol{e}}_y\right), \tag{7.20b}$$

$$\mathsf{Q}^\top \dot{\mathsf{Q}} = [\beta_v \hat{\boldsymbol{e}}_y \times] = \beta_v\left(\hat{\boldsymbol{e}}_x \otimes \hat{\boldsymbol{e}}_z - \hat{\boldsymbol{e}}_z \otimes \hat{\boldsymbol{e}}_x\right). \tag{7.20c}$$

Therefore, in the $\{\hat{\boldsymbol{e}}_x, \hat{\boldsymbol{e}}_y, \hat{\boldsymbol{e}}_z\}$ basis, the tensor $\hat{\mathsf{A}}(t)$ is

$$\hat{\mathsf{A}}(t) = \begin{bmatrix} -\alpha_v(t) & -v(t) & 0 \\ v(t) & 0 & 0 \\ 2\beta_v(t) & 0 & \alpha_v(t) \end{bmatrix}. \tag{7.21}$$

Let

$$\boldsymbol{\xi} = X\hat{\boldsymbol{e}}_x + Y\hat{\boldsymbol{e}}_y + Z\hat{\boldsymbol{e}}_z. \tag{7.22}$$

Equations (7.19) and (7.21) imply that the equations we need to solve are

$$\dot{X} = -\alpha_v X - vY, \quad \dot{Y} = vX, \quad \dot{Z} = 2\beta_v X + \alpha_v Z. \tag{7.23a,b,c}$$

From (7.23a,b), we obtain a separated relation for $Y(t)$,

$$\ddot{Y}(t) + \frac{\dot{v}(t)}{v(t)}\dot{Y}(t) + v(t)^2 Y(t) = 0. \tag{7.24}$$

https://doi.org/10.1017/jfm.2026.11537 Published online by Cambridge University Press

This is the equation for a parametric oscillator, where the time-dependent damping term is $\alpha_\nu = \dot{\nu}/\nu$. After the usual change of variable $\mathcal{Y}(t) \equiv \nu(t)^{1/2} Y(t)$, (7.24) transforms into

$$\ddot{\mathcal{Y}}(t) + \Omega^2(t)\mathcal{Y}(t) = 0, \quad \text{where} \quad \Omega^2 \equiv \nu^2 + \frac{1}{4}\left(\frac{\dot{\nu}}{\nu}\right)^2 - \frac{1}{2}\frac{\ddot{\nu}}{\nu}. \tag{7.25a,b}$$

The solution to (7.25*a*) depends on the particular form of $\nu(t)$. In the simple case of a linear time dependence,

$$\nu(t) = \nu_1 + \mu_0(t - t_1), \quad \mu_0 \equiv \frac{\nu_2 - \nu_1}{t_2 - t_1}, \tag{7.26a,b}$$

and the damping term is

$$\alpha_\nu(t) = \frac{\dot{\nu}(t)}{\nu(t)} = \frac{\mu_0}{\nu(t)}. \tag{7.27}$$

In the case $\nu_2 \neq \nu_1$, the oscillator equation (7.24) simplifies to

$$\ddot{Y}(t) + \frac{1}{t - t_*}\dot{Y}(t) + \mu_0^2(t - t_*)^2 Y(t) = 0, \quad \text{with} \quad t_* \equiv t_1 - \nu_1/\mu_0, \tag{7.28}$$

and

$$\frac{\dot{\nu}(t)}{\nu(t)} = \frac{1}{t - t_*}. \tag{7.29}$$

Defining $z \equiv (\mu_0/2)(t - t_*)^2$, (7.28) transforms into

$$z^2\frac{d^2Y}{dz^2} + z\frac{dY}{dz} + z^2 Y = 0, \tag{7.30}$$

which is the Bessel equation of order zero, and therefore the fundamental solutions are

$$Y(t) = c_1 J_0\left(\frac{\mu_0}{2}(t - t_*)^2\right) + c_2 Y_0\left(\frac{\mu_0}{2}(t - t_*)^2\right). \tag{7.31}$$

The simplest case, however, is that in which the amplitude of the background angular velocity $\nu(t)$ is constant, that is, $\nu_2 = \nu_1 = \nu_0$, and the damping term vanishes $\alpha_\nu(t) = 0$. In this case, the parametric oscillator (7.24) simplifies to the undamped oscillator,

$$\ddot{Y}(t) + \nu_0^2 Y(t) = 0. \tag{7.32}$$

For undamped oscillations, the deformation gradient $\mathsf{F}_R(t; t_1)$ in the rotated reference frame is

$$\mathsf{F}_R(t; t_1) \equiv \begin{bmatrix} \cos\Theta(t) & -\sin\Theta(t) & 0 \\ \sin\Theta(t) & \cos\Theta(t) & 0 \\ A(t) & B(t) & 1 \end{bmatrix}, \quad \Theta(t) \equiv \nu_0(t - t_1), \quad \det\mathsf{F}_R = 1, \tag{7.33}$$

where the terms depending on the rate of change of the scattering angle $\beta_\nu(t) \equiv \dot{\theta}_\nu(t)$ are

$$A(t) \equiv 2\int_{t_1}^{t} \beta_\nu(\tau)\cos(\nu_0(\tau - t_1))\,\mathrm{d}\tau, \tag{7.34a}$$

$$B(t) \equiv -2\int_{t_1}^{t} \beta_\nu(\tau)\sin(\nu_0(\tau - t_1))\,\mathrm{d}\tau. \tag{7.34b}$$

https://doi.org/10.1017/jfm.2026.11537 Published online by Cambridge University Press

Then, the solution to (7.19) is

$$\boldsymbol{\xi}(t) = \boldsymbol{X}(t; t_1) = \mathsf{F}_R(t; t_1)\boldsymbol{X}_0. \tag{7.35}$$

In the co-rotating reference frame the effect of the deformation gradient $\mathsf{F}_R(t; t_1)$ on the XY-plane is a planar rotation with constant angular rate ν_0,

$$X(t) = X_0 \cos\Theta(t) - Y_0 \sin\Theta(t), \tag{7.36a}$$

$$Y(t) = X_0 \sin\Theta(t) + Y_0 \cos\Theta(t), \tag{7.36b}$$

where $\{X_0, Y_0, Z_0\} = \boldsymbol{\xi}(0) = \mathsf{Q}^\top(0)\boldsymbol{x}_0$. The coordinate $Z(t)$ of the particle along the instantaneous rotation axis $\hat{\boldsymbol{\nu}}(t)$ is

$$Z(t) = Z_0 + 2\int_{t_1}^{t} \beta_\nu(\tau)\,(X_0\cos\Theta(\tau) - Y_0\sin\Theta(\tau))\;\mathrm{d}\tau. \tag{7.37}$$

In fact, $Z(t) = \boldsymbol{\xi}(t)\cdot\hat{\boldsymbol{e}}_z = \hat{\boldsymbol{\nu}}(t)\cdot\boldsymbol{r}(t)$. The temporal change of $Z(t)$ is due to temporal change of angular velocity direction, $\beta_\nu(t) \equiv \dot{\theta}_\nu(t)$. Term $\beta_\nu(t)$ is associated with a tilt-induced shear. The term $2\beta_\nu X$ transforms transverse offset X, the coordinate along $\hat{\boldsymbol{e}}_x \mapsto \hat{\boldsymbol{\nu}}_\perp$, into axial motion. When the axis tilts ($\beta_\nu \neq 0$), points off the axis are pumped along $\hat{\boldsymbol{\nu}}$. Thus, $Z(t)$, is the projection of $\boldsymbol{r}(t)$ on the instantaneous angular-velocity direction.

We need the inverse deformation gradient $\mathsf{F}_R(t; t_1)^{-1}$ in the rotated frame, which, from (7.33), is

$$\mathsf{F}_R(t; t_1)^{-1} \equiv \begin{bmatrix} \cos\Theta(t) & \sin\Theta(t) & 0 \\ -\sin\Theta(t) & \cos\Theta(t) & 0 \\ -A(t)\cos\Theta(t) + B(t)\sin\Theta(t) & -A(t)\sin\Theta(t) - B(t)\cos\Theta(t) & 1 \end{bmatrix}. \tag{7.38}$$

Finally, the solutions, in the laboratory reference frame, for the deformation gradient and the flow map are

$$\mathsf{F}(t) = \mathsf{Q}(t)\mathsf{F}_R(t; t_1)\mathsf{Q}^\top(t_1), \quad \boldsymbol{r}_v(\boldsymbol{x}_0, t) = \mathsf{F}(t)\boldsymbol{x}_0, \tag{7.39a,b}$$

and the inverse deformation gradient and the inverse flow map are

$$\mathsf{F}^{-1}(t) = \mathsf{Q}(t_1)\mathsf{F}_R(t; t_1)^{-1}\mathsf{Q}^\top(t), \quad \boldsymbol{R}_v(\boldsymbol{x}, t) = \mathsf{F}(t)^{-1}\boldsymbol{x}. \quad \text{(a,b)} \tag{7.40a,b}$$

The inverse map $\boldsymbol{R}_v(\boldsymbol{x}, t)$ in (7.40b) is

$$\boldsymbol{R}_v(\boldsymbol{x}, t) = \mathsf{R}_{\boldsymbol{y}}(\theta_v(t_1))\mathsf{F}_R(t; t_1)^{-1}\mathsf{R}_{\boldsymbol{y}}(-\theta_v(t))\boldsymbol{x}, \tag{7.41}$$

which is the desired inverse flow map of the advecting flow $\boldsymbol{v}_b(\boldsymbol{x}, t)$ as a function of the initial θ_1 and final θ_2 scattering angles.

We provide next a graphical example of elastic scattering produced by a background velocity pulse with parameters $\theta_1 = \pi/2$ and $\theta_2 = \pi/4$. The scattering angle difference $\Delta\theta \equiv |\theta_2 - \theta_1| = \pi/4$ has been taken excessively large to visualise the deformation from the Beltrami initial flow. The initial time is $t_1 = 0$ and the final time is $t_2 = 1$. The angular frequency is $\nu_0 \equiv 2\pi$, so that the pulse lasts an interval time of one cycle. The wavenumber $k_0 = 1$. The background angular velocity is

$$\boldsymbol{v}(t) = 2\pi\left(\cos\left(\frac{\pi}{4}t\right)\hat{\boldsymbol{x}} + \sin\left(\frac{\pi}{4}t\right)\hat{\boldsymbol{z}}\right), \quad t \subset [0, 1]. \tag{7.42}$$

$$\boldsymbol{v}(t_1) = \nu_0\hat{\boldsymbol{x}} \quad \text{and} \quad \boldsymbol{v}(t_2) = \frac{\sqrt{2}}{2}\nu_0(\hat{\boldsymbol{x}} + \hat{\boldsymbol{y}}), \quad |\boldsymbol{v}(t_1)| = |\boldsymbol{v}(t_2)| = |\nu_0|. \tag{7.43a,b,c}$$

https://doi.org/10.1017/jfm.2026.11537 Published online by Cambridge University Press

The scattering angle $\theta(t)$ and its rate of change $\dot{\theta}(t)$ are

$$\theta(t) \equiv \theta_1 + \beta_v (t - t_1), \quad \dot{\theta} = \beta_v = \frac{\theta_2 - \theta_1}{t_2 - t_1} = -\frac{\pi}{4}. \tag{7.44}$$

The rotation tensors are

$$\mathsf{Q}(t) = \begin{pmatrix} \sin(\pi t/4) & 0 & \cos(\pi t/4) \\ 0 & 1 & 0 \\ -\cos(\pi t/4) & 0 & \sin(\pi t/4) \end{pmatrix}, \quad \mathsf{Q}(0) = \begin{pmatrix} 0 & 0 & 1 \\ 0 & 1 & 0 \\ -1 & 0 & 0 \end{pmatrix}, \tag{7.45}$$

and the Z-stretchings in the tilted reference frame are

$$A(t; t_1) = -\frac{1}{4}\sin(2\pi t) \quad \text{and} \quad B(t; t_1) = \frac{1}{2}\left(\sin(\pi t)\right)^2. \tag{7.46a,b}$$

The deformation gradient $\mathsf{F}_R(t)$ in the tilted reference frame is

$$\mathsf{F}_R(t) = \begin{pmatrix} \cos(2\pi t) & -\sin(2\pi t) & 0 \\ \sin(2\pi t) & \cos(2\pi t) & 0 \\ -\dfrac{1}{4}\sin(2\pi t) & \dfrac{1}{2}\sin^2(\pi t)) & 1 \end{pmatrix}, \tag{7.47}$$

and its inverse $\mathsf{F}_R(t)^{-1}$ is

$$\mathsf{F}_R(t)^{-1} = \begin{pmatrix} \cos(2\pi t) & \sin(2\pi t) & 0 \\ -\sin(2\pi t) & \cos(2\pi t) & 0 \\ \dfrac{1}{4}\sin(2\pi t) & \dfrac{1}{2}\sin^2(\pi t)) & 1 \end{pmatrix}, \tag{7.48}$$

and, finally, the inverse map of the advecting flow $\boldsymbol{v}_b(\boldsymbol{x}, t)$ is

$$\boldsymbol{R}_v(\boldsymbol{x}, t) = \mathsf{Q}(0)\mathsf{F}_R(t)^{-1}\mathsf{Q}(t)^{\top}\boldsymbol{x}, \quad t \subset [0, 1]. \tag{7.49}$$

In the following figures, we represent contours or isosurfaces of $\eta(\boldsymbol{x}, t) \equiv \eta_{s1}(\boldsymbol{R}_v(\boldsymbol{x}, t))$ where the seed function,

$$\eta_{S1}(\boldsymbol{x}) = j_1(k_0\|\boldsymbol{x}\|)\boldsymbol{k}_0 \cdot \frac{\boldsymbol{x}}{\|\boldsymbol{x}\|}, \tag{7.50}$$

is representative of the spherical Beltrami vortex of order $\ell = 1$ (Viúdez 2025*c*). The order $\ell = 0$ function $\eta_{S0}(\boldsymbol{x}) = j_0(k_0\|\boldsymbol{x}\|)$ is also representative of the spherical Beltrami vortex of order $\ell = 1$, but the precession of the vortex, that is, the rotation of the wavevector $\boldsymbol{k}(t)$, and its initial orientation is better described by $\eta_{S1}(\boldsymbol{x})$.

We visualise two examples of scattering. In the first example (figures 1, 3(*a*) and 4), the vortex is initially aligned along the $\hat{\boldsymbol{z}}$-axis, that is, $\boldsymbol{k}_0 = \hat{\boldsymbol{z}}$ and therefore $\boldsymbol{k}_0 \perp \boldsymbol{v}(0)$, and the vortex precesses around the axis defined by $\boldsymbol{v}(t)$, which is its instantaneous direction of propagation. In the second example (figures 2, 3(*b*) and 5), the vortex is initially aligned along the $\hat{\boldsymbol{x}}$-axis, that is, $\boldsymbol{k}_0 = \hat{\boldsymbol{x}}$, and therefore $\boldsymbol{k}_0 \parallel \boldsymbol{v}(0)$, and the vortex does not precess around its direction of propagation.

The initial ($t = 0$), middle ($t = 1/2$) and final ($t = 1$) distributions of $\eta(\boldsymbol{x}, t)$ on different planes (figures 1 and 2) display the distortion of the spherical vortex at $t = 1/2$, which implies its departure from a Beltrami field, and its recovery at the end of the background pulse. The final state is the same spherical Beltrami field, but whose wavevector has rotated $\pi/4$ in the x–z plane. The vortex precession is visualised as a double spiral isosurfaces of $\eta(\boldsymbol{x}, t) = \pm\eta_0$ in the space (y, z, t) in figure 3(*a*), The vortex departure

https://doi.org/10.1017/jfm.2026.11537 Published online by Cambridge University Press

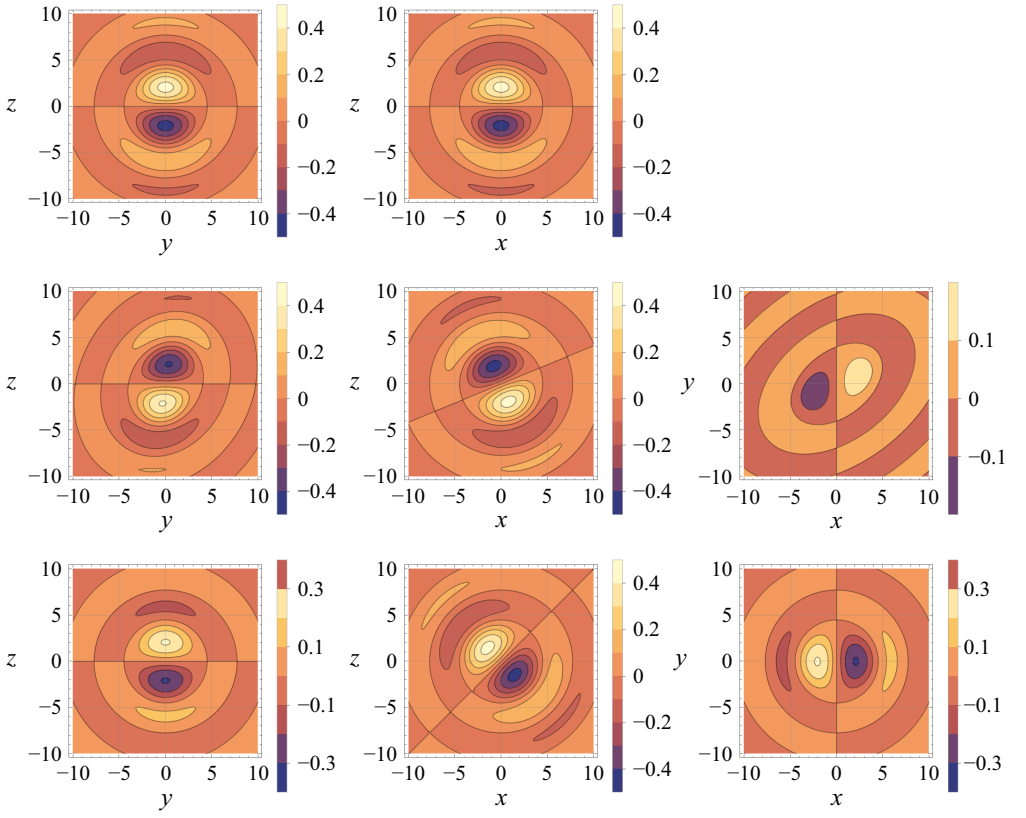


Figure 1. Time evolution of the distributions of $\eta(0, y, z, t)$ (left column), $\eta(x, 0, z, t)$ (central column) and $\eta(x, y, 0, t)$ (right column), in the case the spherical spin $\ell = 1$ vortex dipole is initially aligned along the z-axis, that is, $\hat{\boldsymbol{k}}_0 = \hat{\boldsymbol{z}}$, at the initial time $t = 0$ (top row), $t = 1/2$ (middle row) and $t = 1$ (bottom row). The initial distribution of $\eta(x, y, 0, 0) = 0$ is not included. We notice the evolution of $\eta(x, 0, z, t)$ in the x–z plane (mid column) is just a rotation of the field. The vortex recovers its spherical geometry at $t = 1$ (bottom row). These distributions are plotted in the frame in which $\boldsymbol{c}(t) = \boldsymbol{0}$.

from its initial spherical Beltrami configuration is visualised better in the non-precessing case from isosurfaces of $\eta(\boldsymbol{x}, t) = \pm\eta_0$ in the space (y, z, t) in figure 3(b). The vortex scattering, in both examples, can be visualised from the superposition of isosurfaces of $\eta(\boldsymbol{x}, t_i) = \pm\eta_0$ at different times t_i in figures 4 and 5. The large deformation of the isosurfaces at $t = 1/2$, relative to those at $t = 0$ and $t = 1$, is due to the large differential scattering angle $\Delta\theta = \pi/2$ prescribed. Smaller values of $\Delta\theta$, typical of forward scattering, would provide much smaller deformations.

8. Concluding remarks

We have provided in this work exact and approximate solutions to the barotropic vorticity equation in which the time evolution of a Beltrami field $\boldsymbol{\mathcal{U}}(\boldsymbol{x}, t)$, independently of its particular geometry, is completely determined by the presence of a time-dependent linear background flow. In particular, the Beltrami field may precess, expand/contract and displace, due to the presence of a background velocity field $\boldsymbol{u}_b(\boldsymbol{x}, t)$ whose velocity gradient consists of an isotropic time-dependent expansion/contraction and a homogeneous time-dependent rotation. In this case, the dynamical constraint for the

https://doi.org/10.1017/jfm.2026.11537 Published online by Cambridge University Press

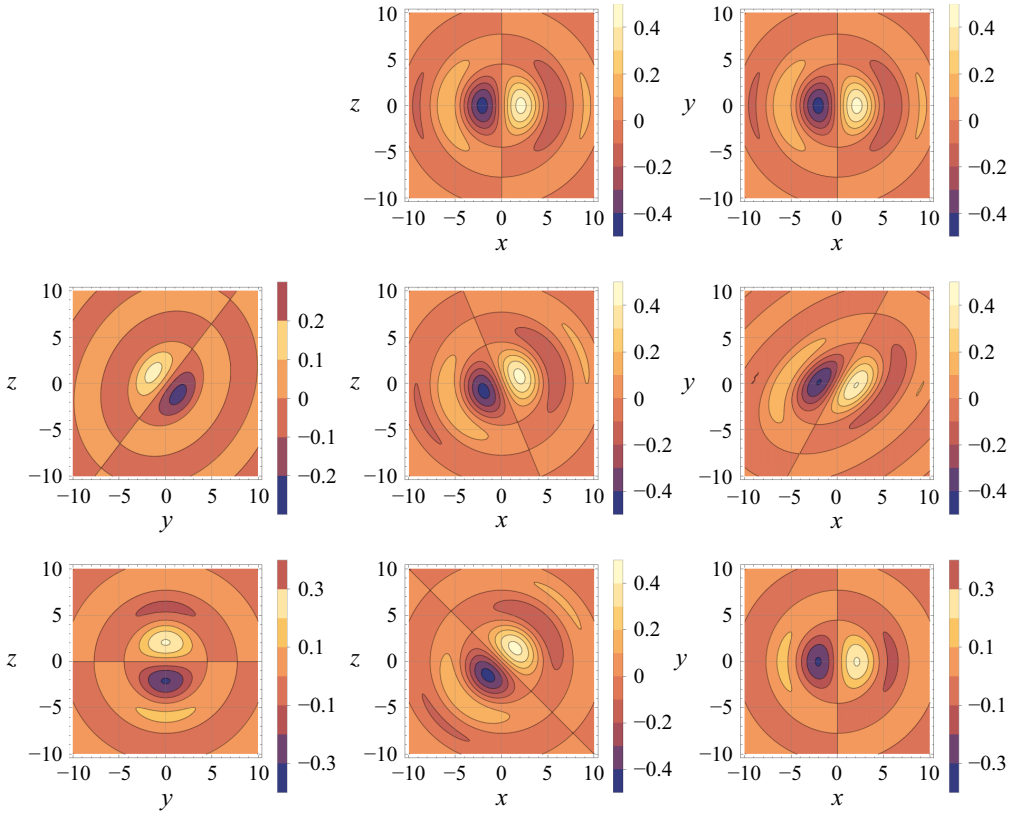


Figure 2. Same as figure 1, but in the case the spherical spin $\ell = 1$ vortex dipole is initially aligned along the x-axis, that is, $\hat{\boldsymbol{k}}_0 = \hat{\boldsymbol{x}}$. The initial distribution of $\eta(0, y, z, 0) = 0$ is not included.

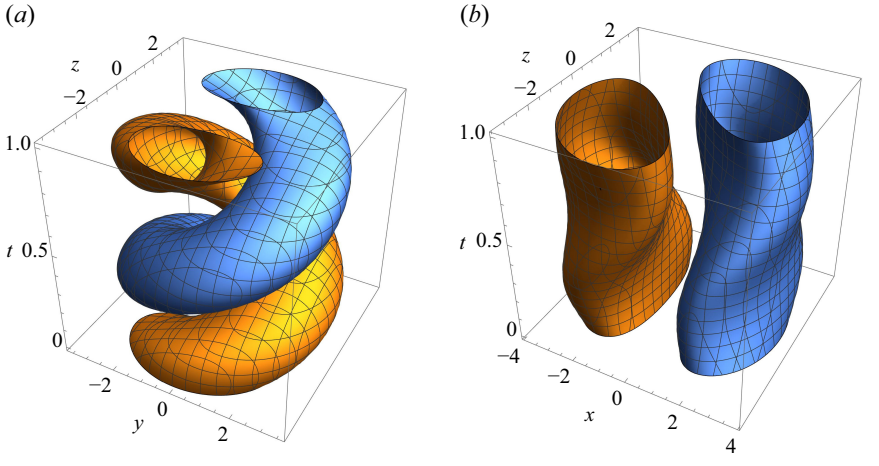


Figure 3. Isosurfaces of (*a*) $\eta(x_0, y, z, t) = \pm 0.2$ for $x_0 = 0$ in the (y, z, t) space in the case the spherical spin $\ell = 1$ vortex dipole is initially aligned along the z-axis ($\boldsymbol{k}_0 = \hat{\boldsymbol{z}}$), and (*b*) $\eta(x, y_0, z, t) = \pm 0.2$ for $y_0 = 0$ in the case the vortex dipole is initially aligned along the x-axis ($\boldsymbol{k}_0 = \hat{\boldsymbol{x}}$).

https://doi.org/10.1017/jfm.2026.11537 Published online by Cambridge University Press

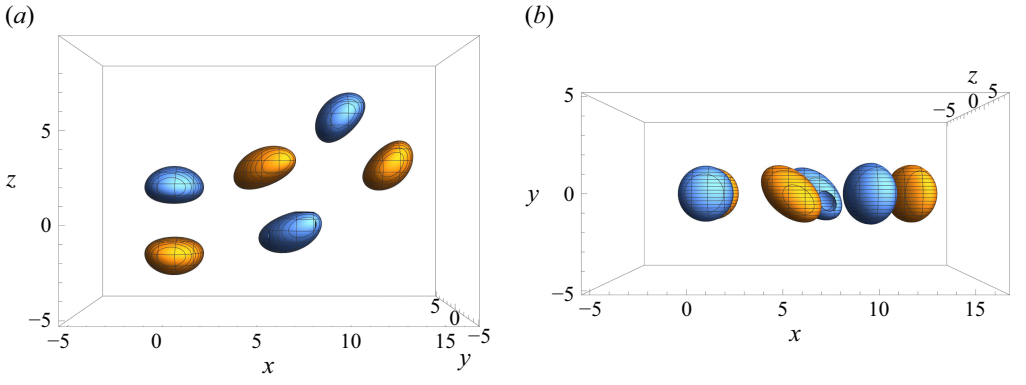


Figure 4. (*a*) Front and (*b*) top views of the superposition of isosurfaces of $\eta(x, y, z, t) = \pm 0.3$ in the (x, y, z) space at three different times $t \in \{0, 1/2, 1\}$ for the case where the spherical spin $\ell = 1$ vortex dipole is initially aligned along the z-axis.

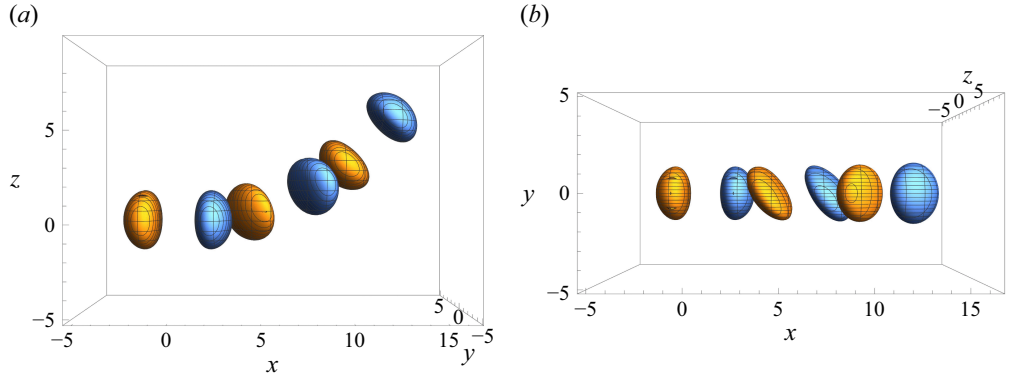


Figure 5. (*a*) Front and (*b*) top views as in figure 4, but for the case where the spherical spin $\ell = 1$ vortex dipole is initially aligned along the x-axis.

background flow does not allow direction changes in the background angular velocity $\boldsymbol{v}(t)$, and hence the Beltrami field cannot change its direction of propagation. The most interesting cases, however, are those in which the background velocity includes a time-dependent deviatoric tensor $\mathsf{D}_0(t)$. In this case, changes in the direction of the background angular velocity vector $\boldsymbol{v}(t)$ are allowed and, hence, directional changes in the Beltrami field displacement velocity. The presence of anisotropic strain caused by $\mathsf{D}_0(t)$, however, breaks in the general case the Beltrami property of the initial Beltrami field, and this fact complicates the existence of exact time-dependent solutions in the theoretical approach presented in this study. Nevertheless, an approximation method, called here the Beltrami field approximation and which assumes that the oscillating field departs only slightly from its initial Beltrami property, allows the linearisation of the vorticity equation assuming that the oscillating field continues to be frozen in the advecting velocity field $\boldsymbol{v}_b(\boldsymbol{x}, t)$, as it were still a Beltrami field. This approximation allows the investigation of elastic scattering of vortices by pulses of a background flow with a time-dependent deviatoric strain tensor $\mathsf{D}_0(t) \neq \mathsf{0}$.

The Beltrami field, which using the Chandrasekhar–Kendall approach admits any geometry in which the scalar Helmholtz equation is separable, is frozen in the background flow and, hence, the time evolution of the Beltrami field is completely determined by the

https://doi.org/10.1017/jfm.2026.11537 Published online by Cambridge University Press

background flow. The velocity gradient $\nabla \boldsymbol{u}_b$ has nine time-dependent components, but the vorticity equation imposes a condition on the time evolution of its antisymmetric part, the spin tensor or the vorticity vector $2\boldsymbol{v}(t)$, which leads to six, the symmetric components, the number of independent time-dependent functions. These six degrees of freedom may be distributed into the six components of the deviatoric strain tensor $\mathsf{D}_0(t)$, subjected to $\mathrm{tr}\mathsf{D}_0(t) = 0$, and the background divergence $\delta(t)$.

The main results may be explained in the following way. In the general case, the barotropic vorticity equation may be expressed as the Cauchy vorticity formula $\boldsymbol{\omega}(\boldsymbol{x}, t) = (1/J(\boldsymbol{x}, t))\mathsf{F}(\boldsymbol{x}, t)\boldsymbol{\omega}_0(\boldsymbol{R}(\boldsymbol{x}, t))$, where $\boldsymbol{\omega}_0$ is the vorticity in the reference configuration. This expression includes the inverse map of the total flow $\boldsymbol{R}(\boldsymbol{x}, t)$. However, the self-advection of Beltrami fields vanishes, since the vorticity of the Beltrami field is frozen in its own flow. Since the background flow is spatially homogeneous, Cauchy vorticity formula reduces to $\boldsymbol{\mathcal{W}}(\boldsymbol{x}, t) = (1/J_v(t))\mathsf{F}_v(t)\boldsymbol{\mathcal{W}}_0(\boldsymbol{R}_v(\boldsymbol{x}, t))$, that is, the Beltrami field is frozen in the advecting velocity. The advecting velocity $\boldsymbol{v}_b(\boldsymbol{x}, t)$ is spatially homogeneous and its inverse map $\boldsymbol{R}_v(\boldsymbol{x}, t)$ may be obtained in a closed form. Hence, those initial Beltrami fields, which remain Beltrami after being advected by $\boldsymbol{v}_b(\boldsymbol{x}, t)$, are exact solutions to the barotropic vorticity equation. The Beltrami property is preserved when the advecting flow induces a similarity, that is, an isotropic expansion/contraction and a solid body rotation. In this case, exact solutions are possible, which describe an arbitrary time-dependent isotropic expansion/contraction and the precession of the Beltrami field.

Independent of its geometry, a main property of the Beltrami field is its time-dependent wavevector $\boldsymbol{k}(t)$. This wavevector expands/contracts, precesses, displaces and changes its direction guided by the time-dependent background flow. This seems to be conceptually very relevant since a time-dependent wavevector associated with a displacing Beltrami field may be interpreted as a particle-like property of a wave field. This description of motion is therefore consistent with the wave–particle duality as a property of matter. The wave–particle description depends on our ability to assign time-dependent vector or scalar-valued functions to a set of oscillating modal fields.

Acknowledgements. I thank the three anonymous reviewers for their careful reading and constructive comments, which helped improve the manuscript. I acknowledge the 'Severo Ochoa Centre of Excellence' accreditation (CEX2019-000928-S). Portions of the manuscript text were edited for clarity and grammar using artificial intelligence (AI) tools (ChatGPT 5.2). The author reviewed and verified all AI-assisted text and takes full responsibility for the content.

Funding. This work was funded by the Spanish Government through the project SAGA (Ministerio de Ciencia, Innovación y Universidades, Ref. No. RTI2018-100844-B-C33).

Declaration of interests. The author declares no competing interests.

Appendix A. Oceanographic application

The theory of Beltrami flows in the presence of a background current may be applied to the ocean, in an inertial frame, where the background flow $\boldsymbol{u}_b(\boldsymbol{x})$ is taken as the steady solid body rotation $\boldsymbol{u}_b(\boldsymbol{x}) \equiv \Omega_b \hat{\boldsymbol{z}} \times \boldsymbol{x}$, where Ω_b is the Earth angular frequency. The Beltrami field consists of a superposition of spherical Beltrami modes

$$\boldsymbol{\mathcal{U}}(\boldsymbol{x}, t) \equiv \sum_{\ell \geq 1} \sum_{|m| \leq \ell} \boldsymbol{\mathcal{U}}_{\ell m}(\boldsymbol{x}, t), \tag{A1}$$

and the Beltrami modes, in terms of the vector spherical harmonic basis $\{\boldsymbol{Y}_{\ell m}(\theta, \varphi), \boldsymbol{\Psi}_{\ell m}(\theta, \varphi), \boldsymbol{\Phi}_{\ell m}(\theta, \varphi)\}$, are

https://doi.org/10.1017/jfm.2026.11537 Published online by Cambridge University Press

$$\boldsymbol{\mathcal{U}}_{\ell m}(\boldsymbol{x},t) \equiv \ell(\ell+1)\frac{\chi_\ell(kr)}{kr}\boldsymbol{Y}_{\ell m}(\theta,\varphi) + \left((\ell+1)\frac{\chi_\ell(kr)}{kr} - \chi_{\ell+1}(kr)\right)\boldsymbol{\Psi}_{\ell m}(\theta,\varphi) + \chi_\ell(kr)\boldsymbol{\Phi}_{\ell m}(\theta,\varphi), \tag{A2}$$

where now

$$\chi_{\ell m}(r) \equiv \hat{u}_{\ell m} j_l(kr) + \hat{v}_{\ell m} y_\ell(kr), \tag{A3}$$

and $\{\hat{u}_{\ell m}, \hat{v}_{\ell m}\}$ are arbitrary amplitudes. The modes are applied to a spherical shell with inner r_1 and outer $r_2 > r_1$ radii whose mean is equal to the mean radius of the Earth and a thickness $r_2 - r_1$ equal to the mean depth of the ocean. Since this shell does not include $r = 0$, the singularity of the spherical Bessel function of the second kind $y_\ell(z)$ at $z = 0$ is not a problem. Vanishing radial velocity at $r = r_1, r_2$, implies that $\chi_{\ell m}(kr_1) = \chi_{\ell m}(kr_2) = 0$ is possible if the determinant of this system of equations vanishes,

$$j_{\ell m}(kr_1)y_{\ell m}(kr_2) - j_{\ell m}(kr_2)y_{\ell m}(kr_1) = 0. \tag{A4}$$

The positive roots $k = k_{\ell n}$, with $n = 1, 2, \ldots$, are the discrete radial wavenumbers. The radial wavenumber is therefore quantised. For typical ocean values $r_1 \approx 6371$ km and $r_2 \approx 6375$ km, the spherical shell is very thin, then $kr_1 \approx kr_2 \gg 1$ and (A4) is very well approximated by

$$\sin(k(r_2 - r_1)) = 0, \quad k_{\ell n} \approx \frac{n\pi}{r_2 - r_1} = \frac{n\pi}{4\,\mathrm{km}}, \quad n = 1, 2, \ldots \tag{A5}$$

or a radial wavelength

$$\lambda_n \equiv \frac{2\pi}{k_n} \approx \frac{8}{n}\,\mathrm{km}. \tag{A6}$$

The ℓ-dependence in $k_{\ell n}$ is negligible unless for very large values of ℓ. Once $k_{\ell n}$ is a root, the ratio between the coefficients

$$\frac{\hat{v}_{\ell m}}{\hat{u}_{\ell m}} = -\frac{j_\ell(k_{\ell n}r_1)}{y_\ell(k_{\ell n}r_1)} = -\frac{j_\ell(k_{\ell n}r_2)}{y_\ell(k_{\ell n}r_2)} \tag{A7}$$

is fixed.

Since the L^2 (square-integrable) norm on the unit sphere S^2 of $\boldsymbol{\Phi}_{\ell m}$ is $\|\boldsymbol{\Phi}_{\ell m}\|_{L^2(S^2)} = \sqrt{\ell(\ell+1)}\|Y_{\ell m}\|_{L^2(S^2)}$, the root mean square (r.m.s.) radial versus tangent (to $Y_{\ell m}$ levels) speed ratio is

$$\frac{\|u_r\|_{rms}}{\|\boldsymbol{u}_{\boldsymbol{\Phi}}\|_{rms}} = \frac{\sqrt{\ell(\ell+1)}}{kr}. \tag{A8}$$

For the first radial wavenumber root, $k_1 \simeq \pi/(4\,\mathrm{km}) \simeq 0.785398\,\mathrm{km}^{-1}$, and hence across the shell, $k_1 r \in [k_1 r_1, k_1 r_2] = [5003.77, 5006.91]$ so that we can safely take $k_1 r \approx 5005$, and the ratio $\|u_r\|_{rms}/\|\boldsymbol{u}_{\boldsymbol{\Phi}}\|_{rms}$ ranges from $\approx 2.83 \times 10^{-4}$ for $\ell = 1$ to $\approx 2.10 \times 10^{-3}$ for $\ell = 10$, whose orders of magnitude are the common scalings for the vertical to horizontal ratio of the secondary circulation in ocean vortices.

However if, instead of assuming that vortex flow satisfies the Helmholtz equation $\nabla^2\boldsymbol{\mathcal{U}} = -k^2\boldsymbol{\mathcal{U}}$, we assume, in the same background velocity field $\boldsymbol{u}_b(\boldsymbol{x},t) \equiv \Omega_b\hat{\boldsymbol{z}} \times \boldsymbol{x}$, a vortex flow $\bar{\boldsymbol{u}}(\boldsymbol{x},t)$ tangent to the spherical surfaces such that its steady streamfunction, in the absence of background velocity, $\bar{\psi}_0(\theta,\varphi)$ satisfies the Helmholtz equation in the unit sphere

https://doi.org/10.1017/jfm.2026.11537 Published online by Cambridge University Press

$$\nabla_S^2 \bar{\psi}_0 = -\kappa^2 \bar{\psi}_0, \tag{A9}$$

where ∇_S^2 is the surface Laplacian operator on the sphere. Then, $\bar{\psi}_0(\theta, \varphi)$ is a single Laplace–Beltrami eigenmode on the sphere

$$\bar{\psi}_0(\theta, \varphi) = \hat{\psi}_{\ell m} Y_\ell^m(\theta, \varphi), \quad \kappa^2 = \ell(\ell+1), \tag{A10}$$

the vortex velocity is

$$\bar{\boldsymbol{u}}_0(\boldsymbol{x}, t) = \boldsymbol{\nabla} \times (\bar{\psi}_0(\theta, \varphi)\hat{\boldsymbol{r}}), \quad \bar{u}_{0r} = 0. \tag{A11}$$

The radial vorticity is

$$\bar{\zeta}_0 \equiv \hat{\boldsymbol{r}} \cdot (\boldsymbol{\nabla} \times \bar{\boldsymbol{u}}_0) = -\frac{1}{r^2}\nabla_S^2 \bar{\psi}_0 = \frac{\kappa^2}{r^2}\bar{\psi}_0. \tag{A12}$$

Since the nonlinear self-advection term vanishes $\bar{\boldsymbol{u}} \cdot \boldsymbol{\nabla}\bar{\zeta} = 0$, the barotropic vorticity equation reduces to a linear transport law for the time-dependent radial vorticity $\bar{\zeta}(\theta, \varphi, t)$,

$$\frac{\partial \bar{\zeta}}{\partial t} + \bar{\boldsymbol{v}} \cdot \boldsymbol{\nabla}\bar{\zeta} = 0, \quad \bar{\boldsymbol{v}}(\boldsymbol{x}) = \bar{\Omega}_\ell \hat{\boldsymbol{z}} \times \boldsymbol{x}, \quad \bar{\Omega}_\ell \equiv \Omega_b \left(1 - \frac{2}{\ell(\ell+1)}\right), \tag{A13}$$

where

$$\bar{\zeta}(\theta, \varphi, t) = \bar{\zeta}_0(\theta, \varphi - \bar{\Omega}_\ell t), \quad \bar{\psi}(\theta, \varphi, t) = \bar{\psi}_0(\theta, \varphi - \bar{\Omega}_\ell t) = \hat{\psi}_{\ell m} Y_\ell^m(\theta, \varphi - \bar{\Omega}_\ell t)$$
$$= \hat{\psi}_{\ell m} Y_\ell^m(\theta, \varphi) \mathrm{e}^{-im\bar{\Omega}_\ell t}. \tag{A14}$$

Thus, the radial vorticity satisfies

$$\frac{\partial \bar{\zeta}}{\partial t} + \Omega_b \left(1 - \frac{2}{\ell(\ell+1)}\right) \frac{\partial \bar{\zeta}}{\partial \varphi} = 0. \tag{A15}$$

Therefore, these eigenmode vortices rotate rigidly with a drift velocity $\rho\bar{\Omega}_\ell \hat{\boldsymbol{\varphi}}$, or a drift angular velocity relative to the background flow equal to

$$\bar{\boldsymbol{c}} = -\frac{2\Omega_b}{\ell(\ell+1)}\hat{\boldsymbol{\varphi}} = \bar{c}_\ell \hat{\boldsymbol{\varphi}}, \tag{A16}$$

that is, opposite to the background flow, or westward. These are the Rossby–Haurwitz waves (Rossby *et al.* 1939; Haurwitz 1940), which are usually defined in the rotating reference frame as

$$\psi(\theta, \varphi, t) = \hat{\psi}_{\ell m} Y_\ell^m(\theta, \varphi) \mathrm{e}^{-i\sigma_\ell t}, \tag{A17}$$

where the Rossby–Haurwitz dispersion relation is expressed in terms of the local (relative to the rotating frame) frequency

$$\sigma_\ell \equiv -m\frac{2\Omega_b}{\ell(\ell+1)}, \tag{A18}$$

and the angular phase speed

$$c_\ell = \frac{\sigma_\ell}{m} = -\frac{2\Omega_b}{\ell(\ell+1)} \tag{A19}$$

coincides with $\bar{c}_\ell$ in (A16). Both the Rossby–Haurwitz solutions and the spherical Beltrami constructions exploit a common eigenmode principle on the sphere: by choosing fields built from spherical eigenfunctions, the nonlinear advection terms simplify and the

https://doi.org/10.1017/jfm.2026.11537 Published online by Cambridge University Press

resulting pattern can persist while being Doppler-shifted/advected by the same solid-body background rotation $\boldsymbol{u}_b = \Omega_b\,\hat{\boldsymbol{z}} \times \boldsymbol{x}$. In the Rossby–Haurwitz case, the motion is purely tangential and non-divergent, $\boldsymbol{u} = \boldsymbol{\nabla} \times (\psi\,\hat{\boldsymbol{r}})$, with $\Delta_S\psi = -\ell(\ell+1)\psi$ so that the relative vorticity satisfies $\bar{\zeta} = -(1/r^2)\Delta_S\psi \propto \psi$, yielding an exact nonlinear solution of the barotropic vorticity equation whose frequency is the intrinsic Rossby drift plus the Doppler shift by Ω_b. In contrast, spherical Beltrami flows are three-dimensional helical modes satisfying $\boldsymbol{\nabla} \times \boldsymbol{\mathcal{U}} = k\,\boldsymbol{\mathcal{U}}$, and hence, $\boldsymbol{\mathcal{U}}$ obeys the vector Helmholtz equation $\nabla^2\boldsymbol{\mathcal{U}} + k^2\boldsymbol{\mathcal{U}} = 0$; their vorticity is proportional to the velocity itself and in the presence of $\boldsymbol{u}_b$, the mode is likewise transported and Doppler-shifted by the background rotation, but with a three-dimensional (3-D) curl-eigenfield structure rather than a surface vorticity wave. Both phenomena can be understood as a consequence of the mismatch between the background velocity and the effective advecting velocity.

Appendix B. Analogy to quantum field theory (QFT) solutions

The analogy of the approach described in § 3 with the approach developed in QFT is based in that in § 3, we have a linear, time-dependent ordinary differential equation along each material label $\boldsymbol{x}_0$ in the form

$$\frac{\partial \boldsymbol{r}}{\partial t}(\boldsymbol{x}_0, t) = \mathsf{L}(t)\boldsymbol{r}(\boldsymbol{x}_0, t). \tag{B1}$$

Introduce the fundamental matrix $\mathsf{U}(t, t_0)$, which is the deformation gradient in this homogeneous case, by

$$\dot{\mathsf{U}}(t, t_0) = \mathsf{L}(t)\mathsf{U}(t, t_0), \quad \mathsf{U}(t_0, t_0) = \mathsf{I}, \tag{B2}$$

then the particle position is

$$\boldsymbol{r}(\boldsymbol{x}_0, t) = \mathsf{U}(t, t_0)\boldsymbol{r}(\boldsymbol{x}_0, t_0). \tag{B3}$$

If $\mathsf{L}(t)$ does not commute with $\mathsf{L}(t')$ at different times, the solution is the time-ordered exponential

$$\mathsf{U}(t, t_0) = \mathcal{T}\exp\left(\int_{t_0}^{t} \mathsf{L}(\tau)\,\mathrm{d}\tau\right). \tag{B4}$$

Equivalently, we may use the Dyson series (Dyson 1949*a*, *b*),

$$\mathsf{U}(t, t_0) = \mathsf{I} + \int_{t_0}^{t} \mathrm{d}\tau_1\,\mathsf{L}(\tau_1) + \int_{t_0}^{t} \mathrm{d}\tau_1 \int_{t_0}^{\tau_1} \mathrm{d}\tau_2\,\mathsf{L}(\tau_1)\,\mathsf{L}(\tau_2) + \cdots \tag{B5}$$

That is mathematically the same structure as quantum time evolution in 0+1 dimensions (time dependence but no space dependence) in which the QFT evolution operator $\hat{H}(t)$ (the Hamiltonian operator) acts on the wavefunction $\psi(t)$ in the Schrödinger equation

$$\mathrm{i}\frac{d}{\mathrm{d}t}|\psi(t)\rangle = \hat{H}(t)|\psi(t)\rangle \quad \Longrightarrow \quad |\psi(t)\rangle = \hat{U}(t, t_0)|\psi(t_0)\rangle, \tag{B6}$$

with the evolution operator

$$\hat{U}(t, t_0) = \mathcal{T}\exp\left(-\mathrm{i}\int_{t_0}^{t} \hat{H}(\tau)\,\mathrm{d}\tau\right). \tag{B7}$$

In quantum mechanics the Hamiltonian operator $\hat{H}(t)$ is Hermitian, $\hat{H}^\dagger(t) = \hat{H}(t)$, which implies that the evolution operator (B7) is unitary, $\hat{U}^\dagger\hat{U} = \hat{I}$, and therefore preserves the

https://doi.org/10.1017/jfm.2026.11537 Published online by Cambridge University Press

norm $\langle\psi|\psi\rangle$. With the identification $\hat{H}(t) = \mathrm{i}\,\mathsf{L}(t)$, this property corresponds to $\mathsf{L}^{\dagger}(t) = -\mathsf{L}(t)$, i.e. $\mathsf{L}(t)$ is anti-Hermitian. For real-valued velocity gradients, this reduces to $\mathsf{L}^{\top}(t) = -\mathsf{L}(t)$, so that $\mathsf{L}(t)$ is skew-symmetric and generates a pure rotation. By contrast, for a general fluid velocity gradient $\mathsf{L}(t)$ containing strain (symmetric part), the propagator is not unitary and the particle separation $\|\boldsymbol{r}\|$ can be amplified or attenuated, even though the evolution retains the same time-ordering (Dyson-series) structure as in Schrödinger dynamics.

Although this setting is purely classical, it is useful to note a structural analogy with gauge transport in quantum theory. In the homogeneous background case $\boldsymbol{\nabla u}_b = \mathsf{L}(t)$, the deformation/transport of a vector quantity along a material label is governed by a linear non-autonomous system whose fundamental matrix is $\mathsf{U}(t, t_0)$ with time ordering required when $[\mathsf{L}(t), \mathsf{L}(t')] \neq \mathsf{0}$. This is mathematically the same propagator structure as quantum time evolution, $\hat{U}(t, t_0)$, and may be viewed as a classical 'connection' generating parallel transport of the field components. In this sense, the background velocity gradient $\mathsf{L}(t)$ plays the role of an effective gauge potential acting on the transported object (here the Beltrami excitation), while the resulting drift/deflection can be interpreted as the analogue of a non-trivial holonomy. A non-trivial holonomy in this homogeneous-flow analogy corresponds to a situation where, after a cycle of the background (e.g. $\mathsf{L}(t + T) = \mathsf{L}(t)$), the one-period propagator is not the identity, i.e. $\mathsf{U}(t_0 + T, t_0) \neq \mathsf{I}$, implying a net rotation/stretch (or phase-like change) of transported directions or modes even though the background has completed a full 'cycle'. This is a formal analogy (acting in physical-space frames rather than an internal gauge space), included to clarify the role of the time-ordered propagator.

Appendix C. On the 'Gauss potential' and the role of the seed function η

In the Chandrasekhar–Kendall-type construction, we take $\boldsymbol{n} = \hat{\boldsymbol{z}}$ and define

$$\boldsymbol{\chi} \equiv \eta(\boldsymbol{x})\,\hat{\boldsymbol{z}}, \qquad \boldsymbol{\psi} \equiv \boldsymbol{\chi} + \frac{1}{k}\boldsymbol{\nabla}\times\boldsymbol{\chi}, \qquad \boldsymbol{\mathcal{U}} \equiv \boldsymbol{\nabla}\times\boldsymbol{\psi}, \tag{C1}$$

with seed function

$$\eta(\boldsymbol{x}) = j_{\ell}(kr)\,Y_{\ell}^{m}(\theta, \varphi), \tag{C2}$$

which satisfies the scalar Helmholtz equation. Since $\hat{\boldsymbol{z}}$ is constant,

$$\boldsymbol{\nabla}\times(\eta\,\hat{\boldsymbol{z}}) = \boldsymbol{\nabla}\eta\times\hat{\boldsymbol{z}}. \tag{C3}$$

In cylindrical coordinates (ρ, φ, z), using

$$\boldsymbol{\nabla}\eta = \hat{\boldsymbol{\rho}}\,\partial_{\rho}\eta + \hat{\boldsymbol{\varphi}}\,\frac{1}{\rho}\partial_{\varphi}\eta + \hat{\boldsymbol{z}}\,\partial_{z}\eta, \tag{C4}$$

one obtains

$$\boldsymbol{\nabla}\eta\times\hat{\boldsymbol{z}} = \hat{\boldsymbol{\rho}}\,\frac{1}{\rho}\,\partial_{\varphi}\eta - \hat{\boldsymbol{\varphi}}\,\partial_{\rho}\eta, \tag{C5}$$

and therefore the vector potential $\boldsymbol{\psi}$ in (C1) has cylindrical components

$$\psi_{\rho} = \frac{1}{k\rho}\partial_{\varphi}\eta, \qquad \psi_{\varphi} = -\frac{1}{k}\partial_{\rho}\eta, \qquad \psi_{z} = \eta. \tag{C6}$$

For the axisymmetric subset $m = 0$ (hence, $\partial_{\varphi}\eta = 0$), the field is independent of φ and one may introduce the standard axisymmetric flux/stream function, sometimes termed a

https://doi.org/10.1017/jfm.2026.11537 Published online by Cambridge University Press

'Gauss potential', as

$$\Psi_G(\rho, z) \equiv \rho\, \psi_\varphi = -\frac{\rho}{k}\, \partial_\rho \eta. \tag{C7}$$

With this definition, the poloidal component of $\boldsymbol{\mathcal{U}} \equiv \boldsymbol{\nabla} \times \boldsymbol{\psi}$ can be expressed in the familiar flux-function form

$$\boldsymbol{\mathcal{U}}_p = \frac{1}{\rho} \boldsymbol{\nabla} \Psi_G \times \hat{\boldsymbol{\varphi}}, \tag{C8}$$

so that the level sets $\Psi_G = \text{const}$ define poloidal stream-surfaces.

For generic non-axisymmetric modes $m \neq 0$, the field depends on φ (equivalently, $\partial_\varphi \eta \neq 0$), and there is, in general, no global scalar flux/stream function whose level sets foliate the domain into invariant 'flux surfaces' for $\boldsymbol{\mathcal{U}}$. In this fully three-dimensional setting, the natural potential object is the vector potential $\boldsymbol{\psi}$ in (C1).

When we refer to topology preserved under diffeomorphisms, we mean the topology of level sets of suitably chosen scalar fields. In the axisymmetric case $m = 0$, Ψ_G in (C7) provides such a scalar label whose level sets coincide with poloidal stream-surfaces. In the general case (including $m \neq 0$), if one nevertheless wishes to track the deformation/topology of level sets under the diffeomorphisms considered in this work, one may instead use the seed scalar $\eta(\boldsymbol{x})$ (or its real/imaginary part) as a convenient scalar label: its isosurfaces $\eta = \text{const}$ define a well-posed family of reference surfaces, even though they are not, in general, stream/flux surfaces of $\boldsymbol{\mathcal{U}}$.

We consider now the diffeomorphic invariance of field-line topology and the scaling symmetry of k. Let $\boldsymbol{\mathcal{U}}(\boldsymbol{x})$ be a solenoidal field and let Φ_t be the smooth flow map generated by a smooth advecting velocity (so Φ_t is a diffeomorphism for all t before any singularity/caustic formation). The advected/push-forward field may be written schematically as

$$\boldsymbol{\mathcal{U}}_t \;=\; (\Phi_t)_*\, \boldsymbol{\mathcal{U}}_0, \tag{C9}$$

so that field lines are transported by Φ_t as embedded curves. In particular, any field-line connectivity and knot/link type is preserved under such smooth advection: a diffeomorphism can deform field lines but cannot cut, reconnect or change their topological class. In addition, the Beltrami families in this work exhibit a simple scaling symmetry that changes the curl eigenvalue while preserving field-line topology. Indeed, if $\boldsymbol{\mathcal{U}}$ satisfies

$$\boldsymbol{\nabla} \times \boldsymbol{\mathcal{U}} = k\, \boldsymbol{\mathcal{U}} \quad (\text{in } \mathbb{R}^3), \tag{C10}$$

then for any $\lambda > 0$, the rescaled field

$$\boldsymbol{\mathcal{U}}^{(\lambda)}(\boldsymbol{x}) \equiv \boldsymbol{\mathcal{U}}(\lambda \boldsymbol{x}) \tag{C11}$$

satisfies

$$\boldsymbol{\nabla} \times \boldsymbol{\mathcal{U}}^{(\lambda)} = (\lambda k)\, \boldsymbol{\mathcal{U}}^{(\lambda)}. \tag{C12}$$

Since $\boldsymbol{x} \mapsto \lambda \boldsymbol{x}$ is a diffeomorphism of $\mathbb{R}^3$, this transformation preserves the topology of field lines (it amounts to a global change of length scale), while continuously rescaling the parameter k.

The spectral properties of the curl operator (Yoshida & Giga 1990) depend sensitively on the domain and boundary conditions. On bounded domains with physically imposed boundary conditions (e.g. tangential/normal constraints, as in the oceanographic application considered in Appendix A, the curl spectrum is typically discrete, so changing

https://doi.org/10.1017/jfm.2026.11537 Published online by Cambridge University Press

k at fixed domain/BC usually means selecting a different eigenfunction, and it is then unsurprising that field-line geometry/topology may change across eigenmodes. In contrast, on unbounded domains (or in settings where scale is not fixed *a priori*) one naturally encounters continuous families related by symmetries such as translations, rotations and the scaling map above, for which k may vary continuously without forcing a jump to a topologically unrelated eigenfunction. This clarifies why the symmetry-generated families considered here do not support the heuristic 'changing the eigenvalue implies a topology change': in our case, the change in k is produced by an explicit diffeomorphic (and, in particular, topology-preserving) transformation, rather than by moving between distinct eigenfunctions on a fixed bounded domain with fixed boundary conditions.

References

ARNOLD, V.I. 1965 Sur la topologie des écoulements stationnaires des fluides parfaits. *C. R. Acad. Sci. Paris* **261**, 17–20.

ARNOLD, V.I. & KHESIN, B.A. 1998 *Topological Methods in Hydrodynamics, Applied Mathematical Sciences*, vol. 125. Springer.

BARNES, L.A., FRANCIS, M.J., JAMES, J.B. & LEWIS, G.F. 2006 Joining the Hubble flow: implications for expanding space. *Mon. Not. R. Astron. Soc.* **373** (1), 382–390.

BĚLÍK, P., SU, X., DOKKEN, D.P., SCHOLZ, K. & SHVARTSMAN, M.M. 2020 On the axisymmetric steady incompressible Beltrami flows. *Open J. Fluid Dyn.* **10**, 208–238.

CHANDRASEKHAR, S. & KENDALL, P.C. 1957 On force-free magnetic fields. *Astrophys. J.* **126**, 457–460.

CHANDRASEKHAR, S. & WOLTJER, L. 1958 On force-free magnetic fields. *Proc. Natl Acad. Sci. USA* **44** (4), 285–289.

CHAPLYGIN, S.A. 1903 One case of vortex motion in fluid. *Trudy Otdeleniya Fiz. Nauk Imperatorskogo Moskovskogo Obshchestva Lyubitelei Estestvoznaniya* **11** (2), 11–14. In Russian; reprinted in Chaplygin's Collected Works (1933, 1948).

CHAPLYGIN, S.A. 2007 One case of vortex motion in fluid. *Regular Chaotic Dyn.* **12** (2), 219–232. English translation of Chaplygin (1903).

CHELTON, D.B., SCHLAX, M.G. & SAMELSON, R.M. 2011 Global observations of nonlinear mesoscale eddies. *Prog. Oceanogr.* **91** (2), 167–216.

CHILDRESS, S. 1970 New solutions of the kinematic dynamo problem. *J. Math. Phys.* **11** (10), 3063–3076.

COLLETT, E. 2005 *Field Guide to Polarization*. SPIE Press.

DOMBRE, T., FRISCH, U., GREENE, J.M., HÉNON, M., MEHR, A. & SOWARD, A.M. 1986 Chaotic streamlines in the ABC flows. *J. Fluid Mech.* **167**, 353–391.

DRITSCHEL, D.G. 1990 The stability of elliptical vortices in an external straining flow. *J. Fluid Mech.* **210**, 223–261.

DRITSCHEL, D.G. 1991 Generalized helical Beltrami flows in hydrodynamics and magnetohydrodynamics. *J. Fluid Mech.* **222**, 525–541.

DRITSCHEL, D.G. & LEGRAS, B. 1991 The elliptical model of two-dimensional vortex dynamics. II: Disturbance equations. *Phys. Fluids A* **3** (5), 855–869.

DYSON, F.J. 1949*a* The radiation theories of Tomonaga, Schwinger, and Feynman. *Phys. Rev.* **75** (3), 486–502.

DYSON, F.J. 1949*b* The S matrix in quantum electrodynamics. *Phys. Rev.* **75** (11), 1736–1755.

ENCISO, A. & PERALTA-SALAS, D. 2012 Knots and links in steady solutions of the Euler equation. *Proc. Natl Acad. Sci. USA* **109** (23), 9714–9719.

GALLOWAY, D.J. & FRISCH, U. 1986 Dynamo action in a family of flows with chaotic streamlines. *Geophys. Astrophys. Fluid Dyn.* **36** (1), 53–83.

HAURWITZ, B. 1940 The motion of atmospheric disturbances on the spherical Earth. *J. Mar. Res.* **3** (3), 254–267.

HICKS, W.M. 1899 Researches in vortex motion. Part III. On spiral or gyrostatic vortex aggregates. *Phil. Trans. R. Soc. Lond. A* **192**, 33–99.

JACKSON, J.D. 1999 *Classical Electrodynamics*, 3rd edn. Wiley.

JONES, R.C. 1941 A new calculus for the treatment of optical systems. I. Description and discussion of the calculus. *J. Opt. Soc. Am.* **31** (7), 488–493.

KIDA, S. 1981 Motion of an elliptic vortex in a uniform shear flow. *J. Phys. Soc. Japan* **50** (10), 3517–3520.

KLEIN, P. & LAPEYRE, G. 2009 The oceanic vertical pump induced by mesoscale and submesoscale dynamics. *Annu. Rev. Mar. Sci.* **1**, 351–375.

LAMB, H. 1895 *Hydrodynamics*, 2nd edn. Cambridge University Press.

https://doi.org/10.1017/jfm.2026.11537 Published online by Cambridge University Press

LEGRAS, B. & DRITSCHEL, D.G. 1991 The elliptical model of two-dimensional vortex dynamics. I: the basic state. *Phys. Fluids A* **3** (5), 845–854.
KELVIN, L. 1880 Vibrations of a columnar vortex. *Phil. Mag.* **10**, 155–168.
MCWILLIAMS, J.C. 2016 Submesoscale currents in the ocean. *Annu. Rev. Mar. Sci.* **8**, 125–159.
MOFFATT, H.K. 1969 The degree of knottedness of tangled vortex lines. *J. Fluid Mech.* **35** (1), 117–129.
MOFFATT, H.K. 2017 The degree of knottedness of tangled vortex lines—corrigendum. *J. Fluid Mech.* **830**, 821–822.
MORSE, P.M. & FESHBACH, H. 1953 Vector fields. In *International Series in Pure and Applied Physics*, vol. 2, chap. 13. McGraw-Hill Book Company. Part II.
MUNK, W.H. 1950 On the wind-driven ocean circulation. *J. Meteorol.* **7** (2), 79–93.
PEACOCK, J.A. 1999 *Cosmological Physics*. Cambridge University Press.
RINTOUL, S.R., HUGHES, C.W. & OLBERS, D. 2001 The antarctic circumpolar current system. In *Ocean Circulation and Climate* (ed. G. Siedler, J. Church & J. Gould), International Geophysics, vol. 77, pp. 271–302. Academic Press.
ROBINSON, A.C. & SAFFMAN, P.G. 1984 Three-dimensional stability of an elliptical vortex in a straining field. *J. Fluid Mech.* **142**, 451–466.
ROSSBY, C.-G., WILLETT, H.C., HOLMBOE, J., NAMIAS, J., PAGE, L. & ALLEN, R. 1939 Relation between variations in the intensity of the zonal circulation of the atmosphere and the displacements of the semi-permanent centers of action. *J. Mar. Res.* **2** (1), 38–55.
RYDEN, B. 2017 *Introduction to Cosmology*, 2nd edn. Cambridge University Press.
SOWARD, A.M. 1987 Fast dynamo action in a steady flow. *J. Fluid Mech.* **180**, 267–295.
STOMMEL, H. 1948 The westward intensification of wind-driven ocean currents. *Trans. Am. Geophys. Union* **29** (2), 202–206.
VALLIS, G.K. 2017 *Atmospheric and Oceanic Fluid Dynamics*, 2nd edn. Cambridge University Press.
VIÚDEZ, A. 2022 Exact solutions of time-dependent oscillations in multipolar spherical vortices. *J. Fluid Mech.* **949**, A13.
VIÚDEZ, A. 2025 A classical fluid mechanics description of the spin-up and spin-down states that violates the Clauser–Horne–Shimony–Holt inequality. *Phys. Fluids* **37** (11), 112003.
VIÚDEZ, A. 2025*a* Euler fluid mechanics solutions to Dirac quantum mechanics equation using multipolar oscillations in spherical geometry. *Euro. J. Mech. B/Fluids* **111**, 81–86.
VIÚDEZ, A. 2025*b* Isochoric unsteady multipolar spherical oscillations in compressible radial and cylindrical background flows. *J. Fluid Mech.* **1002**, A11.
VIÚDEZ, A. 2025*c* Precession of spherical spin-1 vortices. *Phys. Fluids* **37** (5), 056116.
WOLTJER, L. 1958*a* The stability of force-free magnetic fields. *Astrophys. J.* **128**, 384–389.
WOLTJER, L. 1958*b* A theorem on force-free magnetic fields. *Proc. Natl Acad. Sci. USA* **44** (6), 489–491.
YOSHIDA, Z. & GIGA, Y. 1990 Remarks on spectra of operator rot. *Math. Z.* **204** (2), 235–245.
ZOELLER, V. & VIÚDEZ, A. 2023 Elastic interaction between a mesoscale eddy-pair and an axisymmetrical eddy. *J. Geophys. Res.: Oceans* **128** (3), e2022JC019597.

https://doi.org/10.1017/jfm.2026.11537 Published online by Cambridge University Press